UNIVERSITY OF CALIFORNIA
RIVERSIDE

Mass Spectrometric Investigation on the Formation and Repair of DNA Modifications

A Dissertation submitted in partial satisfaction
of the requirements for the degree of

Doctor of Philosophy

in

Environmental Toxicology

by

Su Guo

December 2022

Dissertation Committee:
Dr. Yinsheng Wang, Chairperson
Dr. Quan Cheng
Dr. Min Xue

The Dissertation of Su Guo is approved:

Committee Chairperson

University of California, Riverside

ACKNOWLEDGEMENTS

In the first place, I'd like to take this opportunity to offer my profound gratitude to Professor Yinsheng Wang for giving me the priceless opportunity to do research in such a passionate and active group and for his inspirational leadership and strategic direction over the past six years. He will always be an excellent example and role model for me to follow because of his sincere pursuit and strong understanding in creating scientific discoveries. Group meetings in the lab are a feast of information and a great chance to learn thanks to Dr. Wang's extensive knowledge in the field and his willingness to share. Dr. Wang is also always encouraging me to think broadly, read extensively. In addition, he provides me with many opportunities to present my research in national conferences, which broaden my vision and connect me with the scientific community.

Along with Dr. Quan Cheng and Dr. Min Xue, I would like to express my profound gratitude for their patient direction, frequent reminders, useful counsel, and insightful questions throughout the preparation of my thesis. This dissertation would not have been possible without them. Additionally, I would like to thank Dr. Jay Gan and Dr. Huinan Liu for being my oral qualifying committee members. They are great professors and taught me to think critically and react scientifically.

I am truly grateful for the support from my lab mates in Wang lab. I am fortunate to have the chance to work with so many talented young scientists in our lab. Especially,

I want to express my sincere gratitude to Dr. Jiapeng Leng, Dr. Yang Yu, Dr. Yuxiang Cui, Dr. Quanqing Zhang and Dr. Ying Tan. Jiapeng synthesized chemical standards for my first project. Yang and Yuxiang taught me how to perform DNA extraction and enzymatic digestion. Quanqing helped me set up a homemade fraction collector. Ying was a good collaborator and contributed a lot to my research. Additionally, my research is set forth on the shoulders of great scientists who previously worked in our lab. I wish them all the best!

I consider myself extremely fortunate to have my supportive parents. They genuinely care about me and are always willing to impart their knowledge and love. I appreciate my old friends coming to see me and sharing their lives with me. I appreciate the faculties and staff in UCR who helped me in the past and appreciate their willingness to aid my research and life.

COPYRIGHT ACKNOWLEDGEMENTS

The text and figures in Chapter 2, in part or in full, are a reprint of the material as it appears in ***Chemical Research in Toxicology*** 2019, 32, 708–717. The coauthor (Dr. Jiapeng Leng) contributed the synthesis of stable isotope-labeled standards; the coauthor (Dr. Yinsheng Wang) listed in that publication directed and supervised the research that forms the basis of this chapter.

The text and figures in Chapter 3, in part or in full, are a reprint of the material as it appears in ***Journal of the American Chemical Society*** 2021, 143, 16197–16205 and ***Chemical Research in Toxicology*** 2022, 35, 1814-1820. The coauthor (Ying Tan) conducted the CTAB assays; the coauthor (Dr. Yinsheng Wang) listed in these publications directed and supervised the research that forms the basis of this chapter.

ABSTRACT OF THE DISSERTATION

Mass Spectrometric Investigation on the Formation and Repair of DNA Modifications

by

Su Guo

Doctor of Philosophy, Graduate Program in Environmental Toxicology
University of California, Riverside, December 2022
Dr. Yinsheng Wang, Chairperson

The advancement of mass spectrometry (MS) facilitates sensitive and unambiguous analysis of DNA modifications. There are two subjects in this area of investigation: 1) discovery of novel DNA modifications; 2) revelation of repair mechanisms of DNA modifications. In this dissertation, we developed LC-MS/MS methods to quantify a number of DNA modifications in mammalian cells and to assess their repair.

In Chapter 2, we employed nLC-nESI-MS/MS coupled with isotope-dilution method that simultaneously quantifies three pyridylhydroxybutyl (PHB) adducts induced by tobacco-specific nitrosamine 4-(methylnitrosamino)-1-(3-pyridyl)-1-butanol (NNAL).

Among them, O^4-[4-(3-pyridyl)-4-hydroxylbut-1-yl]-thymidine (O^4-PHBdT) was first discovered in mammalian genome upon NNAL exposure. The newly discovered O^4-PHBdT, as well as O^2-PHBdT and O^6-PHBdG, was found to display dose-dependent formation both *in vivo* and *in vitro*. In addition, NER was shown to be involved in the removal of O^2-PHBdT and O^4-PHBdT, while direct reversal suicide protein MGMT may counteract the formation of O^6-PHBdG and O^4-PHBdT.

In Chapter 3, we employed metabolic labeling to selectively incorporate N^2-methyl-dG (N^2-MedG) and N^2-*n*-butyl-dG (N^2-*n*BudG) into genomic DNA of cultured cells, and investigated how the levels of the two lesions in cellular DNA are modulated by different DNA repair factors. It was found that NER exerts moderate effects on the removal of N^2-MedG and N^2-*n*BudG from genomic DNA. Translesion synthesis (TLS) polymerases κ and η may contribute to the incorporation of N^2-alkyl-dG into genomic DNA. Pol κ was found to be involved in the repair of both N^2-MedG and N^2-*n*BudG; while Pol η was responsible for the repair of less bulky N^2-MedG, but not N^2-*n*BudG. In addition, loss of ALKBH3 resulted in higher frequencies of N^2-MedG and N^2-*n*BudG incorporation into genomic DNA, suggesting a role of oxidative dealkylation in the reversal of these lesions.

In Chapter 4, we extended the metabolic labeling approach to accommodate genomic incorporation of 2-amino-2'-deoxyadenosine (dZ) and investigated its plausible repair mechanism. Z is a naturally occurring non-canonical nucleobase that has been found in bacteriophages in substitution of adenine (A). It was observed for the first time that dZ could be incorporated into genomic DNA in mammalian cells, and TLS

polymerases ι and REV1 may contribute to its incorporation. In addition, transcription-coupled NER (TC-NER), but not global genome NER (GG-NER), participates in the removal of dZ from human genome.

Table of Contents

List of Schemes

List of Tables

List of Figures

Chapter 1 Introduction

1.1. General overview

Human genome is coded with four types of nucleobases: adenine (A), cytosine (C), guanine (G), and thymine (T), where A pairs with T and C pairs with G.[1] This base pairing system through hydrogen bonding, along with nucleobase stacking, eventually builds up the DNA double helix. However, human genome is susceptible to damage by chemicals from internal and external sources due to the reactive nature of nucleobases and backbone phosphate in DNA. As a result, a number of DNA modifications (lesions) can be introduced into the genome.[2,3]

To counteract the deleterious effects of DNA lesions, cells are equipped with multiple repair machineries, including direct reversal, base excision repair (BER), nucleotide excision repair (NER), mismatch repair (MMR), non-homologous end-joining (NHEJ) and homologous recombination (HR).[3–7] Unrepaired DNA lesions may perturb the efficiency of DNA replication and transcription.[3,8,9] In addition, DNA lesions may not be recognized correctly by the DNA replication machinery, which ultimately elicits mutations in the genome.[10,11] Thus, it is essential to investigate the formation and repair of DNA lesions.

Over the last several decades, many analytical techniques have been applied for the detection and quantitative measurements of modified nucleosides in DNA.[8,12] Since most DNA modifications are induced at extremely low levels in the genome,[12,13] researchers placed emphasis on the development of sensitive and specific analytical

methods. These include, but are not limited to, ^{32}P-postlabeling assays, immunoassays, electrochemical methods and next-generation sequencing.[14–18] These techniques afford highly sensitive analysis of DNA modifications, which as a result enhance the detection ability and decrease sample consumption. However, these assays have disadvantages such as safety issues, ambiguity in the identities of DNA modifications, tedious procedures, and high cost.[8]

Recent advances in mass spectrometry (MS) instrumentation and sample preparation methods render it possible for highly sensitive and unambiguous analysis of DNA modifications.[8,19,20] MS has been widely adopted in qualitative and quantitative analysis of DNA modifications.[21–27] In this dissertation, I focused on the development of LC-MS/MS methods for the quantification of several DNA modifications and utilization of these methods to explore the potential repair mechanisms of DNA lesions. In this chapter, I will discuss the occurrence, repair, and biological consequences of DNA modifications. Next, I will summarize the recent advances in the detection and quantitative analysis of DNA modifications.

1.2. Occurrence of DNA modifications

The integrity of genome is constantly challenged by chemical agents that can induce DNA damage. The multiple nucleophilic sites in nucleobases (the *N*7, O^6, and N^2 position of guanine; the *N*1, *N*3, and *N*7 position of adenine; the O^2 and O^4 position of thymine; and the O^2 and N^4 position of cytosine, etc.) can be attacked by reactive electrophiles.[1,21,28–30] Additionally, phosphate backbone in DNA can also be

alkylated.[27,31,32] In contrast to nucleobases and phosphate backbone, the 2′-deoxyribose is inert to alkylating agents but susceptible to damage from hydroxyl radicals.[33] The resulting DNA modifications on the 2′-deoxyribose can be oxidized derivatives, epimers, or DNA-protein crosslinks.[33,34] (**Scheme 1.1.**)

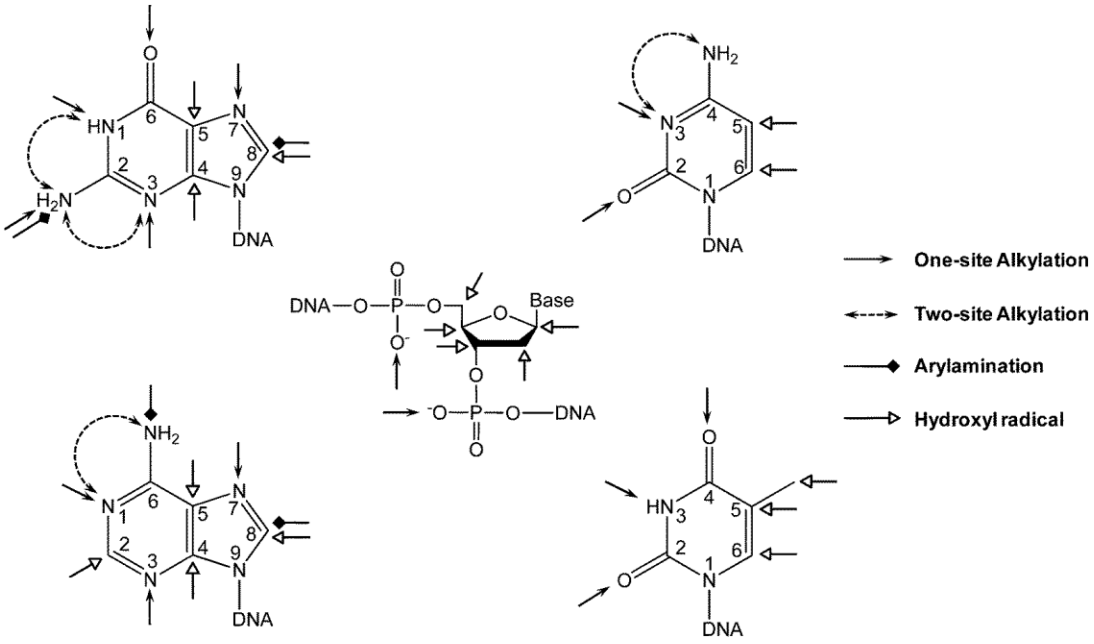

Scheme 1.1. A summary of the reactive sites in DNA. Adapted with permission from Royal Society of Chemistry: Chemical Society Reviews 2015, 44, 7829-7854

1.2.1. Adducts induced by tobacco-specific nitrosamines

4-(methylnitrosamino)-1-(3-pyridyl)-1-butanone (NNK), a major tobacco-specific nitrosamine, and its reduced metabolite 4-(methylnitrosamino)-1-(3-pyridyl)-1-butanol (NNAL) have been found to induce cancer.[35–37] The carcinogenic effects of NNK and NNAL reside on their abilities in inducing the formation of adducts on nucleobases and DNA backbone,[38,39] which may result in diminished replication efficiency and mutations in DNA.[40] NNK and NNAL are bioactivated by cytochrome P450 enzymes, yielding

reactive intermediates that can pyridyloxobutylate and pyridylhydroxybutylate DNA, respectively.[35,41] A number of studies reported the presence of pyridyloxobutylated and pyridylhydroxybutylated DNA lesions in tissues of mammals exposed to NNK and NNAL. These lesions include O^2-POBdT, O^4-POBdT, O^6-POBdG, O^2-PHBdT, O^6-PHBdG, O^2-POBdC, 7-POBG, 7-PHBG, N^6-POBdA, N^6-PHBdA, $N1$-POBdI and $N1$-PHBdI on nucleobases and $B_1p(POB)B_2$ and $B_1p(PHB)B_2$ on phosphate backbone, identified *in vivo*.[42–44] (**Scheme 1.2.**)

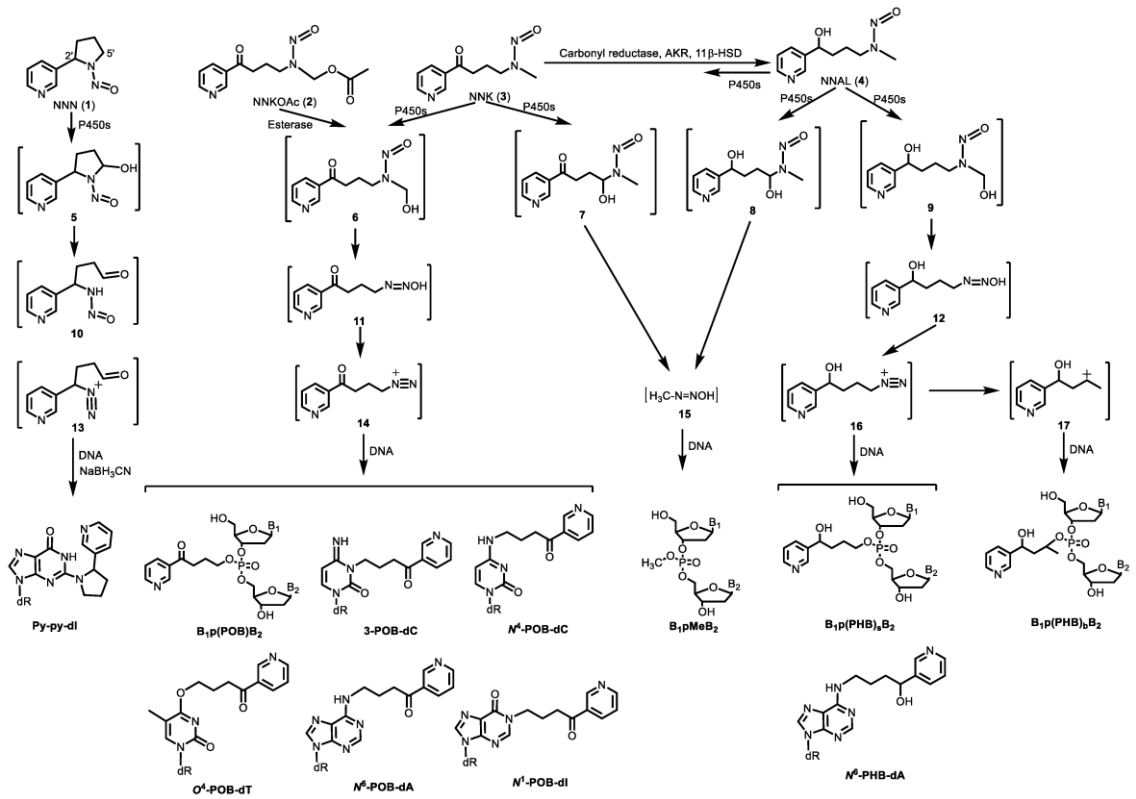

Scheme 1.2. NNK and NNN-derived nucleobase and phosphate adducts characterized. Adapted by permission from MDPI, Basel, Switzerland: Toxics. 2019; 7: 1644

1.2.2. N^2-alkyl-2′-deoxyguanosine

Minor-groove N^2 position of dG is susceptible to modifications by various alkylating agents.[28,45,46] For instance, exposure to benzo[*a*]pyrene results in N^2-BPDE-dG through its metabolite benzo[*a*]pyrene-7,8-diol-9,10-epoxide (BPDE).[47,48] In addition, aldehydes can attack the N^2 position of guanine to yield N^2-alkyl-dG, and the resulting N^2-ethyl-dG in plasma is a biomarker that reflects alcohol consumption.[49,50]

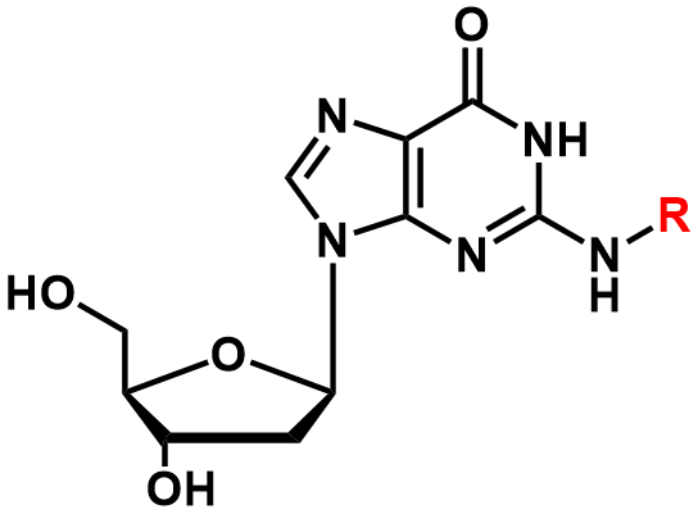

Scheme 1.3. Chemical structure of N2-alkyl-dG

1.2.3. 2,6-diaminopurine

2,6-diaminopurine (Z) was first found in the genome of bacteriophages, where it replaces adenine (A).[51,52] The Z-containing genome is resistant to a spectrum of bacterial endonucleases, empowering bacteriophages a selective advantage.[53,54] This noncanonical, however, does not exist in the genome of higher organisms.[52,55]

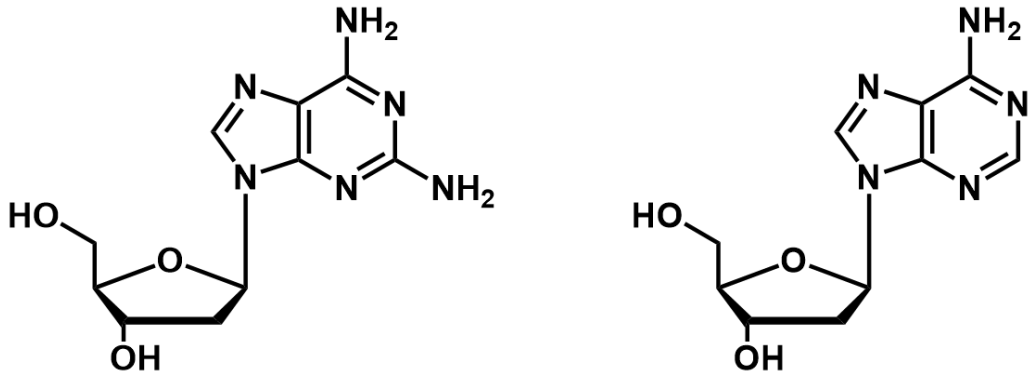

Scheme 1.4. Chemical structure of dZ (left) and dA (right)

1.3. Repair of DNA modifications

The repair processes include direct reversal by alkyltransferases (e.g. MGMT), oxidative reversal by dioxygenases (i.e. AlkB in *Escherichia coli* and AlkB homologs in human), BER, and NER.[3,4,11,56] In this vein, it is worth noting that non-heme Fe(II)/α-ketoglutarate-dependent dioxygenase AlkB family of proteins and their functions have been identified in recent years, and researchers have realized that many of these dioxygenases play critical roles in demethylating epigenetic and epitranscriptomic modifications in DNA and RNA.[57] In addition, translesion synthesis (TLS) polymerases were recently shown to be involved in NER.[58,59]

1.3.1. Direct reversal

A small subset of DNA modifications can be reversed by simple direct reversal mechanisms. There are two major classes of enzymes/proteins that are responsible for the reversal of alkylated bases in mammalian cells.[60,61] The first class consists of suicide proteins, O^6-methylguanine-DNA alkyltransferase (MGMT), which can repair O^6-MedG, O^6-EtdG, O^6-benzyl-dG and even bulky pyridyloxobutyl adducts formed on the O^6 position of guanine.[23,60,62] To a lesser extent, MGMT is involved in the removal of modifications at the O^4 position of thymine. The second class includes AlkB-related α-ketoglutarate-dependent dioxygenases, which repair N-alkylated nucleobases.[60] AlkB family proteins hydroxylate the alkyl group in an α-ketoglutarate-dependent manner, which as a result releases aldehyde and leaves behind unmodified nucleobase.[63,64] AlkB proteins carry out essential repair in bacteria cells and were later found its human analogs (i.e., ALKBH1-8, FTO).[65,66] Among them, ALKBH3 was characterized as a *bona fide* repair protein handling the reversal of N3-methyl-2′-deoxycytidine.[67,68]

1.3.2. NER

NER was first found to be involved in the removal of bulky photoproducts elicited by UV radiation.[3,69] It was later found capacity to repair N^2-BPDE-dG and interstrand crosslink adducts induced by chemotherapeutic drugs.[1,70,71] NER deficiency in humans is a cause of various diseases, including, but are not limited to, xeroderma pigmentosum (XP) and Cockayne syndrome (CS).[72,73]

There are two major branches of NER, global genome NER (GG-NER) and transcription-coupled NER (TC-NER).[74,75] GG-NER was first characterized to be involved in the repair of lesions that result in helix distortion.[3] The mechanisms of GG-NER are complicated, where xeroderma pigmentosum, complementation group C (XPC) detects helix distortion, and XPC-lesion complex recruits transcription initiation factor IIH (TFIIH) that initiates the NER repair process.[48,75,76] The later process of NER consists of the use of XPF–ERCC1 and XPG endonucleases that cleave damaged strand from 5′ and 3′ sides, respectively.[75,77] The final step is gap-filling synthesis and ligation, which ultimately restore genome integrity.[3,74,78]

TC-NER, in contrast, is initiated by stalled transcriptional machinery. First, Cockayne syndrome protein B (CSB) is recruited to the stalled RNA polymerase II, and downstream NER factors are recruited to the complex.[75,79] The subsequent steps of repair in TC-NER are the same as that of GG-NER, despite the drastic difference in repair initiation.[3,80]

1.3.3. TLS polymerases

TLS polymerases are highly conserved proteins that mediate damage bypass when replication machinery encounters unrepaired DNA modifications.[81,82] In humans, a total of eleven TLS polymerases were found (i.e., REV1, Pol η, Pol ι, Pol κ, Pol ζ, Pol μ, Pol λ, Pol β, Pol ν, Pol θ and PrimPol).[82,83] Despite their well-documented roles in lesion bypass, TLS polymerases were found to exhibit versatile functions. For instance, human Pol η can incorporate ribonucleoside triphosphates (rNTPs).[84] The involvement of TLS in

the reversal of DNA modification is in debate, while some researchers suggested that Pol κ is closely connected to NER.[58,59]

1.4. Biological consequences of unrepaired DNA modifications

If DNA modifications are not properly repaired, they may lead to deleterious effects such as cell death or mutations.[1,7] DNA alkylation adducts can impede replication and transcription to varying degrees, depending on the size of the alkyl group. Many DNA modifications have been proven to be highly mutagenic, such as N^2-alkyl-dG, O^6-alkyl-dG, O^4-alkyl-dT and O^2-alkyl-dT.[40,62,85–87] Although some DNA adducts can be removed by DNA repair processes, long-term exposure to carcinogens, such as aflatoxin B1, benzo[*a*]pyrene, and nitrosamines, may ultimately lead to cancer.[3,12,13,35] On the other hand, some cancer chemotherapeutic agents function through deadly effects of DNA alkylation.[1]

1.5. Recent advances in quantitative and qualitative analyses of DNA modifications

1.5.1. Qualitative analysis of DNA modifications

Mass spectrometer measures *m/z* for both parent and daughter ions, working well for structural elucidation.[8] In recent years, electrospray ionization (ESI)-MS is the most adopted platform in DNA adduct detection.[12] Prior to MS analysis, DNA samples are usually digested down to mononucleosides and loaded onto an HPLC column, which allows for separation of different modified nucleosides from each other and from unmodified canonical nucleosides, thereby enhancing the sensitivity of MS detection.[21,30]

Furthermore, the advent of nanoflow HPLC reduces the limit of detection (LOD) of DNA modifications to femtomoles level or lower. The advancement of MS enables the discoveries of novel DNA modifications (e.g., interstrand crosslinks, intrastrand crosslinks and DNA-protein complex) in biological samples.[25,88–90]

1.5.2. Quantitative analysis of DNA modifications

The introduction of nanoflow HPLC and nano-ESI enables more sensitive analyses of trace levels of compounds compared to normal-flow HPLC and ESI.[91,92] However, the execution of the new platform often encounters severe matrix effects.[93,94] Thus, it is essential to develop reliable analytical methods that mitigate matrix effects.[95] The most adopted method for quantitative analysis of DNA modifications is isotope dilution coupled to LC-MS/MS measurement (**Scheme 1.5.**).[12,19,20] The internal standard spiked in the injected sample has the same physiochemical properties as the analytes, which allows for accounting for the effects of sample matrix on the ionization efficiency of analytes.[20]

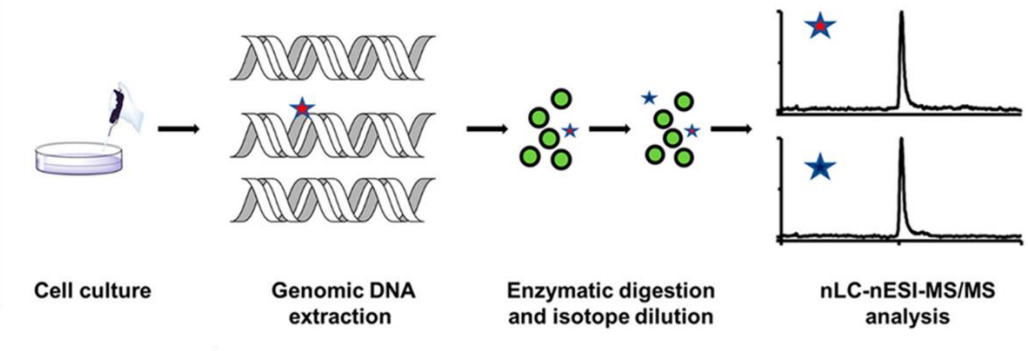

Scheme 1.5. The workflow of isotope dilution coupled to HPLC-MS/MS analysis of DNA modifications.

It is now possible to investigate the DNA repair process by directly monitoring the amounts of DNA adducts with a reliable quantitative MS-based method. When combined with genetic depletion of certain DNA repair proteins, quantitative analysis of DNA modifications can help assess the involvement of repair mechanisms (**Scheme 1.6**.).[23,25,96] For example, O^2-POB-dT was found at an elevated level in XPA- or ERCC1-deficient cell lines (i.e., GM04429, CHO-7-27) compared to their repair-proficient counterparts (i.e., GM00637, CHO-AA8).[23]

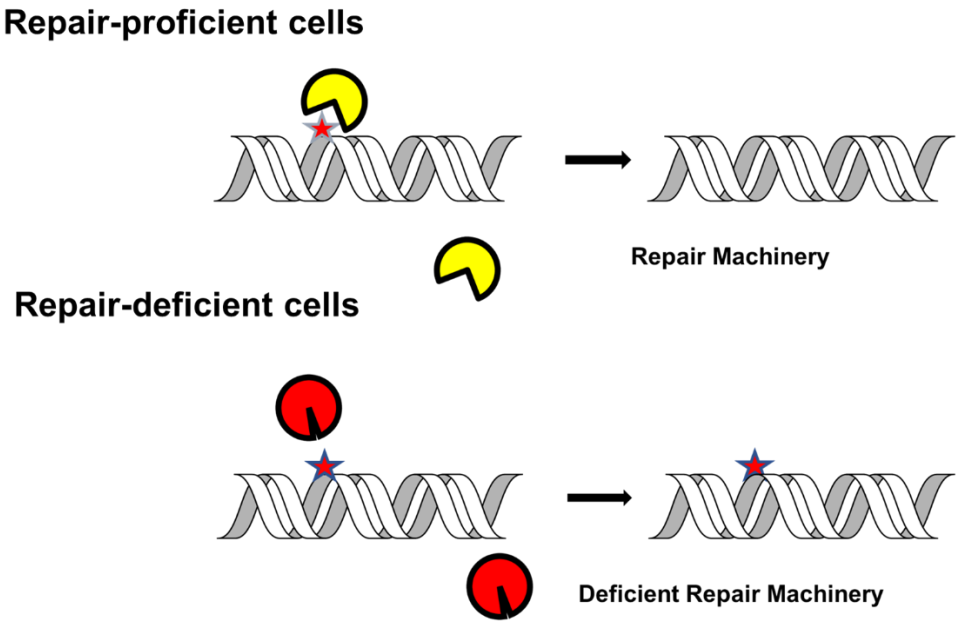

Scheme 1.6. The fate of DNA modifications in repair-proficient and deficient cells.

1.6. Scope of this dissertation

The advancement of mass spectrometry (MS) facilitates sensitive and unambiguous analysis of DNA modifications, which allows for discovery of novel DNA modifications and revelation of the repair mechanisms of DNA modifications. In this dissertation, we developed LC-MS/MS methods to quantify a number of DNA modifications in mammalian cells and to examine their repair.

In Chapter 2, we employed nLC-nESI-MS/MS coupled with isotope-dilution method to quantify simultaneously three pyridylhydroxybutyl (PHB) adducts induced by tobacco-specific nitrosamine 4-(methylnitrosamino)-1-(3-pyridyl)-1-butanol (NNAL). Of

which, O^4-[4-(3-pyridyl)-4-hydroxylbut-1-yl]-thymidine (O^4-PHBdT) was discovered, for the first time, in mammalian genome upon NNAL exposure. The newly discovered O^4-PHBdT, as well as O^2-PHBdT and O^6-PHBdG, was found to display dose-dependent formation both *in vivo* and *in vitro*. In addition, NER was shown to be involved in the removal of O^2-PHBdT and O^4-PHBdT, while direct reversal suicide protein MGMT may counteract the formation of O^6-PHBdG and O^4-PHBdT.

In Chapter 3, we employed metabolic labeling to selectively incorporate N^2-methyl-dG (N^2-MedG) and N^2-*n*-butyl-dG (N^2-*n*BudG) into genomic DNA of cultured cells, and investigated how the levels of the two lesions in cellular DNA are modulated by different DNA repair factors. It was found that NER exerts moderate effects on the removal of N^2-MedG and N^2-*n*BudG from genomic DNA. Translesion synthesis (TLS) polymerases κ and η may contribute to the incorporation of N^2-alkyl-dG into genomic DNA. Pol κ was found to be involved in the repair of both N^2-MedG and N^2-*n*BudG; while Pol η was responsible for the repair of less bulky N^2-MedG, but not N^2-*n*BudG. In addition, loss of ALKBH3 resulted in higher frequencies of N^2-MedG and N^2-*n*BudG incorporation into genomic DNA, suggesting a role of oxidative dealkylation in the reversal of these lesions.

In Chapter 4, we extended the metabolic labeling approach to accommodate genomic incorporation of 2-amino-2'-deoxyadenosine (dZ) and investigated its plausible repair mechanism. Z is a naturally occurring non-canonical nucleobase that has been found in bacteriophages in substitution of adenine (A). We found, for the first time, that dZ could be incorporated into genomic DNA in mammalian cells, and TLS polymerases ι

and REV1 may contribute to the incorporation. In addition, TC-NER, but not GG-NER, participates in the reversal of dZ from human genome.

References

(1) Friedberg, E. C.; Walker, G. C.; Siede, W.; Wood, R. D. *DNA Repair and Mutagenesis*; American Society for Microbiology Press, 2005.

(2) Lindahl, T. Instability and Decay of the Primary Structure of DNA. *Nature* **1993**, *362* (6422), 709–715. https://doi.org/10.1038/362709a0.

(3) Chatterjee, N.; Walker, G. C. Mechanisms of DNA Damage, Repair, and Mutagenesis. *Environ. Mol. Mutagen.* **2017**, *58* (5), 235–263. https://doi.org/10.1002/em.22087.

(4) Lindahl, T.; Wood, R. D. Quality Control by DNA Repair. *Science* **1999**, *286* (5446), 1897–1905. https://doi.org/10.1126/science.286.5446.1897.

(5) Bauer, N. C.; Corbett, A. H.; Doetsch, P. W. The Current State of Eukaryotic DNA Base Damage and Repair. *Nucleic Acids Res.* **2015**, *43* (21), 10083–10101. https://doi.org/10.1093/nar/gkv1136.

(6) Schärer, O. D. Chemistry and Biology of DNA Repair. *Angew. Chem. Int. Ed Engl.* **2003**, *42* (26), 2946–2974. https://doi.org/10.1002/anie.200200523.

(7) Fu, D.; Calvo, J. A.; Samson, L. D. Balancing Repair and Tolerance of DNA Damage Caused by Alkylating Agents. *Nat. Rev. Cancer* **2012**, *12* (2), 104–120. https://doi.org/10.1038/nrc3185.

(8) Liu, S.; Wang, Y. Mass Spectrometry for the Assessment of the Occurrence and Biological Consequences of DNA Adducts. *Chem. Soc. Rev.* **2015**, *44* (21), 7829–7854. https://doi.org/10.1039/C5CS00316D.

(9) You, C.; Dai, X.; Yuan, B.; Wang, J.; Wang, J.; Brooks, P. J.; Niedernhofer, L. J.; Wang, Y. A Quantitative Assay for Assessing the Effects of DNA Lesions on Transcription. *Nat. Chem. Biol.* **2012**, *8* (10), 817–822. https://doi.org/10.1038/nchembio.1046.

(10) Hoeijmakers, J. H. Genome Maintenance Mechanisms for Preventing Cancer. *Nature* **2001**, *411* (6835), 366–374. https://doi.org/10.1038/35077232.

(11) Friedberg, E. C.; Aguilera, A.; Gellert, M.; Hanawalt, P. C.; Hays, J. B.; Lehmann, A. R.; Lindahl, T.; Lowndes, N.; Sarasin, A.; Wood, R. D. DNA Repair: From Molecular Mechanism to Human Disease. *DNA Repair* **2006**, *5* (8), 986–996. https://doi.org/10.1016/j.dnarep.2006.05.005.

(12) Hwa Yun, B.; Guo, J.; Bellamri, M.; Turesky, R. J. DNA Adducts: Formation, Biological Effects, and New Biospecimens for Mass Spectrometric Measurements in Humans. *Mass Spectrom. Rev.* **2020**, *39* (1–2), 55–82. https://doi.org/10.1002/mas.21570.

(13) Yu, Y.; Cui, Y.; Niedernhofer, L. J.; Wang, Y. Occurrence, Biological Consequences, and Human Health Relevance of Oxidative Stress-Induced DNA Damage. *Chem. Res. Toxicol.* **2016**, *29* (12), 2008–2039. https://doi.org/10.1021/acs.chemrestox.6b00265.

(14) Randerath, K.; Reddy, M. V.; Gupta, R. C. 32P-Labeling Test for DNA Damage. *Proc. Natl. Acad. Sci.* **1981**, *78* (10), 6126–6129. https://doi.org/10.1073/pnas.78.10.6126.

(15) Hsu, I. C.; Poirier, M. C.; Yuspa, S. H.; Grunberger, D.; Weinstein, I. B.; Yolken, R. H.; Harris, C. C. Measurement of Benzo(a)Pyrene-DNA Adducts by Enzyme Immunoassays and Radioimmunoassay. *Cancer Res.* **1981**, *41* (3), 1091–1095.

(16) Boysen, G.; Nookaew, I. Current and Future Methodology for Quantitation and Site-Specific Mapping the Location of DNA Adducts. *Toxics* **2022**, *10* (2), 45. https://doi.org/10.3390/toxics10020045.

(17) Yang, Y.; Wang, Z.; Wang, J.; Dai, X.; You, C. Next-Generation Sequencing-Based Analysis of the Effects of N1- and N6-Methyldeoxyadenosine Adducts on DNA Transcription. *Anal. Chem.* **2022**, *94* (32), 11248–11254. https://doi.org/10.1021/acs.analchem.2c01764.

(18) Tang, F.; Liu, S.; Li, Q.-Y.; Yuan, J.; Li, L.; Wang, Y.; Yuan, B.-F.; Feng, Y.-Q. Location Analysis of 8-Oxo-7,8-Dihydroguanine in DNA by Polymerase-Mediated Differential Coding. *Chem. Sci.* **2019**, *10* (15), 4272–4281. https://doi.org/10.1039/c8sc04946g.

(19) Tretyakova, N.; Villalta, P. W.; Kotapati, S. Mass Spectrometry of Structurally Modified DNA. *Chem. Rev.* **2013**, *113* (4), 2395–2436. https://doi.org/10.1021/cr300391r.

(20) Tretyakova, N.; Goggin, M.; Sangaraju, D.; Janis, G. Quantitation of DNA Adducts by Stable Isotope Dilution Mass Spectrometry. *Chem. Res. Toxicol.* **2012**, *25* (10), 2007–2035. https://doi.org/10.1021/tx3002548.

(21) Yu, Y.; Wang, P.; Cui, Y.; Wang, Y. Chemical Analysis of DNA Damage. *Anal. Chem.* **2018**, *90* (1), 556–576. https://doi.org/10.1021/acs.analchem.7b04247.

(22) Wang, J.; Yuan, B.; Guerrero, C.; Bahde, R.; Gupta, S.; Wang, Y. Quantification of Oxidative DNA Lesions in Tissues of Long-Evans Cinnamon Rats by Capillary High-Performance Liquid Chromatography-Tandem Mass Spectrometry Coupled with Stable Isotope-Dilution Method. *Anal. Chem.* **2011**, *83* (6), 2201–2209. https://doi.org/10.1021/ac103099s.

(23) Leng, J.; Wang, Y. Liquid Chromatography-Tandem Mass Spectrometry for the Quantification of Tobacco-Specific Nitrosamine-Induced DNA Adducts in Mammalian Cells. *Anal. Chem.* **2017**, *89* (17), 9124–9130. https://doi.org/10.1021/acs.analchem.7b01857.

(24) Xiao, S.; Guo, J.; Yun, B. H.; Villalta, P. W.; Krishna, S.; Tejpaul, R.; Murugan, P.; Weight, C. J.; Turesky, R. J. Biomonitoring DNA Adducts of Cooked Meat Carcinogens in Human Prostate by Nano Liquid Chromatography-High Resolution Tandem Mass Spectrometry: Identification of 2-Amino-1-Methyl-6-Phenylimidazo[4,5-b]Pyridine DNA Adduct. *Anal. Chem.* **2016**, *88* (24), 12508–12515. https://doi.org/10.1021/acs.analchem.6b04157.

(25) Liu, S.; Wang, Y. A Quantitative Mass Spectrometry-Based Approach for Assessing the Repair of 8-Methoxypsoralen-Induced DNA Interstrand Cross-Links and Monoadducts in Mammalian Cells. *Anal. Chem.* **2013**, *85* (14), 6732–6739. https://doi.org/10.1021/ac4012232.

(26) Cui, Y.; Wang, P.; Yu, Y.; Yuan, J.; Wang, Y. Normalized Retention Time for Targeted Analysis of the DNA Adductome. *Anal. Chem.* **2018**, *90* (24), 14111–14115. https://doi.org/10.1021/acs.analchem.8b04660.

(27) Ma, B.; Villalta, P. W.; Zarth, A. T.; Kotandeniya, D.; Upadhyaya, P.; Stepanov, I.; Hecht, S. S. Comprehensive High-Resolution Mass Spectrometric Analysis of DNA Phosphate Adducts Formed by the Tobacco-Specific Lung Carcinogen 4-(Methylnitrosamino)-1-(3-Pyridyl)-1-Butanone. *Chem. Res. Toxicol.* **2015**, *28* (11), 2151–2159. https://doi.org/10.1021/acs.chemrestox.5b00318.

(28) Pfeifer, G. P.; Denissenko, M. F.; Olivier, M.; Tretyakova, N.; Hecht, S. S.; Hainaut, P. Tobacco Smoke Carcinogens, DNA Damage and P53 Mutations in Smoking-Associated Cancers. *Oncogene* **2002**, *21* (48), 7435–7451. https://doi.org/10.1038/sj.onc.1205803.

(29) Burcham, P. C. Genotoxic Lipid Peroxidation Products: Their DNA Damaging Properties and Role in Formation of Endogenous DNA Adducts. *Mutagenesis* **1998**, *13* (3), 287–305. https://doi.org/10.1093/mutage/13.3.287.

(30) Yuan, B.-F. Assessment of DNA Epigenetic Modifications. *Chem. Res. Toxicol.* **2020**, *33* (3), 695–708. https://doi.org/10.1021/acs.chemrestox.9b00372.

(31) Ma, B.; Zarth, A. T.; Carlson, E. S.; Villalta, P. W.; Upadhyaya, P.; Stepanov, I.; Hecht, S. S. Identification of More than 100 Structurally Unique DNA-Phosphate Adducts Formed during Rat Lung Carcinogenesis by the Tobacco-Specific Nitrosamine 4-(Methylnitrosamino)-1-(3-Pyridyl)-1-Butanone. *Carcinogenesis* **2018**, *39* (2), 232–241. https://doi.org/10.1093/carcin/bgx135.

(32) Jones, G. D. D.; Le Pla, R. C.; Farmer, P. B. Phosphotriester Adducts (PTEs): DNA's Overlooked Lesion. *Mutagenesis* **2010**, *25* (1), 3–16. https://doi.org/10.1093/mutage/gep038.

(33) Marnett, L. J. Oxyradicals and DNA Damage. *Carcinogenesis* **2000**, *21* (3), 361–370. https://doi.org/10.1093/carcin/21.3.361.

(34) Du, H.; Wang, P.; Li, L.; Amato, N. J.; Wang, Y. Cytotoxic and Mutagenic Properties of C1′ and C3′-Epimeric Lesions of 2′-Deoxyribonucleosides in Human Cells. *ACS Chem. Biol.* **2019**, *14* (3), 478–485. https://doi.org/10.1021/acschembio.8b01126.

(35) Hecht, S. S. DNA Adduct Formation from Tobacco-Specific N-Nitrosamines. *Mutat. Res. Mol. Mech. Mutagen.* **1999**, *424* (1), 127–142. https://doi.org/10.1016/S0027-5107(99)00014-7.

(36) Hecht, S. S. Tobacco Carcinogens, Their Biomarkers and Tobacco-Induced Cancer. *Nat. Rev. Cancer* **2003**, *3* (10), 733–744. https://doi.org/10.1038/nrc1190.

(37) Hecht, S. S.; DeMarini, D. M. Tobacco Smoke and Its Constituents. In *Tumour Site Concordance and Mechanisms of Carcinogenesis*; Baan, R. A., Stewart, B. W., Straif, K., Eds.; IARC Scientific Publications; International Agency for Research on Cancer: Lyon (FR), 2019.

(38) Hecht, S. S. Lung Carcinogenesis by Tobacco Smoke. *Int. J. Cancer* **2012**, *131* (12), 2724–2732. https://doi.org/10.1002/ijc.27816.

(39) Li, Y.; Hecht, S. S. Metabolism and DNA Adduct Formation of Tobacco-Specific N-Nitrosamines. *Int. J. Mol. Sci.* **2022**, *23* (9), 5109. https://doi.org/10.3390/ijms23095109.

(40) Du, H.; Leng, J.; Wang, P.; Li, L.; Wang, Y. Impact of Tobacco-Specific Nitrosamine-Derived DNA Adducts on the Efficiency and Fidelity of DNA Replication in Human Cells. *J. Biol. Chem.* **2018**, *293* (28), 11100–11108. https://doi.org/10.1074/jbc.RA118.003477.

(41) Hecht, S. S.; Carmella, S. G.; Foiles, P. G.; Murphy, S. E. Biomarkers for Human Uptake and Metabolic Activation of Tobacco-Specific Nitrosamines. *Cancer Res.* **1994**, *54* (7 Suppl), 1912s–1917s.

(42) Hecht, S. S.; Stepanov, I.; Carmella, S. G. Exposure and Metabolic Activation Biomarkers of Carcinogenic Tobacco-Specific Nitrosamines. *Acc. Chem. Res.* **2016**, *49* (1), 106–114. https://doi.org/10.1021/acs.accounts.5b00472.

(43) Ma, B.; Zarth, A. T.; Carlson, E. S.; Villalta, P. W.; Stepanov, I.; Hecht, S. S. Pyridylhydroxybutyl and Pyridyloxobutyl DNA Phosphate Adduct Formation in Rats Treated Chronically with Enantiomers of the Tobacco-Specific Nitrosamine Metabolite 4-(Methylnitrosamino)-1-(3-Pyridyl)-1-Butanol. *Mutagenesis* **2017**, *32* (6), 561–570. https://doi.org/10.1093/mutage/gex031.

(44) Ma, B.; Stepanov, I.; Hecht, S. S. Recent Studies on DNA Adducts Resulting from Human Exposure to Tobacco Smoke. *Toxics* **2019**, *7* (1), E16. https://doi.org/10.3390/toxics7010016.

(45) Mulderrig, L.; Garaycoechea, J. I.; Tuong, Z. K.; Millington, C. L.; Dingler, F. A.; Ferdinand, J. R.; Gaul, L.; Tadross, J. A.; Arends, M. J.; O'Rahilly, S.; Crossan, G. P.; Clatworthy, M. R.; Patel, K. J. Aldehyde-Driven Transcriptional Stress Triggers an Anorexic DNA Damage Response. *Nature* **2021**, *600* (7887), 158–163. https://doi.org/10.1038/s41586-021-04133-7.

(46) Cheng, G.; Shi, Y.; Sturla, S. J.; Jalas, J. R.; McIntee, E. J.; Villalta, P. W.; Wang, M.; Hecht, S. S. Reactions of Formaldehyde Plus Acetaldehyde with Deoxyguanosine and DNA: Formation of Cyclic Deoxyguanosine Adducts and Formaldehyde Cross-Links. *Chem. Res. Toxicol.* **2003**, *16* (2), 145–152. https://doi.org/10.1021/tx025614r.

(47) Zhang, Y.; Wu, X.; Guo, D.; Rechkoblit, O.; Geacintov, N. E.; Wang, Z. Two-Step Error-Prone Bypass of the (+)- and (-)-Trans-Anti-BPDE-N2-DG Adducts by Human DNA Polymerases Eta and Kappa. *Mutat. Res.* **2002**, *510* (1–2), 23–35. https://doi.org/10.1016/s0027-5107(02)00249-x.

(48) Gillet, L. C. J.; Schärer, O. D. Molecular Mechanisms of Mammalian Global Genome Nucleotide Excision Repair. *Chem. Rev.* **2006**, *106* (2), 253–276. https://doi.org/10.1021/cr040483f.

(49) Matsuda, T.; Yabushita, H.; Kanaly, R. A.; Shibutani, S.; Yokoyama, A. Increased DNA Damage in ALDH2-Deficient Alcoholics. *Chem. Res. Toxicol.* **2006**, *19* (10), 1374–1378. https://doi.org/10.1021/tx060113h.

(50) Fang, J. L.; Vaca, C. E. Detection of DNA Adducts of Acetaldehyde in Peripheral White Blood Cells of Alcohol Abusers. *Carcinogenesis* **1997**, *18* (4), 627–632. https://doi.org/10.1093/carcin/18.4.627.

(51) Kirnos, M. D.; Khudyakov, I. Y.; Alexandrushkina, N. I.; Vanyushin, B. F. 2-Aminoadenine Is an Adenine Substituting for a Base in S-2L Cyanophage DNA. *Nature* **1977**, *270* (5635), 369–370. https://doi.org/10.1038/270369a0.

(52) Zhou, Y.; Xu, X.; Wei, Y.; Cheng, Y.; Guo, Y.; Khudyakov, I.; Liu, F.; He, P.; Song, Z.; Li, Z.; Gao, Y.; Ang, E. L.; Zhao, H.; Zhang, Y.; Zhao, S. A Widespread Pathway for Substitution of Adenine by Diaminopurine in Phage Genomes. *Science* **2021**, *372* (6541), 512–516. https://doi.org/10.1126/science.abe4882.

(53) Szekeres, M.; Matveyev, A. V. Cleavage and Sequence Recognition of 2,6-Diaminopurine-Containing DNA by Site-Specific Endonucleases. *FEBS Lett.* **1987**, *222* (1), 89–94. https://doi.org/10.1016/0014-5793(87)80197-7.

(54) Czernecki, D.; Bonhomme, F.; Kaminski, P.-A.; Delarue, M. Characterization of a Triad of Genes in Cyanophage S-2L Sufficient to Replace Adenine by 2-Aminoadenine in Bacterial DNA. *Nat. Commun.* **2021**, *12* (1), 4710. https://doi.org/10.1038/s41467-021-25064-x.

(55) Tan, Y.; You, C.; Park, J.; Kim, H. S.; Guo, S.; Schärer, O. D.; Wang, Y. Transcriptional Perturbations of 2,6-Diaminopurine and 2-Aminopurine. *ACS Chem. Biol.* **2022**. https://doi.org/10.1021/acschembio.2c00369.

(56) Mishina, Y.; Yang, C.-G.; He, C. Direct Repair of the Exocyclic DNA Adduct 1,N6-Ethenoadenine by the DNA Repair AlkB Proteins. *J. Am. Chem. Soc.* **2005**, *127* (42), 14594–14595. https://doi.org/10.1021/ja055957m.

(57) Perry, G. S.; Das, M.; Woon, E. C. Y. Inhibition of AlkB Nucleic Acid Demethylases: Promising New Epigenetic Targets. *J. Med. Chem.* **2021**, *64* (23), 16974–17003. https://doi.org/10.1021/acs.jmedchem.1c01694.

(58) Albertella, M. R.; Green, C. M.; Lehmann, A. R.; O'Connor, M. J. A Role for Polymerase Eta in the Cellular Tolerance to Cisplatin-Induced Damage. *Cancer Res.* **2005**, *65* (21), 9799–9806. https://doi.org/10.1158/0008-5472.CAN-05-1095.

(59) Ogi, T.; Lehmann, A. R. The Y-Family DNA Polymerase Kappa (Pol Kappa) Functions in Mammalian Nucleotide-Excision Repair. *Nat. Cell Biol.* **2006**, *8* (6), 640–642. https://doi.org/10.1038/ncb1417.

(60) Mishina, Y.; Duguid, E. M.; He, C. Direct Reversal of DNA Alkylation Damage. *Chem. Rev.* **2006**, *106* (2), 215–232. https://doi.org/10.1021/cr0404702.

(61) Kaina, B.; Christmann, M.; Naumann, S.; Roos, W. P. MGMT: Key Node in the Battle against Genotoxicity, Carcinogenicity and Apoptosis Induced by Alkylating Agents. *DNA Repair* **2007**, *6* (8), 1079–1099. https://doi.org/10.1016/j.dnarep.2007.03.008.

(62) Du, H.; Wang, P.; Li, L.; Wang, Y. Repair and Translesion Synthesis of O6-Alkylguanine DNA Lesions in Human Cells. *J. Biol. Chem.* **2019**, *294* (29), 11144–11153. https://doi.org/10.1074/jbc.RA119.009054.

(63) Fedeles, B. I.; Singh, V.; Delaney, J. C.; Li, D.; Essigmann, J. M. The AlkB Family of Fe(II)/α-Ketoglutarate-Dependent Dioxygenases: Repairing Nucleic Acid Alkylation Damage and Beyond. *J. Biol. Chem.* **2015**, *290* (34), 20734–20742. https://doi.org/10.1074/jbc.R115.656462.

(64) Samson, L.; Cairns, J. A New Pathway for DNA Repair in Escherichia Coli. *Nature* **1977**, *267* (5608), 281–283. https://doi.org/10.1038/267281a0.

(65) Sedgwick, B.; Bates, P. A.; Paik, J.; Jacobs, S. C.; Lindahl, T. Repair of Alkylated DNA: Recent Advances. *DNA Repair* **2007**, *6* (4), 429–442. https://doi.org/10.1016/j.dnarep.2006.10.005.

(66) Yi, C.; He, C. DNA Repair by Reversal of DNA Damage. *Cold Spring Harb. Perspect. Biol.* **2013**, *5* (1), a012575. https://doi.org/10.1101/cshperspect.a012575.

(67) Bian, K.; Lenz, S. A. P.; Tang, Q.; Chen, F.; Qi, R.; Jost, M.; Drennan, C. L.; Essigmann, J. M.; Wetmore, S. D.; Li, D. DNA Repair Enzymes ALKBH2, ALKBH3, and AlkB Oxidize 5-Methylcytosine to 5-Hydroxymethylcytosine, 5-Formylcytosine and 5-Carboxylcytosine in Vitro. *Nucleic Acids Res.* **2019**, *47* (11), 5522–5529. https://doi.org/10.1093/nar/gkz395.

(68) Jia, G.; Yang, C.-G.; Yang, S.; Jian, X.; Yi, C.; Zhou, Z.; He, C. Oxidative Demethylation of 3-Methylthymine and 3-Methyluracil in Single-Stranded DNA and

RNA by Mouse and Human FTO. *FEBS Lett.* **2008**, *582* (23–24), 3313–3319. https://doi.org/10.1016/j.febslet.2008.08.019.

(69) Truglio, J. J.; Croteau, D. L.; Van Houten, B.; Kisker, C. Prokaryotic Nucleotide Excision Repair: The UvrABC System. *Chem. Rev.* **2006**, *106* (2), 233–252. https://doi.org/10.1021/cr040471u.

(70) Hess, M. T.; Gunz, D.; Luneva, N.; Geacintov, N. E.; Naegeli, H. Base Pair Conformation-Dependent Excision of Benzo[a]Pyrene Diol Epoxide-Guanine Adducts by Human Nucleotide Excision Repair Enzymes. *Mol. Cell. Biol.* **1997**, *17* (12), 7069–7076. https://doi.org/10.1128/MCB.17.12.7069.

(71) Kitsera, N.; Rodriguez-Alvarez, M.; Emmert, S.; Carell, T.; Khobta, A. Nucleotide Excision Repair of Abasic DNA Lesions. *Nucleic Acids Res.* **2019**, *47* (16), 8537–8547. https://doi.org/10.1093/nar/gkz558.

(72) Friedberg, E. C. The Discovery That Xeroderma Pigmentosum (XP) Results from Defective Nucleotide Excision Repair. *DNA Repair* **2004**, *3* (2), 183, 195.

(73) de Boer, J.; Hoeijmakers, J. H. J. Nucleotide Excision Repair and Human Syndromes. *Carcinogenesis* **2000**, *21* (3), 453–460. https://doi.org/10.1093/carcin/21.3.453.

(74) Marteijn, J. A.; Lans, H.; Vermeulen, W.; Hoeijmakers, J. H. J. Understanding Nucleotide Excision Repair and Its Roles in Cancer and Ageing. *Nat. Rev. Mol. Cell Biol.* **2014**, *15* (7), 465–481. https://doi.org/10.1038/nrm3822.

(75) Schärer, O. D. Nucleotide Excision Repair in Eukaryotes. *Cold Spring Harb. Perspect. Biol.* **2013**, *5* (10), a012609. https://doi.org/10.1101/cshperspect.a012609.

(76) Aboussekhra, A.; Biggerstaff, M.; Shivji, M. K.; Vilpo, J. A.; Moncollin, V.; Podust, V. N.; Protić, M.; Hübscher, U.; Egly, J. M.; Wood, R. D. Mammalian DNA Nucleotide Excision Repair Reconstituted with Purified Protein Components. *Cell* **1995**, *80* (6), 859–868. https://doi.org/10.1016/0092-8674(95)90289-9.

(77) Li, L.; Elledge, S. J.; Peterson, C. A.; Bales, E. S.; Legerski, R. J. Specific Association between the Human DNA Repair Proteins XPA and ERCC1. *Proc. Natl. Acad. Sci. U. S. A.* **1994**, *91* (11), 5012–5016. https://doi.org/10.1073/pnas.91.11.5012.

(78) Sugasawa, K. Mechanism and Regulation of DNA Damage Recognition in Mammalian Nucleotide Excision Repair. *The Enzymes* **2019**, *45*, 99–138. https://doi.org/10.1016/bs.enz.2019.06.004.

(79) Yan, C.; Dodd, T.; Yu, J.; Leung, B.; Xu, J.; Oh, J.; Wang, D.; Ivanov, I. Mechanism of Rad26-Assisted Rescue of Stalled RNA Polymerase II in Transcription-Coupled Repair. *Nat. Commun.* **2021**, *12* (1), 7001. https://doi.org/10.1038/s41467-021-27295-4.

(80) Sugasawa, K. Mechanism and Regulation of DNA Damage Recognition in Mammalian Nucleotide Excision Repair. *The Enzymes* **2019**, *45*, 99–138. https://doi.org/10.1016/bs.enz.2019.06.004.

(81) Makridakis, N.; Reichardt, J. Translesion DNA Polymerases and Cancer. *Front. Genet.* **2012**, *3*.

(82) Goodman, M. F.; Woodgate, R. Translesion DNA Polymerases. *Cold Spring Harb. Perspect. Biol.* **2013**, *5* (10), a010363. https://doi.org/10.1101/cshperspect.a010363.

(83) Johnson, R. E.; Washington, M. T.; Haracska, L.; Prakash, S.; Prakash, L. Eukaryotic Polymerases Iota and Zeta Act Sequentially to Bypass DNA Lesions. *Nature* **2000**, *406* (6799), 1015–1019. https://doi.org/10.1038/35023030.

(84) Su, Y.; Ghodke, P. P.; Egli, M.; Li, L.; Wang, Y.; Guengerich, F. P. Human DNA Polymerase η Has Reverse Transcriptase Activity in Cellular Environments. *J. Biol. Chem.* **2019**, *294* (15), 6073–6081. https://doi.org/10.1074/jbc.RA119.007925.

(85) Wu, J.; Du, H.; Li, L.; Price, N. E.; Liu, X.; Wang, Y. The Impact of Minor-Groove N2-Alkyl-2′-Deoxyguanosine Lesions on DNA Replication in Human Cells. *ACS Chem. Biol.* **2019**, *14* (8), 1708–1716. https://doi.org/10.1021/acschembio.9b00129.

(86) Wu, J.; Li, L.; Wang, P.; You, C.; Williams, N. L.; Wang, Y. Translesion Synthesis of O4-Alkylthymidine Lesions in Human Cells. *Nucleic Acids Res.* **2016**, *44* (19), 9256–9265. https://doi.org/10.1093/nar/gkw662.

(87) Tan, Y.; Guo, S.; Wu, J.; Du, H.; Li, L.; You, C.; Wang, Y. DNA Polymerase η Promotes the Transcriptional Bypass of N2-Alkyl-2'-Deoxyguanosine Adducts in Human Cells. *J. Am. Chem. Soc.* **2021**, *143* (39), 16197–16205. https://doi.org/10.1021/jacs.1c07374.

(88) Hong, H.; Wang, Y. Formation of Intrastrand Cross-Link Products between Cytosine and Adenine from UV Irradiation of d((Br)CA) and Duplex DNA Containing a 5-Bromocytosine. *J. Am. Chem. Soc.* **2005**, *127* (40), 13969–13977. https://doi.org/10.1021/ja0531677.

(89) Price, N. E.; Catalano, M. J.; Liu, S.; Wang, Y.; Gates, K. S. Chemical and Structural Characterization of Interstrand Cross-Links Formed between Abasic Sites and Adenine Residues in Duplex DNA. *Nucleic Acids Res.* **2015**, *43* (7), 3434–3441. https://doi.org/10.1093/nar/gkv174.

(90) Rozelle, A. L.; Cheun, Y.; Vilas, C. K.; Koag, M.-C.; Lee, S. DNA Interstrand Cross-Links Induced by the Major Oxidative Adenine Lesion 7,8-Dihydro-8-Oxoadenine. *Nat. Commun.* **2021**, *12* (1), 1897. https://doi.org/10.1038/s41467-021-22273-2.

(91) Karas, M.; Bahr, U.; Dülcks, T. Nano-Electrospray Ionization Mass Spectrometry: Addressing Analytical Problems beyond Routine. *Fresenius J. Anal. Chem.* **2000**, *366* (6–7), 669–676. https://doi.org/10.1007/s002160051561.

(92) Becker, J. S.; Jakubowski, N. The Synergy of Elemental and Biomolecular Mass Spectrometry: New Analytical Strategies in Life Sciences. *Chem. Soc. Rev.* **2009**, *38* (7), 1969–1983. https://doi.org/10.1039/b618635c.

(93) Zhou, W.; Yang, S.; Wang, P. G. Matrix Effects and Application of Matrix Effect Factor. *Bioanalysis* **2017**, *9* (23), 1839–1844. https://doi.org/10.4155/bio-2017-0214.

(94) Trufelli, H.; Palma, P.; Famiglini, G.; Cappiello, A. An Overview of Matrix Effects in Liquid Chromatography–Mass Spectrometry. *Mass Spectrom. Rev.* **2011**, *30* (3), 491–509. https://doi.org/10.1002/mas.20298.

(95) Kumar, D.; Gautam, N.; Alnouti, Y. Analyte Recovery in LC-MS/MS Bioanalysis: An Old Issue Revisited. *Anal. Chim. Acta* **2022**, *1198*, 339512. https://doi.org/10.1016/j.aca.2022.339512.

(96) Yu, Y.; Wang, J.; Wang, P.; Wang, Y. Quantification of Azaserine-Induced Carboxymethylated and Methylated DNA Lesions in Cells by Nanoflow Liquid Chromatography-Nanoelectrospray Ionization Tandem Mass Spectrometry Coupled with the Stable Isotope-Dilution Method. *Anal. Chem.* **2016**, *88* (16), 8036–8042. https://doi.org/10.1021/acs.analchem.6b01349.

Chapter 2 Quantification of DNA Lesions induced by 4-(methylnitrosamino)-1-(3-pyridyl)-1-butanol in Mammalian Cells

2.1. Introduction

The human genome is susceptible to damage by endogenous metabolites and exogenous chemicals.[1, 2] The resulting DNA damage leads to perturbations of genomic stability, which may give rise to mutagenesis and other adverse biological consequences.[3] Tobacco-specific nitrosamines may contribute to human cancer, and they are associated with the elevated lung cancer rate in the cohorts of active tobacco users in several epidemiology studies.[4-6] 4-(methylnitrosamino)-1-(3-pyridyl)-1-butanone (NNK), a major tobacco-specific nitrosamine, and its reduced metabolite 4-(methylnitrosamino)-1-(3-pyridyl)-1-butanol (NNAL) have been found to induce cancer in rodents in pioneering studies by Hecht and co-workers.[7-9] The carcinogenic effects of NNK and NNAL reside on their abilities in inducing the formation of adducts on nucleobases and on DNA backbone, which may result in compromised replication that gives rise to mutations in DNA.[10, 11]

Some earlier studies by Hecht and others demonstrated subsets of cytochrome P450 enzymes participated in activation of NNK and NNAL,[11-14] which as a result gives rise to reactive intermediates that can pyridyloxobutylate and pyridylhydroxybutylate DNA, respectively. There are a number of studies reporting the presence of DNA lesions in mammalian genome due to pyridyloxobutylation and pyridylhydroxybutylation. The resulting modifications include O^2-POBdT,[15-17] O^4-POBdT,[18] O^6-POBdG,[15, 17, 19] O^2-PHBdT,[15] O^6-PHBdG,[15, 17] O^2-POBdC,[17] 7-POBG,[15, 17] 7-PHBG,[15] N^6-POBdA,[20] N^6-

PHBdA,[20] *N*1-POBdI[20] and *N*1-PHBdI[20] on nucleobases and $B_1p(POB)B_2$[21-23] and $B_1p(PHB)B_2$ [21-23] on phosphate backbone, identified *in vivo*. Most lesions mentioned above exhibited cytotoxic and mutagenic properties, which, if not properly repaired, may compromise the transmission of genetic information by disrupting DNA replication and transcription machineries. Du et al.,[24] in a recent publication, demonstrated that O^2-POBdT and O^4-POBdT could moderately block DNA replication, which elicited T→A transversion and T→C transition, respectively, whereas G→A transition was the major type of mutation induced by O^6-POBdG. The activated form of NNK and NNAL may also serve as a potent methylating agent. The resulting level of O^6-methylguanine (O^6-mG) following exposure of NNK showed a coherent relationship with tumorgenicity.[19, 25] Ma et al.[26] also demonstrated recently that B_1pmeB_2 can be induced *in vivo* upon exposure to NNK and NNAL.

Cells are equipped with a complex arsenal of DNA repair proteins to remove the deleterious DNA lesions.[1, 2, 27] In this vein, various classes of mammalian DNA repair proteins capable of removing pyridyloxobutylated and pyridylhydroxybutylated DNA-modifications. O^6-alkylguanine-DNA alkyltransferase (AGT) was found capable of removing directly the POB remnant from O^6-POBdG.[17, 19, 28] There are also studies revealing that O^2-POBdT contributes to the elevated occurrence of AT→TA mutation in nucleotide excision repair (NER)-deficient cells, suggesting the involvement of NER in removing this lesion.[28]

Although the implications of tobacco-specific nitrosamines in carcinogenesis have been well documented,[14, 29, 30] there is still gaps to be filled in establishing reliable

quantification methods to meet the increasing demands for the risk assessment of consumption of tobacco products. In this respect, efforts have been made to develop methods including ^{32}P-postlaeling assay, excision assay and immunoblot analysis for measuring the levels and assessing the repair process of targeted DNA lesions *in vitro* and *in vivo*.[31, 32] Due to its sensitivity and its capacity in providing structural information,[18, 33-41] mass spectrometry has become a tool of choice for DNA adduct analysis. Attempts have been made to use LC-MS/MS in combination with solid-phase extraction to quantify several pyridyloxobutyl and pyridylhydroxybutyl DNA lesions. [17, 21, 23, 26, 28]

Herein, we developed a highly sensitive nanoflow liquid chromatography-nanoelectrospray ionization tandem mass spectrometry (nLC-nESI-MS/MS) coupled with the stable isotope-dilution method for the simultaneous measurements of O^4-PHBdT, O^2-PHBdT, and O^6-PHBdG, where O^4-PHBdT was identified here for the first time (**Scheme 2.1.**). By employing this method, we further explored the repair of the three lesions in cultured mammalian cells.

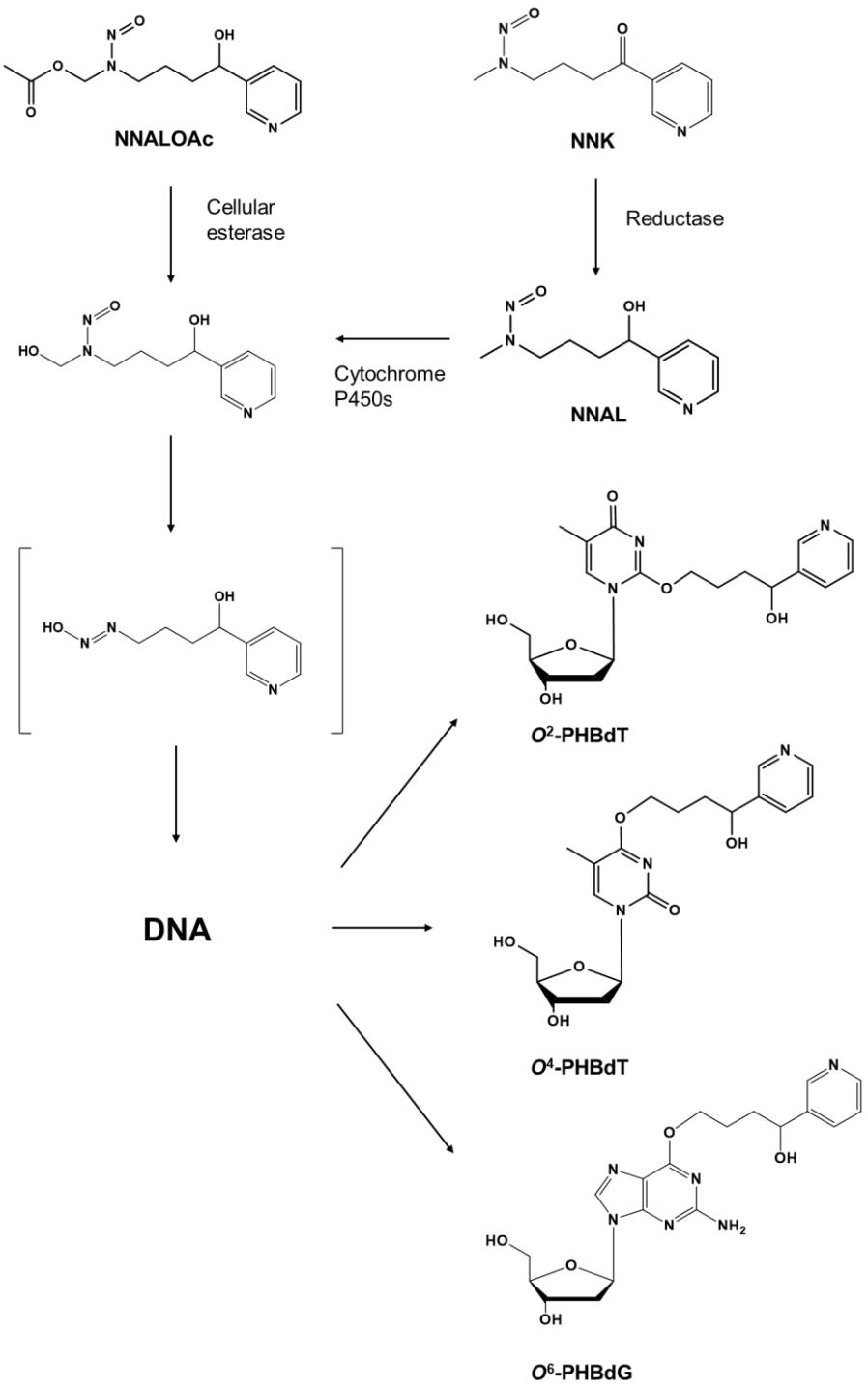

Scheme 2.1. Activation of NNALOAc by cellular esterase and the metabolic activation of NNAL/ NNK by cytochrome P450 enzymes; followed by the reaction of their shared intermediate with DNA which yields the product lesions: O4-PHBdT, O2-PHBdT, and O6-PHBdG.

2.2. Experimental sections

2.2.1. Materials

Unless otherwise noted, all chemicals were obtained from Sigma-Aldrich (St. Louis, MO) and enzymes were obtained from New England Biolabs (Ipswich, WA). NNALOAc was obtained by the reduction of NNKOAc (Toronto Research Chemicals Inc., North York, Ontario) using $NaBH_4$. The reaction was carried out under a condition where NNKOAc (10 mg) was mixed with 5 equivalents of $NaBH_4$ in methanol at room temperature for 30 min, and the product NNALOAc was then isolated from the reaction mixture using HPLC. Stable isotope-labeled compounds were purchased from Cambridge Isotope Laboratories (Cambridge, MA). *Erythro*-9-(2-hydroxy-3-nonyl)adenine (EHNA) hydrochloride was purchased from Tocris Bioscience (Ellisville, MO). Repair-competent AA8 Chinese hamster ovary (CHO) cells and the isogenic CHO cells depleted of excision repair cross-complementing rodent repair deficiency, complementation group 1 (ERCC1, CHO-7-27)[42] were provided by M. M. Seidman (National Institute of Aging, Bethesda, MD). Human skin fibroblasts that are repair-proficient (GM00637) or deficient in xeroderma pigmentosum complementation group A (XPA, GM04429) were kind gifts from G. P. Pfeifer (Van Andel Research Institute, Grand Rapids, MI).

2.2.2. Preparation of Standards

O^2-PHBdT, O^6-PHBdG, O^4-PHBdT and their corresponding stable isotope-labeled derivatives were obtained by reduction with $NaBH_4$ of previously synthesized O^2-POBdT, O^6-POBdG, O^4-POBdT.[18] The reaction was carried out by mixing O^4-POBdT (100 µg) with 5 equivalents of $NaBH_4$ in 100 µL methanol at room temperature for 10 minutes. The solution was diluted with 9 volumes of water, which was then subjected to extraction with an equal volume of ethyl acetate for three times. The aqueous layer was collected, and the overall yield was 80%. Exact mass measurement (Thermo Q-Exactive Plus) yielded *m/z* 392.1820 and 396.2076 for the $[M+H]^+$ ions of the O^4-PHBdT and [pyridine-D_4]-O^4-PHBdT, respectively, which in line with their respective calculated *m/z* values of 392.1822 and 396.2073. O^2-PHBdT and O^6-PHBdG were prepared following the same procedures (**Tabel 2.1.**). Unlabeled and stable isotope-labeled O^4-PHBdT were synthesized for the first time in this study.

Table 2.1. Exact mass for [M+H]+ ions of O2-PHBdT, O4-PHBdT, and O6-PHBdG and their stable isotope-labeled counterparts.

Assignment	Calculated *m/z*	Observed *m/z*	Mass Error in part per million (ppm)
O^2-PHBdT	392.1822	392.1823	0.3
[pyridine-D_4]-O^2-PHBdT	396.2073	396.2075	0.5
O^4-PHBdT	392.1822	392.1820	0.5
[pyridine-D_4]-O^4-PHBdT	396.2073	396.2076	0.8
O^6-PHBdG	417.1886	417.1883	0.7
[pyridine-D_4]-O^6-PHBdG	421.2137	421.2135	0.5

2.2.3. Treatment of Calf Thymus DNA with NNALOAc and Esterase

Calf thymus DNA (25 μg) was incubated with 10 and 50 μg NNALOAc in the presence of porcine liver esterase (0.4 U) in 0.1 M phosphate buffer (1 mL, pH 7.0) at 37°C overnight. The resulting mixture was extracted sequentially with an equal-volume mixture of $CHCl_3$/isoamyl alcohol (24:1) and ethyl acetate. The DNA was precipitated from the aqueous phase by adding cold ethanol, washed with 70% ethanol and then with pure ethanol, allowed to air dry at room temperature, redissolved in doubly distilled water and stored at -20°C until enzymatic digestion and subsequent LC-MS/MS analysis.

2.2.4. Cell Culture and NNALOAc Treatment

The cells were maintained at 37°C, in a 5% CO_2 atmosphere, where human skin fibroblasts were cultured in Dulbecco's modified Eagle's medium (Gibco), and CHO cells were cultured in Alpha Minimum Essential Medium (Gibco) without ribonucleosides or 2′-deoxyribonucleosides. All culture media were supplemented with 10% fetal bovine serum and 100 IU/mL penicillin before use. Approximately $1-1.5\times10^6$ cells were seeded in 75 cm^2 flasks in complete medium and cultured for 24 h. The cells were unexposed or exposed with 5, 10, or 25 μM of NNALOAc (with or without the presence of 20 μM O^6-benzylguanine, an AGT inhibitor, in GM00637 XPA-proficient human skin fibroblast cells). After a 24 h-treatment, the medium was removed from the flask and the cells were washed twice with phosphate-buffered saline (1×PBS) to remove residual medium and NNALOAc. For the repair study, the cells were cultured at 37°C in the corresponding fresh media for different time intervals, detached by using trypsin-

EDTA and harvested by centrifugation.

2.2.5. DNA extraction, enzymatic digestion, and HPLC enrichment

Experimental procedures for DNA extraction, enzymatic digestion, and HPLC enrichment of targeted pyridylhydroxybutylated nucleosides were similar to those described previously.[18, 36, 38]

Extraction and enzymatic digestion of DNA

A high-salt method was employed for genomic and DNA extraction. A lysis buffer (75 μL) containing 20 mM Tris (pH 8.1), 20 mM EDTA, 400 mM NaCl, 1% SDS (w/v), and 15 μL of proteinase K (20 mg/mL) was added to the cell pellet and the mixture was incubated at 55°C overnight. Saturated sodium chloride solution (0.5 volume) was subsequently added, and the mixture was vortexed briefly and incubated at 55°C for 15 min. The mixture was subsequently centrifuged at 13000 rpm for 30 min at 4°C, and the nucleic acids were precipitated from the supernatant using 2 volumes of ethanol. The RNA in the resulting nucleic acid mixture was removed by digestion with 2 μL of RNase A (10 mg/mL) and 2 μL of RNase T1 (25 units/μL) at 37°C overnight followed by extraction with an equal volume of chloroform/isoamyl alcohol (24:1, v/v). The DNA was then precipitated from the aqueous layer with ethanol and centrifuged at 13000 rpm for 10 min. The resulting DNA pellet was washed twice with 70% cold ethanol, allowed to air dry at room temperature, and redissolved in doubly distilled water. The DNA was quantified using Nanodrop (Thermo Fisher, Waltham, MA) by measuring UV absorbance at 260 nm. Approximately 15 μg of DNA was obtained from $1-1.5\times10^6$ cells.

The NNALOAc-treated calf thymus DNA or cellular DNA (10 μg) was digested with 1 unit of nuclease P1 and 0.00125 unit of phosphodiesterase II in a 15-μL buffer containing 300 mM sodium acetate (pH 5.6), 10 mM $ZnCl_2$, and 2.5 nmol of EHNA; the labeled standards were also added to the mixture: 30 fmol of [pyridine-D_4]-O^2-PHBdT, 30 fmol of [pyridine-D_4]-O^6-PHBdG, and 15 fmol of [pyridine-D_4]-O^4-PHBdT. EHNA served as an inhibitor for adenine deaminase and minimized the deamination of dA to 2'-deoxyinosine (dI). The above mixture was incubated at 37°C for 48 h. Next, 1.0 unit of alkaline phosphatase, 0.0025 unit of phosphodiesterase I, and a 20-μL buffer containing 0.5 M Tris-HCl (pH 8.9) were added. After incubation at 37°C for 2 h, the digestion mixture was neutralized with 9.5 μL of 1.0 M formic acid. The enzymes in the digestion mixture were subsequently removed by extraction with an equal volume of chloroform. The aqueous layer was concentrated to approximate 200 μL and was subjected to off-line HPLC enrichment.

HPLC Enrichment

A Hypersil Gold C18 column (4.6 × 250 mm, 5 μm in particle size, 180 Å in pore size, Thermo Scientific Inc., CA) was used for the enrichment of the digestion mixture containing O^2-PHBdT, O^4-PHBdT and O^6-PHBdG. A solution of 10 mM ammonium formate and acetonitrile were used as mobile phases A and B, respectively, and the gradient comprised of 3% B in 0 min, 10% B in 15 min, and 50% B in 20 min, with the flow rate being 0.8 mL/min. The HPLC fractions in the retention time range of 19.5−23.5 min were pooled for the three modified nucleosides (**Figure 2.1.**). Subsequently, the

eluents were dried in a Speed-vac, redissolved in doubly distilled water, and injected for nLC-nESI-MS/MS analysis.

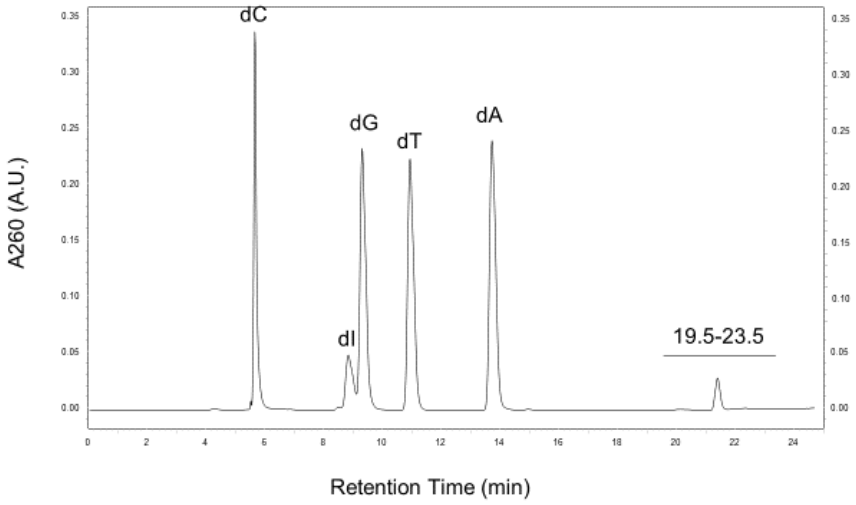

Figure 2.1. A representative HPLC trace for the enrichment of O^2-PHBdT, O^4-PHBdT and O^6-PHBdG from the nucleoside mixture arising from digestion of genomic DNA isolated from human skin fibroblasts (XPA-deficient, GM04429) treated with NNALOAc. The collection window was set at 19.5-23.5 minutes. 'dC', 'dI', 'dG', 'dT', and 'dA' designate 2'-deoxycytidine, 2'-deoxyinosine, 2'-deoxyguanosine, thymidine, and 2'-deoxyadenosine, respectively.

2.2.6. nLC-nESI-MS/MS Analysis

Online nLC-nESI-MS/MS measurements were conducted on a TSQ-Vantage triple quadrupole mass spectrometer (Thermo Fisher Scientific, CA) equipped with a nanoelectrospray ionization source and coupled with an EASY nLC II system (Thermo Fisher Scientific, CA). HPLC separation was conducted by employing a homemade trapping column (150 μm × 40 mm) and an analytical column (75 μm × 200 mm), both packed with Magic C18 AQ (200 Å, 5 μm, Michrom BioResource, Auburn, CA). Mobile

phases A and B were 0.1% formic acid in doubly distilled H_2O and acetonitrile, respectively. Initially, the sample was loaded, at a flow rate of 3 μL/min for 5 min, onto the trapping column with mobile phase A. The modified nucleosides of interest were then eluted by using a 40-min linear gradient of 0−50% mobile phase B at a flow rate of 300 nL/min. The TSQ-Vantage mass spectrometer was operated in the selected-reaction monitoring (SRM) mode. We monitored the transitions corresponding to the neutral loss of a deoxyribose (116 Da) from the $[M+H]^+$ ions of the three modified nucleosides (i.e. *m/z* 392→276, 392→276, and 417→301 for O^2-PHBdT, O^4-PHBdT and O^6-PHBdG, respectively) and their stable isotope-labeled counterparts (i.e. *m/z* 396→280, 396→280, and 421→305, **Figure 2.2.**). The voltage for electrospray was set at 2.0 kV and the temperature for the ion transfer tube was maintained at 275°C. The widths for precursor ion and product ion isolation were 3 Da and 0.7 Da, respectively, with a cycle time for 5 s. The collision gas was 1.2 mTorr nitrogen, and the collision energy was 15 V. The limit of quantitation (LOQ), reported as the mean signal plus 10 times of standard deviations from three blank runs in the selected-ion chromatograms (SICs) plotted for the transitions used for quantification.

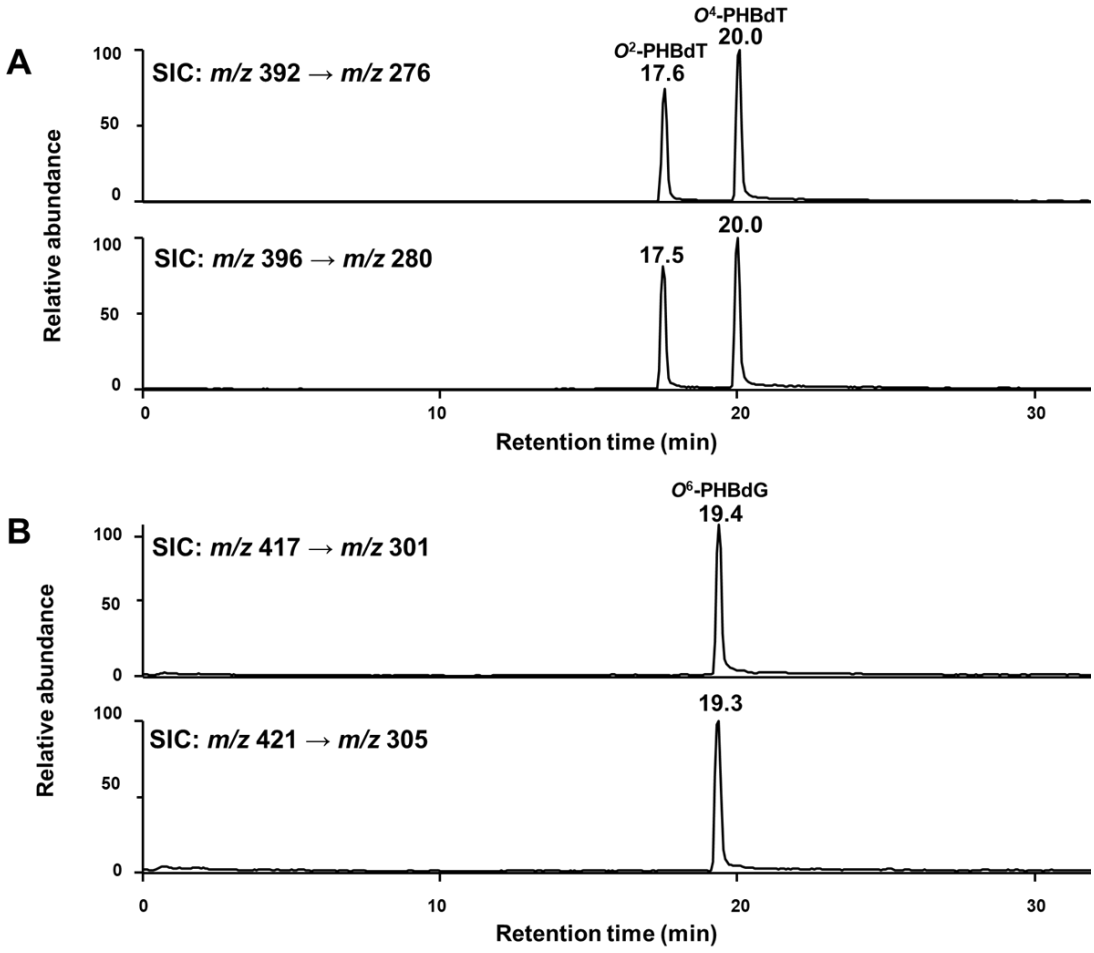

Figure 2.2. Representative selected-ion chromatograms (SICs) of the *m/z* 392 → 276 (A, top panel), 396 → 280 (A, bottom panel), 417 → 301 (B, top panel) and 421 → 305 (B, bottom panel) transitions for the $[M + H]^+$ ions of the unlabeled and stable isotope-labeled O^2- and O^4-PHBdT (A), and O^6-PHBdG (B), respectively, in the enriched modified nucleoside mixture of genomic DNA extracted from the GM04429 cells treated with 10 μM NNALOAc for 24 h.

2.2.7. Method Development

The intra- and inter-day precision and accuracy were evaluated by analyzing samples of O^2-PHBdT, O^4-PHBdT and O^6-PHBdG at three different concentrations. The samples used for calibration curve generation or precision and accuracy test were comprised of 5 μg calf thymus DNA mixed with standard solutions of three lesion-containing oligodeoxyribonucleotides (ODNs, 5'-ATGGCGXGCTAT-3', 'X' represents O^2-PHBdT, O^4-PHBdT or O^6-PHBdG) and their corresponding stable isotope-labeled mononucleosides; these samples were prepared following the previously described procedures[18, 36, 38] for the cellular DNA samples (including DNA digestion, chloroform extraction, and offline HPLC enrichment) and were subjected to LC-MS/MS measurement. Each calibration curve was obtained from triplicate analyses, where the molar ratios of the unlabeled ODNs to their corresponding labeled mononucleoside adducts were 0.10, 0.50, 1.00, 2.00, 5.00, 10.0, and 20.0 for O^2-PHBdT and O^6-PHBdG, and O^4-PHBdT, with the amount of the labeled nucleosides being 5 fmol each. The data, based on peak area ratios of responses of unlabeled/labeled adduct standard versus the molar ratios of unlabeled/labeled adduct standard, were fit to straight lines which were used as calibration curves (**Figure 2.3.**). The moles of DNA lesions in the nucleoside mixtures were calculated from the peak area ratios found in the SICs for the analytes and compared to their corresponding stable isotope-labeled counterparts. The final DNA lesion levels, displayed as number of lesions per 10^8 nucleosides, were calculated by dividing the moles of the modified DNA nucleosides by the total number of nucleosides (in moles) in the digested DNA.

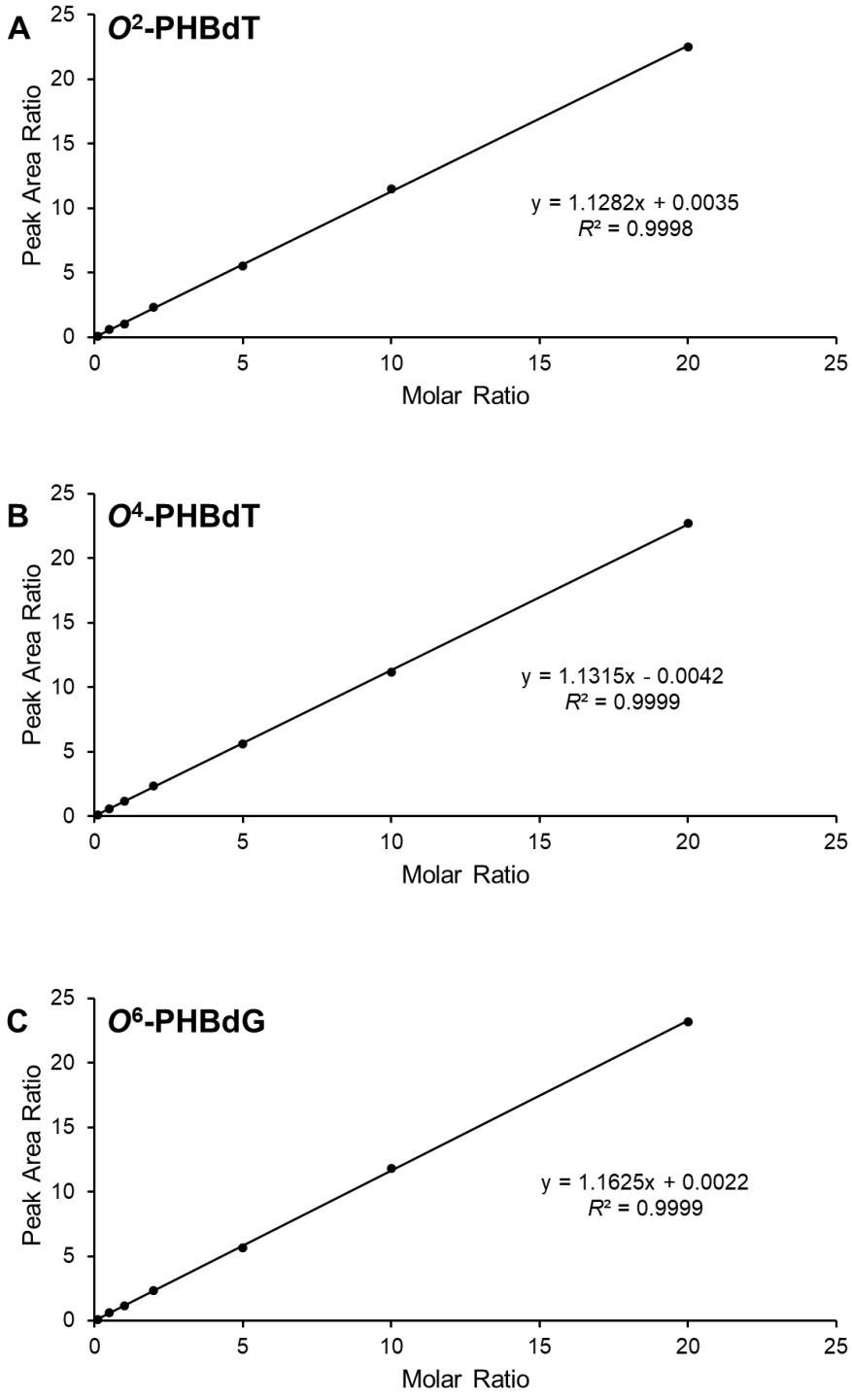

Figure 2.3. Calibration curves for the quantitation of O^2-PHBdT (A), O^4-PHBdT (B), and O^6-PHBdG (C). Plotted are the peak area ratio of unlabeled over labeled nucleoside standard vs. their molar ratios.

2.3. Results

The primary goals of this study are to set up a robust nLC-nESI-MS/MS coupled with stable-isotope-dilution method for quantification of *O*-pyridylhydroxybutylated dT and dG lesions in enzymatically digested cellular DNA, and to employ the method by assessing the occurrence and repair of these lesions in mammalian cells.

2.3.1. Syntheses of Unlabeled and Stable Isotope-Labeled Standards

We first synthesized standards for the unlabeled and stable isotope-labeled O^2-PHBdT, O^4-PHBdT, and O^6-PHBdG (see Experimental Section). O^4-PHBdT is a novel pyridylhydroxylbutylated DNA lesion that we synthesized through reduction from O^4-POBdT, which was prepared in a previous study.[18]

2.3.2. nLC-nESI-MS/MS for the Quantifications of O^2-PHBdT, O^4-PHBdT, and O^6-PHBdG

We next set out to employ the nLC-nESI-MS/MS method for accurate quantification of O^2-PHBdT, O^4-PHBdT, and O^6-PHBdG. The LOQs of these three analytes were determined to be 24.0, 19.0 and 8.5 amol (7.4, 5.9 and 2.6 per 10^{10} nucleosides in 10 μg DNA), respectively. The sample preparation was described in detail in the Experimental Section, where the cellular samples were subjected to DNA extraction using a high-salt method, RNA removal, and enzymatic digestion with a cocktail of four enzymes – including both 3′ and 5′ exonucleases to liberate lesions of

interest as mononucleosides. The stable isotope-labeled O^2-PHBdT, O^4-PHBdT, and O^6-PHBdG were added prior to DNA digestion, which corrects for the potential loss of analytes during chloroform extraction and offline HPLC enrichment. We then evaluated the intra- and inter-day precision and accuracy by triplicate measurements of calf thymus DNA (10 μg) spiked with different concentrations of lesion-bearing ODNs. The results demonstrated that the method offered good precision and accuracy (**Table 2.2.**).

Table 2.2. Intra-day and inter-day evaluation on precision and accuracy for the measurements of O^2-PHBdT, O^4-PHBdT, and O^6-PHBdG.

ODN amount (fmol)	expected lesion frequency in 10 μg DNA (/10^8 nucleosides)	Intraday		interday	
		RSD (%)	recovery (%)	RSD (%)	recovery (%)
O^2-PHBdT					
5.0	15.4	8.1	91.2	14.9	84.9
15	46.2	5.6	89.3	9.1	90.0
50	154.0	7.4	90.5	11.6	87.1
O^4-PHBdT					
5.0	15.4	9.2	93.4	11.0	90.4
15	46.2	7.7	88.2	13.9	89.5
50	154.0	10.1	92.5	10.7	87.8
O^6-PHBdG					
5.0	15.4	7.8	95.2	9.5	89.6
15	46.2	6.1	94.6	14.3	97.1
50	154.0	3.8	90.7	11.5	91.0

The detection of DNA modifications of low abundance is challenging; the sensitivity of measuring analytes is sometimes compromised by much greater amounts of canonical mononucleosides and buffer salts added during the enzymatic digestion. To address this issue, we conducted offline LC enrichment prior to LC-MS/MS analysis. The LC-MS/MS conditions were optimized prior to sample analysis. Better sensitivity could be achieved in positive-ion mode, which was used along with 0.1% formic acid (v/v) in the mobile phase to improve protonation of the analytes.

2.3.3. Dose-dependent formation of O^2-PHBdT, O^4-PHBdT and O^6-PHBdG in mammalian cells

After successfully establishing a robust nLC-nESI-MS/MS method, we subsequently quantified the levels of O^2-PHBdT, O^4-PHBdT, and O^6-PHBdG in genomic DNA isolated from human skin fibroblasts and Chinese hamster ovary cells, each exposed to different concentrations of NNALOAc. NNALOAc was used as a cell membrane-permeable precursor to the reactive intermediate in the presence of cellular esterase. The quantification data revealed dose-dependent formation of the three modified nucleosides in these cells (**Figure 2.4.**). When the dose of NNALOAc was increased from 5 to 25 μM, the levels of O^4-PHBdT in the XPA-proficient GM00637 cells and XPA-deficient GM04429 cells increased from 5.8 to 33.0 and from 9.5 to 53.1 lesions per 10^8 nucleosides, respectively (**Figure 2.4. B**). Similar elevated levels of O^4-PHBdT were observed in Chinese hamster ovary cells, where in ERCC1-deficient CHO-7-27 cells and

in repair-proficient CHO-AA8 cells, the frequencies of O^4-PHBdT were 16.4 to 71.5 and 12.0 to 47.4 lesions per 10^8 nucleosides, respectively (**Figure 2.4. E**). Our quantification data also revealed that the level of O^2-PHBdT and O^6-PHBdG were significantly higher than the observed level of O^4-PHBdT in mammalian cells.

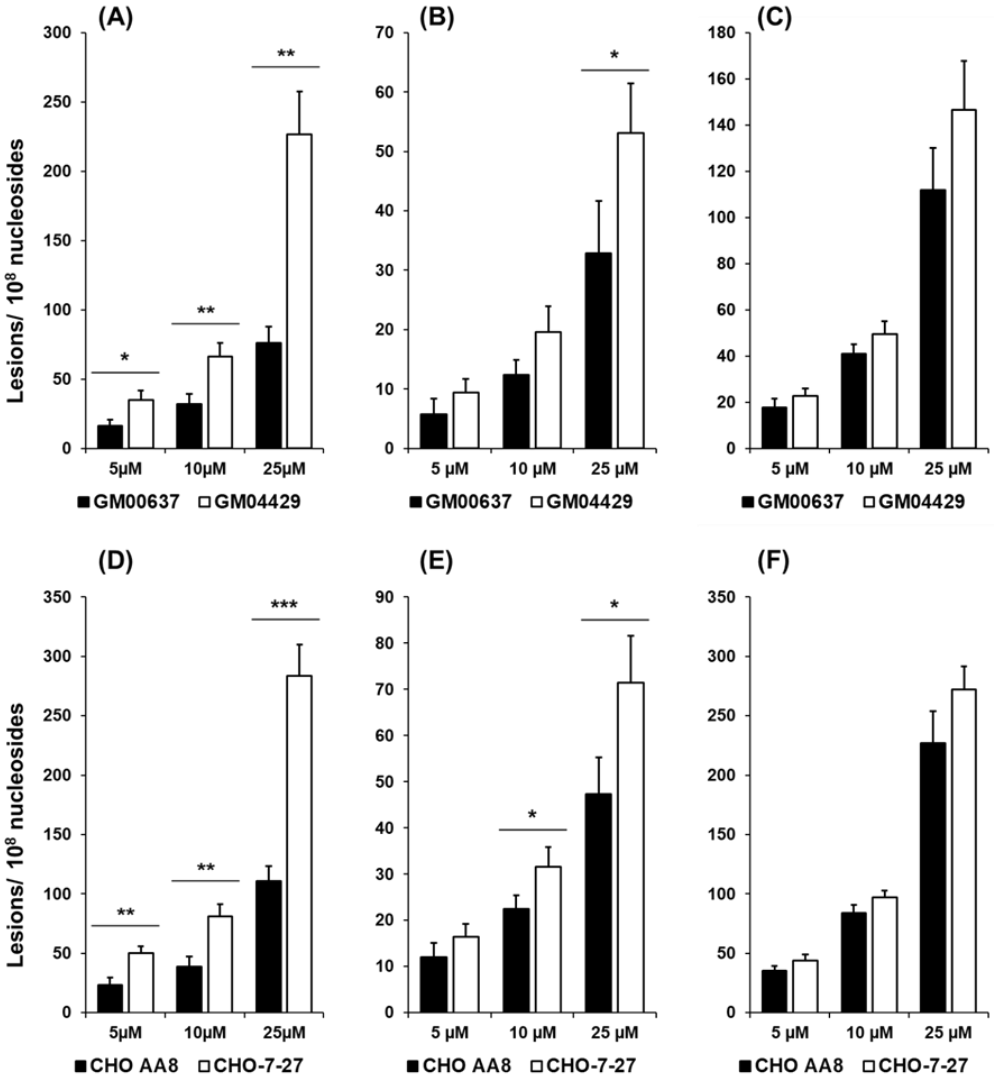

Figure 2.4. The frequencies of O^2-PHBdT (A, D), O^4-PHBdT (B, E), and O^6-PHBdG (C, F) in DNA samples isolated from human skin fibroblast cells (A-C) that are repair-proficient (GM00637) or deficient in XPA (GM04429) and Chinese hamster ovary cells (D-F) that are repair-competent (CHO-AA8) or deficient in ERCC1 (CHO-7-27); all cells were exposed to increasing concentrations of NNALOAc for 24 h. The data represent the means and standard deviations of results obtained from three independent experiments. *, $0.01 < p < 0.05$; **, $0.001 < p < 0.01$; ***, $p < 0.001$. The *p* values were calculated by using unpaired two-tailed student's *t*-test.

The pronounced difference in occurrence between O^2-PHBdT and its regioisomeric O^4-PHBdT could be attributed to the differences in either their rate of formation or repair. To explore these two possibilities, we exposed calf thymus DNA to NNALOAc with the presence of porcine liver esterase at 37°C overnight, and measured the levels of the three lesions using the same workflow (**Figure 2.5.**). Our *in vitro* results validated the preferential formation O^2-PHBdT over O^4-PHBdT, while O^6-PHBdG formed at higher levels than either of the other two lesions. Additionally, the relative levels of O^2-PHBdT, O^4-PHBdT and O^6-PHBdG were in line with previously reported data for the corresponding POB adducts in calf thymus DNA exposed to NNKOAc.[18, 22, 39]

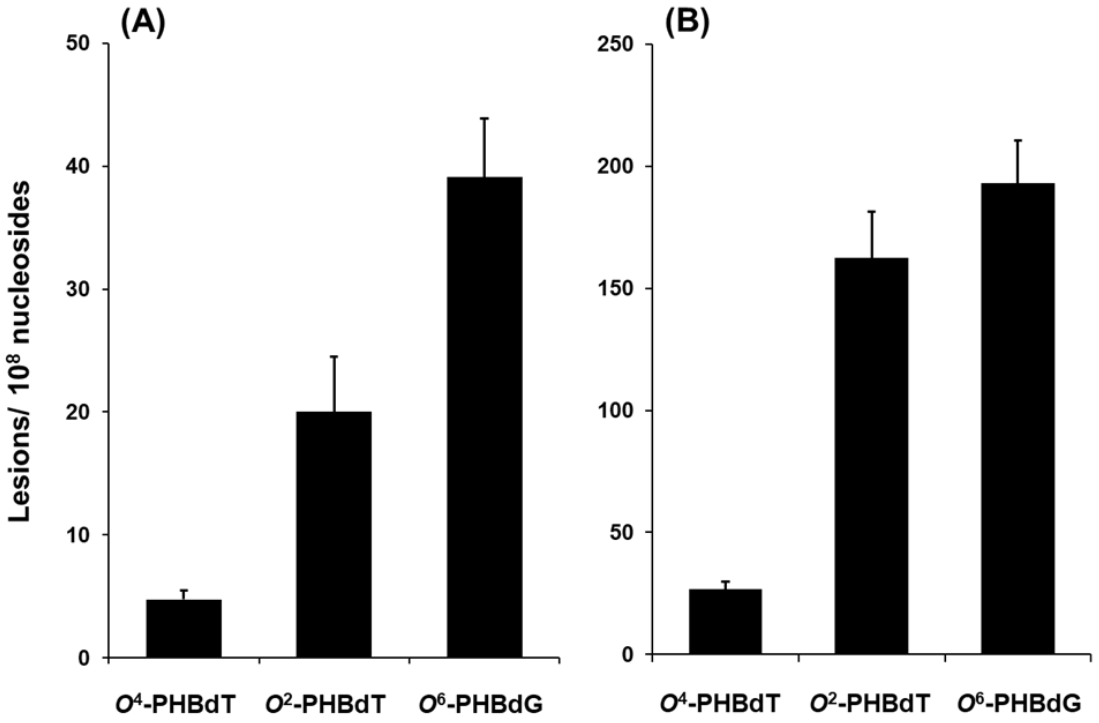

Figure 2.5. The frequencies of O^4-PHBdT, O^2-PHBdT, and O^6-PHBdG in calf thymus DNA treated with: A) 10 µg (37.4 µM) and B) 50 µg (187 µM) NNALOAc in the presence of porcine liver esterase.

2.3.4. Removal of O^2-PHBdT, O^4-PHBdT, and O^6-PHBdG in mammalian cells

Our quantification results reveal that the two lines of NER-deficient cells (XPA-deficient GM04429, ERCC1-deficient CHO-7-27) exhibited a higher level of these three lesions compared to their corresponding repair-proficient counterparts (XPA-proficient GM00637, ERCC1-proficient CHO-AA8), especially in the case of O^2-PHBdT. These results suggest that NER may be involved in repair of these three lesions. To further assess the role of NER in repairing these lesions, we next measured the frequencies of the three pyridylhydroxybutyl lesions in the cells at 0, 12, 24 h after exposure to 10 µM NNALOAc (Figure 4). No pronounced cell death was observed at the end of NNALOAc

exposure. The levels of O^2-PHBdT in NER-proficient and NER-deficient cells were significantly different at all three time points following NNALOAc exposure, suggesting that O^2-PHBdT is a good substrate for NER (**Figure 2.6.**). The rates of removal of this specific lesion in both human fibroblasts cells and Chinese hamster ovary cells were similar, suggesting a similar mechanism is involved with the repair of O^2-PHBdT in these two types of cells. To a lesser extent, O^4-PHBdT is also affected by NER, as the quantification data reveal a significant difference between NER-deficient cells and their repair-proficient counterparts (**Figure 2.6. B, E**). O^6-PHBdG was not found to be an NER substrate as no significant difference in repair was found between cells that are competent or deficient in NER (**Figure 2.6. C, F**). We found the CHO cells and human skin fibroblasts cells exhibited different repair efficiencies for O^6-PHBdG, suggesting that, aside from NER, AGT may be involved in repairing this specific lesion, since there is no AGT expression in CHO cells.[17, 19, 28, 43]

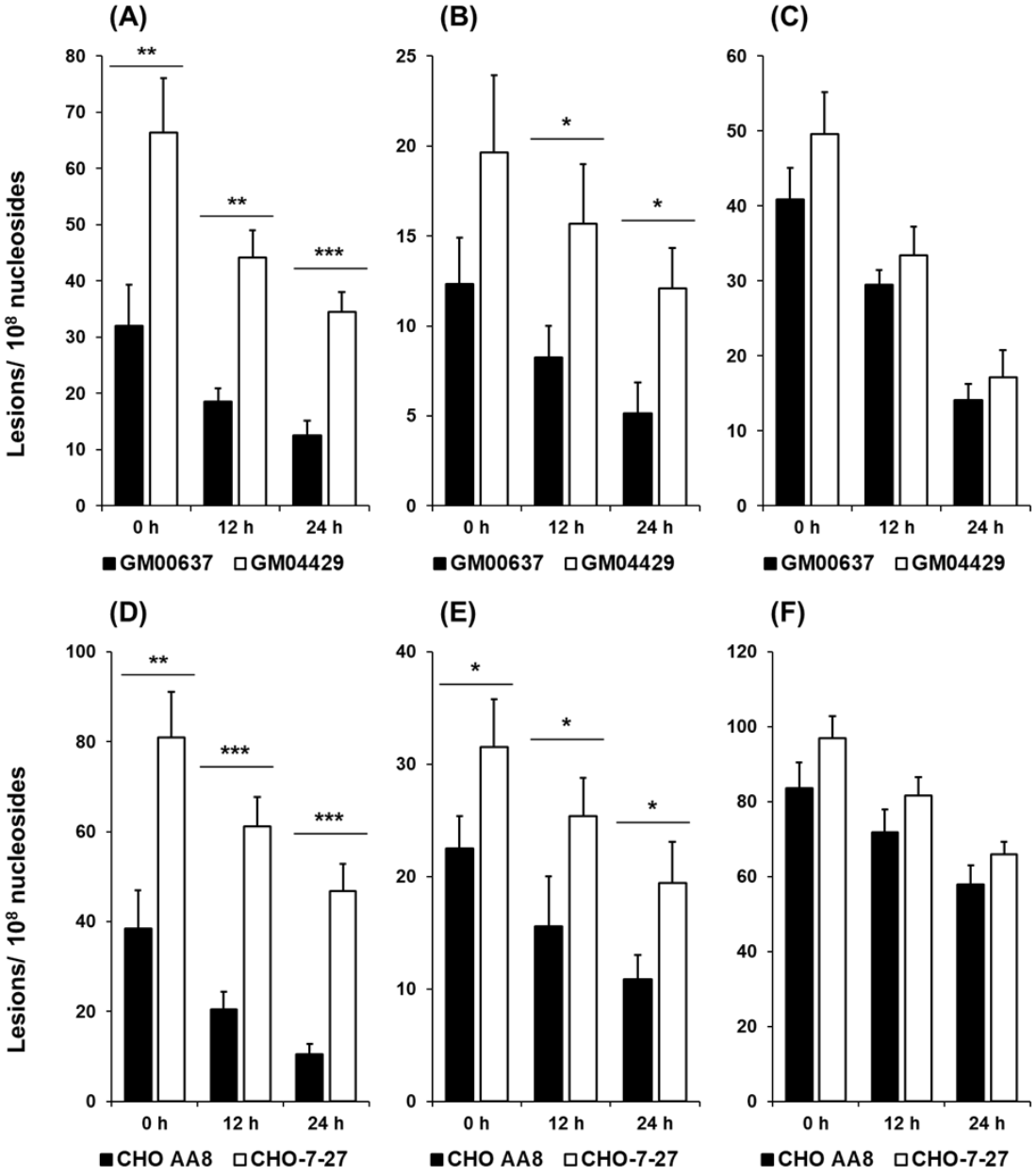

Figure 2.6. LC-MS/MS results for the repair of O^2-PHBdT (A, D), O^4-PHBdT (B, E), and O^6-PHBdG (C, F) in human skin fibroblast (A-C) and Chinese hamster ovary (D-F) cells; after a 24-h exposure to 10 μM NNALOAc, the media was exchanged and the cells were harvested immediately, or 12 or 24 h later. The data represent the means and standard deviations of results obtained from three independent experiments. *, 0.01< p < 0.05; **, 0.001< p < 0.01; ***, p < 0.001. The p values were calculated by using unpaired two-tailed student's t-test.

During further examination, we asked whether AGT participated in the removal of the three lesions. O^6-benzylguanine (20 μM) was used to inactivate AGT in cells, and GM00637 cells were examined after exposure to 10 μM NNALOAc (**Figure 2.7.**). The results showed that the levels of O^2-PHBdT in the AGT proficient and AGT inactive cells were almost the same. We detected a small difference in the O^4-PHBdT levels, indicating that AGT may also be involved in the removal of O^4-PHBdT.[27, 44] The difference in O^6-PHBdG levels was the largest among the three lesions, suggesting that AGT will readily repair this lesion.

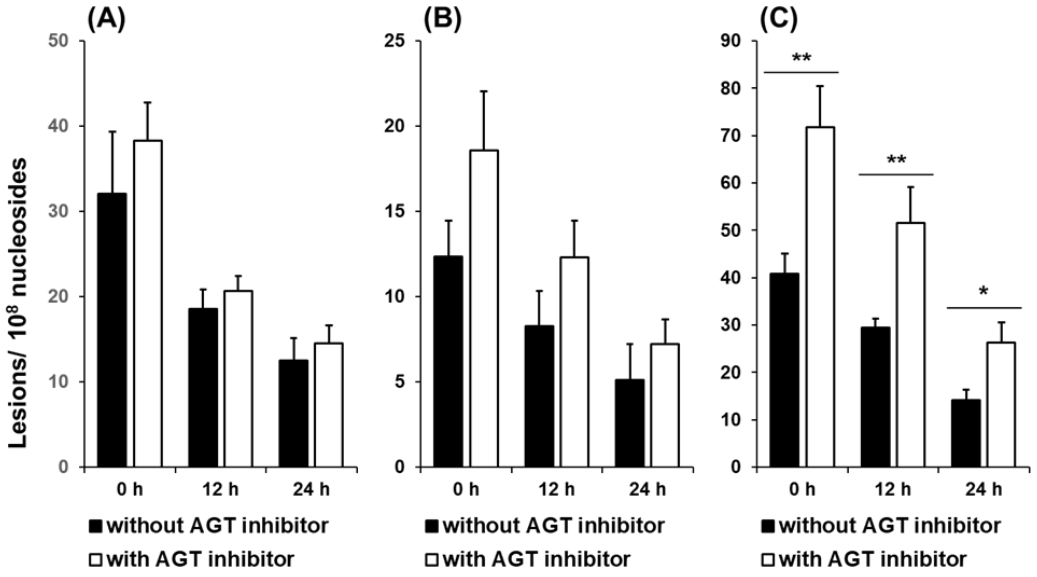

Figure 2.7. The repair of *O*^{2}-PHBdT (A), *O*^{4}-PHBdT (B), and *O*^{6}-PHBdG (C) in human skin fibroblast GM00637 cells following a 24-h exposure to 10 μM NNALOAc with the presence of 20 μM *O*^{6}-benzylguanine (to inactive AGT). The data represent the means and standard deviations of results obtained from three independent experiments. *, 0.01< *p* < 0.05; **, *p* < 0.01. The *p* values were calculated by using unpaired two-tailed student's *t*-test.

2.4. Discussion

LC-MS/MS in combination with the stable isotope-dilution method enables specific, accurate and highly sensitive analysis of DNA lesions in complex biological matrices.[18, 33-41] It provides an advantage over conventional DNA adduct measurement methods (e.g., immunoblot assay, ^{32}P -postlabeling[45-47]) by offering structural information to enable identification, and by facilitating reliable absolute quantification when spiked with known amounts of stable isotope-labeled standards.[40, 48, 49] In this study stable isotope-labeled standards were added prior to enzymatic digestion, which helps correct

for the loss of analytes during chloroform extraction and offline enrichment; thereby providing more accurate quantification for the three lesions. Offline HPLC was employed in this study to eliminate the more abundant canonical mononucleosides in digestion mixtures and remove buffer salts used during the enzymatic digestion. Our offline HPLC enrichment method provides higher sensitivity in subsequent LC-MS/MS analysis compared to previously reported solid-phase extraction methods for targeted nucleoside enrichment; this lower sensitivity may have been due to incomplete removal of unmodified nucleosides and buffer salts during solid-phase extraction.[50, 51] The calibration curve set up in this study employed calf thymus DNA spiked with lesion-bearing ODNs, which not only aided in evaluation of ionization efficiency for labeled and unlabeled mononucleosides, but also allowed us to correct for potential incomplete release of modified nucleosides from DNA during the digestion step.

Mammalian cells are equipped with an arsenal of DNA repair proteins that can be dispatched in response to numerous types of damage, thus protecting genomic stability. In this study, we used four mammalian cell lines that are proficient or deficient in key NER proteins and we investigated the role of NER in the removal of O^2-PHBdT, O^4-PHBdT and O^6-PHBdG from genomic DNA. Dose-dependent formation was observed for O^2-PHBdT, O^4-PHBdT and O^6-PHBdG in the four cell lines, where O^2-PHBdT and O^6-PHBdG displayed higher frequencies of formation than O^4-PHBdT. In the repair study, we carefully compared the levels of these lesions in NER-proficient and NER-deficient cells. Our results revealed that O^2-PHBdT and, to a lesser extent, O^4-PHBdT may serve as substrates for NER, whereas O^6-PHBdG cannot be repaired by NER. It is of note that

similar repair observed between pyridylhydroxybutylated and pyridyloxobutylated lesions. Our previous study on O^2-POBdT, O^4-POBdT and O^6-POBdG reveals that the formation of the three POB lesions are dose-dependent, and O^2-POBdT is most readily repaired by NER, O^4-POBdT can be repaired at a lesser degree, whereas O^6-POBdG is not subjected to be repaired by NER.[18] The different repair capacity of O^6-PHBdG between Chinese hamster ovary cells and human fibroblasts cells may suggest that AGT is responsible for the removal of this specific modification,[17, 19, 28, 43] which in line with our previous finding that different levels in occurrence of O^6-POBdG in GM and CHO cells could be observed.[18] Thus, we interrogated the levels of three lesions by employing an AGT inhibitor, O^6-benzylguanine. O^6-benzylguanine was reported to covalently react with AGT, rendering it inactive. The results confirmed our hypothesis that AGT plays an important role in the reversal of O^6-PHBdG; to a lesser degree, O^4-PHBdT was repaired, which is in line with existing evidences that AGT recognizes major-groove lesions.[27, 44]

In summary, here we reported a LC-MS/MS method for the simultaneous quantification of the pyridylhydroxybutyl lesions O^2-PHBdT, O^4-PHBdT and O^6-PHBdG; where O^4-PHBdT was, for the first time, found to be induced in mammalian cells upon exposure to pyridylhydroxybutylating agents. The method demonstrated high sensitivity in quantification of targeted DNA lesions and its capacity to snapshot the levels of lesions in a repair study at different time intervals. The method may serve as a tool to investigate the involvement of DNA pyridylhydroxybutylation as a biomarker related to tobacco-induced cancer.

References

(1) Lindahl, T.; Wood, R. D., Quality control by DNA repair. *Science* **1999,** *286*, 1897-1905.

(2) Fu, D.; Calvo, J. A.; Samson, L. D., Balancing repair and tolerance of DNA damage caused by alkylating agents. *Nat. Rev. Cancer* **2012,** *12*, 104-120.

(3) Shrivastav, N.; Li, D.; Essigmann, J. M., Chemical biology of mutagenesis and DNA repair: cellular responses to DNA alkylation. *Carcinogenesis* **2010,** *31*, 59-70.

(4) Wynder, E. L.; Muscat, J. E., The changing epidemiology of smoking and lung cancer histology. *Environ. Health Perspect.* **1995,** *103 Suppl 8*, 143-148.

(5) Hackshaw, A. K.; Law, M. R.; Wald, N. J., The accumulated evidence on lung cancer and environmental tobacco smoke. *BMJ* **1997,** *315*, 980-988.

(6) Nyberg, F.; Pershagen, G., Passive smoking and lung cancer. Accumulated evidence on lung cancer and environmental tobacco smoke. *BMJ* **1998,** *317*, 347-348.

(7) Hoffmann, D.; Hecht, S. S., Nicotine-derived *N*-nitrosamines and tobacco-related cancer: current status and future directions. *Cancer Res.* **1985,** *45*, 935-944.

(8) Hecht, S. S.; Hoffmann, D., Tobacco-specific nitrosamines, an important group of carcinogens in tobacco and tobacco smoke. *Carcinogenesis* **1988,** *9*, 875-884.

(9) Hecht, S. S., Biochemistry, biology, and carcinogenicity of tobacco-specific *N*-nitrosamines. *Chem. Res. Toxicol.* **1998,** *11*, 559-603.

(10) Hecht, S. S., Tobacco smoke carcinogens and lung cancer. *J. Natl. Cancer Inst.* **1999,** *91*, 1194-1210.

(11) Hecht, S. S., DNA adduct formation from tobacco-specific *N*-nitrosamines. *Mutat. Res.* **1999,** *424*, 127-142.

(12) Hecht, S. S.; Villalta, P. W.; Sturla, S. J.; Cheng, G.; Yu, N.; Upadhyaya, P.; Wang, M., Identification of O^2-substituted pyrimidine adducts formed in reactions of 4-(acetoxymethylnitrosamino)- 1-(3-pyridyl)-1-butanone and 4-(acetoxymethylnitrosamino)-1-(3-pyridyl)-1-butanol with DNA. *Chem. Res. Toxicol.* **2004,** *17*, 588-597.

(13) Hecht, S. S.; Stepanov, I.; Carmella, S. G., Exposure and metabolic activation biomarkers of carcinogenic tobacco-specific nitrosamines. *Acc. Chem. Res.* **2016,** *49*, 106-114.

(14) Peterson, L. A., Context matters: contribution of specific DNA adducts to the genotoxic properties of the tobacco-specific nitrosamine NNK. *Chem. Res. Toxicol.* **2017,** *30*, 420-433.

(15) Stepanov, I.; Hecht, S. S., Mitochondrial DNA adducts in the lung and liver of F344 rats chronically treated with 4-(methylnitrosamino)-1-(3-pyridyl)-1-butanone and (*S*)-4-(methylnitrosamino)-1-(3-pyridyl)-1-butanol. *Chem. Res. Toxicol.* **2009,** *22*, 406-414.

(16) Balbo, S.; Johnson, C. S.; Kovi, R. C.; James-Yi, S. A.; O'Sullivan, M. G.; Wang, M.; Le, C. T.; Khariwala, S. S.; Upadhyaya, P.; Hecht, S. S., Carcinogenicity and DNA adduct formation of 4-(methylnitrosamino)-1-(3-pyridyl)-1-butanone and enantiomers of its metabolite 4-(methylnitrosamino)-1-(3-pyridyl)-1-butanol in F-344 rats. *Carcinogenesis* **2014,** *35*, 2798-2806.

(17) Urban, A. M.; Upadhyaya, P.; Cao, Q.; Peterson, L. A., Formation and repair of pyridyloxobutyl DNA adducts and their relationship to tumor yield in A/J mice. *Chem. Res. Toxicol.* **2012,** *25*, 2167-2178.

(18) Leng, J.; Wang, Y., Liquid chromatography-tandem mass spectrometry for the quantification of tobacco-specific nitrosamine-induced DNA adducts in mammalian cells. *Anal. Chem.* **2017,** *89*, 9124-9130.

(19) Mijal, R. S.; Thomson, N. M.; Fleischer, N. L.; Pauly, G. T.; Moschel, R. C.; Kanugula, S.; Fang, Q.; Pegg, A. E.; Peterson, L. A., The repair of the tobacco specific nitrosamine derived adduct O^6-[4-Oxo-4-(3-pyridyl)butyl]guanine by O^6-alkylguanine-DNA alkyltransferase variants. *Chem. Res. Toxicol.* **2004,** *17*, 424-434.

(20) Carlson, E. S.; Upadhyaya, P.; Villalta, P. W.; Ma, B.; Hecht, S. S., Analysis and identification of 2'-deoxyadenosine-derived adducts in lung and liver DNA of F-344 rats treated with the tobacco-specific carcinogen 4-(Methylnitrosamino)-1-(3-pyridyl)-1-butanone and enantiomers of its metabolite 4-(Methylnitrosamino)-1-(3-pyridyl)-1-butanol. *Chem. Res. Toxicol.* **2018,** *31*, 358-370.

(21) Ma, B.; Zarth, A. T.; Carlson, E. S.; Villalta, P. W.; Stepanov, I.; Hecht, S. S., Pyridylhydroxybutyl and pyridyloxobutyl DNA phosphate adduct formation in rats treated chronically with enantiomers of the tobacco-specific nitrosamine metabolite 4-(methylnitrosamino)-1-(3-pyridyl)-1-butanol. *Mutagenesis* **2017,** *32*, 561-570.

(22) Lao, Y.; Villalta, P. W.; Sturla, S. J.; Wang, M.; Hecht, S. S., Quantitation of pyridyloxobutyl DNA adducts of tobacco-specific nitrosamines in rat tissue DNA by high-performance liquid chromatography-electrospray ionization-tandem mass spectrometry. *Chem. Res. Toxicol.* **2006,** *19*, 674-682.

(23) Ma, B.; Villalta, P. W.; Zarth, A. T.; Kotandeniya, D.; Upadhyaya, P.; Stepanov, I.; Hecht, S. S., Comprehensive high-resolution mass spectrometric analysis of DNA phosphate adducts formed by the tobacco-specific lung carcinogen 4-(Methylnitrosamino)-1-(3-pyridyl)-1-butanone. *Chem. Res. Toxicol.* **2015,** *28*, 2151-2159.

(24) Du, H.; Leng, J.; Wang, P.; Li, L.; Wang, Y., Impact of tobacco-specific nitrosamine-derived DNA adducts on the efficiency and fidelity of DNA replication in human cells. *J. Biol. Chem.* **2018,** *293*, 11100-11108.

(25) Ronai, Z. A.; Gradia, S.; Peterson, L. A.; Hecht, S. S., G to A transitions and G to T transversions in codon 12 of the Ki-*ras* oncogene isolated from mouse lung tumors induced by 4-(methylnitrosamino)-1-(3-pyridyl)-1-butanone (NNK) and related DNA methylating and pyridyloxobutylating agents. *Carcinogenesis* **1993,** *14*, 2419-2422.

(26) Ma, B.; Zarth, A. T.; Carlson, E. S.; Villalta, P. W.; Upadhyaya, P.; Stepanov, I.; Hecht, S. S., Methyl DNA phosphate adduct formation in rats treated chronically with 4-(Methylnitrosamino)-1-(3-pyridyl)-1-butanone and enantiomers of its metabolite 4-(Methylnitrosamino)-1-(3-pyridyl)-1-butanol. *Chem. Res. Toxicol.* **2018,** *31*, 48-57.

(27) Mishina, Y.; Duguid, E. M.; He, C., Direct reversal of DNA alkylation damage. *Chem. Rev.* **2006,** *106*, 215-232.

(28) Li, L.; Perdigao, J.; Pegg, A. E.; Lao, Y.; Hecht, S. S.; Lindgren, B. R.; Reardon, J. T.; Sancar, A.; Wattenberg, E. V.; Peterson, L. A., The influence of repair pathways on the cytotoxicity and mutagenicity induced by the pyridyloxobutylation pathway of tobacco-specific nitrosamines. *Chem. Res. Toxicol.* **2009,** *22*, 1464-1472.

(29) Hecht, S. S., Lung carcinogenesis by tobacco smoke. *Int. J. Cancer* **2012,** *131*, 2724-2732.

(30) Peterson, L. A.; Hecht, S. S., Tobacco, e-cigarettes, and child health. *Curr. Opin. Pediatr.* **2017,** *29*, 225-230.

(31) Choi, J. Y.; Guengerich, F. P., Kinetic analysis of translesion synthesis opposite bulky N^2- and O^6-alkylguanine DNA adducts by human DNA polymerase REV1. *J. Biol. Chem.* **2008,** *283*, 23645-23655.

(32) Weerasooriya, S.; Jasti, V. P.; Bose, A.; Spratt, T. E.; Basu, A. K., Roles of translesion synthesis DNA polymerases in the potent mutagenicity of tobacco-specific nitrosamine-derived O^2-alkylthymidines in human cells. *DNA Repair (Amst)* **2015,** *35*, 63-70.

(33) Dator, R.; von Weymarn, L. B.; Villalta, P. W.; Hooyman, C. J.; Maertens, L. A.; Upadhyaya, P.; Murphy, S. E.; Balbo, S., In vivo stable-isotope labeling and mass-

spectrometry-based metabolic profiling of a potent tobacco-specific carcinogen in rats. *Anal. Chem.* **2018,** *90*, 11863-11872.

(34) Guo, J.; Yun, B. H.; Upadhyaya, P.; Yao, L.; Krishnamachari, S.; Rosenquist, T. A.; Grollman, A. P.; Turesky, R. J., Multiclass carcinogenic DNA adduct quantification in formalin-fixed paraffin-embedded tissues by ultraperformance liquid chromatography-tandem mass spectrometry. *Anal. Chem.* **2016,** *88*, 4780-4787.

(35) Monien, B. H.; Schumacher, F.; Herrmann, K.; Glatt, H.; Turesky, R. J.; Chesne, C., Simultaneous detection of multiple DNA adducts in human lung samples by isotope-dilution UPLC-MS/MS. *Anal. Chem.* **2015,** *87*, 641-648.

(36) Wang, J.; Yuan, B.; Guerrero, C.; Bahde, R.; Gupta, S.; Wang, Y., Quantification of oxidative DNA lesions in tissues of Long-Evans Cinnamon rats by capillary high-performance liquid chromatography-tandem mass spectrometry coupled with stable isotope-dilution method. *Anal. Chem.* **2011,** *83*, 2201-2209.

(37) Xiao, S.; Guo, J.; Yun, B. H.; Villalta, P. W.; Krishna, S.; Tejpaul, R.; Murugan, P.; Weight, C. J.; Turesky, R. J., Biomonitoring DNA adducts of cooked meat carcinogens in human prostate by nano liquid chromatography-high resolution tandem mass spectrometry: identification of 2-Amino-1-methyl-6-phenylimidazo[4,5-b]pyridine DNA adduct. *Anal. Chem.* **2016,** *88*, 12508-12515.

(38) Yu, Y.; Wang, J.; Wang, P.; Wang, Y., Quantification of azaserine-induced carboxymethylated and methylated DNA lesions in cells by nanoflow liquid chromatography-nanoelectrospray ionization tandem mass spectrometry coupled with the stable isotope-dilution method. *Anal. Chem.* **2016,** *88*, 8036-8042.

(39) Sturla, S. J.; Scott, J.; Lao, Y.; Hecht, S. S.; Villalta, P. W., Mass spectrometric analysis of relative levels of pyridyloxobutylation adducts formed in the reaction of DNA with a chemically activated form of the tobacco-specific carcinogen 4-(methylnitrosamino)-1-(3-pyridyl)-1-butanone. *Chem. Res. Toxicol.* **2005,** *18*, 1048-1055.

(40) Liu, S.; Wang, Y., Mass spectrometry for the assessment of the occurrence and biological consequences of DNA adducts. *Chem. Soc. Rev.* **2015,** *44*, 7829-7854.

(41) Guo, C.; Xie, C.; Chen, Q.; Cao, X.; Guo, M.; Zheng, S.; Wang, Y., A novel malic acid-enhanced method for the analysis of 5-methyl-2'-deoxycytidine, 5-hydroxymethyl-2'-deoxycytidine, 5-methylcytidine and 5-hydroxymethylcytidine in human urine using hydrophilic interaction liquid chromatography-tandem mass spectrometry. *Anal. Chim. Acta* **2018,** *1034*, 110-118.

(42) Rolig, R. L.; Layher, S. K.; Santi, B.; Adair, G. M.; Gu, F.; Rainbow, A. J.; Nairn, R. S., Survival, mutagenesis, and host cell reactivation in a Chinese hamster ovary

cell ERCC1 knock-out mutant. *Mutagenesis* **1997,** *12*, 277-283.

(43) Peterson, L. A.; Liu, X. K.; Hecht, S. S., Pyridyloxobutyl DNA adducts inhibit the repair of O^6-methylguanine. *Cancer Res.* **1993,** *53*, 2780-2785.

(44) Mitra, S., MGMT: a personal perspective. *DNA Repair (Amst)* **2007,** *6* (8), 1064-1070.

(45) Wang, P.; Wang, Y., Cytotoxic and mutagenic properties of O^6-alkyl-2'-deoxyguanosine lesions in Escherichia coli cells. *J. Biol. Chem.* **2018,** *293*, 15033-15042.

(46) Wang, P.; Amato, N. J.; Zhai, Q.; Wang, Y., Cytotoxic and mutagenic properties of O^4-alkylthymidine lesions in Escherichia coli cells. *Nucleic Acids Res.* **2015,** *43*, 10795-10803.

(47) Zhai, Q.; Wang, P.; Cai, Q.; Wang, Y., Syntheses and characterizations of the in vivo replicative bypass and mutagenic properties of the minor-groove O^2-alkylthymidine lesions. *Nucleic Acids Res.* **2014,** *42*, 10529-10537.

(48) Yu, Y.; Cui, Y.; Niedernhofer, L. J.; Wang, Y., Occurrence, biological consequences, and human health relevance of oxidative stress-induced DNA damage. *Chem. Res. Toxicol.* **2016,** *29*, 2008-2039.

(49) Yu, Y.; Wang, P.; Cui, Y.; Wang, Y., Chemical analysis of DNA damage. *Anal. Chem.* **2018,** *90*, 556-576.

(50) Vanden Bussche, J.; Moore, S. A.; Pasmans, F.; Kuhnle, G. G.; Vanhaecke, L., An approach based on ultra-high pressure liquid chromatography-tandem mass spectrometry to quantify O^6-methyl and O^6-carboxymethylguanine DNA adducts in intestinal cell lines. *J. Chromatogr. A* **2012,** *1257*, 25-33.

(51) Da Pieve, C.; Sahgal, N.; Moore, S. A.; Velasco-Garcia, M. N., Development of a liquid chromatography/tandem mass spectrometry method to investigate the presence of biomarkers of DNA damage in urine related to red meat consumption and risk of colorectal cancer. *Rapid Commun. Mass Spectrom.* **2013,** *27*, 2493-2503.

Chapter 3 LC-MS/MS for Assessing the Incorporation and Repair of N^2-alkyl-2'-deoxyguanosine in Genomic DNA

3.1. Introduction

In all domains of life, genetic information has to be faithfully transmitted during cell division.[1] However, DNA is susceptible to chemical modifications induced by various endogenous and exogenous DNA damaging agents.[2,3] If not properly repaired, DNA lesions can impede DNA replication and transcription, and introduce mutations to nascent DNA or RNA, which may contribute to cancer initiation.[4,5] Hence, it is important to have a comprehensive understanding about how various structurally defined DNA lesions are repaired.

Multi-disciplinary efforts have been devoted toward developing reliable approaches to study DNA damage and repair.[6,7] Among them, liquid chromatography coupled with tandem mass spectrometry (LC-MS/MS) is the most widely adopted.[8,9] Numerous DNA lesions have been reliably quantified using LC-MS/MS coupled with the stable isotope-dilution technique.[6,10] To study the formation and repair of DNA adducts in a laboratory setting, researchers frequently expose experimental animals and/or cultured cells to DNA damaging agents.[6,11] This approach not only enables accurate quantifications of known DNA lesions, but also leads to the discovery of novel DNA modifications elicited by certain chemicals, which facilitate risk assessment.[9,11] Due to the lack of chemical specificity of the DNA damaging agents, the approach, however, frequently does not permit the induction of only one specific type of lesion in DNA.[12–14]

Alternatively, modified nucleobases or nucleosides could be added to the cell culture medium to enable their metabolic incorporation into genomic DNA.[15–17] For instance, 6-thioguanine (^{S}G), 6-thio-2′-deoxyguanosine (^{S}dG), and 5-aza-2′-deoxycytidine were shown to be efficiently incorporated into genomic DNA, and these modified nucleobases and nucleosides have been successfully used as chemotherapeutic agents.[15,18,19] Additionally, 5-ethynyl-2′-deoxyuridine (EdU) could be incorporated into genomic DNA and its 'clickable' property allows for its further application in biorthogonal assays.[17,20] Moreover, 5-hydroxymethyl-2′-deoxycytidine and 5-formyl-2′-deoxycytidine could exert anti-tumor effects through their deamination to the corresponding dU derivatives and subsequent incorporation of the deaminated nucleosides into genomic DNA of cancer cells.[21] While the incorporation of these modified nucleosides into genomic DNA may involve replicative DNA polymerases, translesion synthesis (TLS) DNA polymerases have been documented to enable the incorporation of some of the modified nucleosides into genomic DNA. For instance, polymerase (Pol) λ and Pol κ were found to promote the incorporation of N^6-methyl-2′-deoxyadenosine and N^2-substituted-dG into genomic DNA of mammalian cells, respectively.[22–24] Thus, metabolic labeling of modified nucleosides and nucleobases may serve as a useful tool for studying the repair of modified nucleosides in genomic DNA.

Minor-groove N^2 position of dG is susceptible to modifications by various alkylating agents. For instance, exposure to benzo[*a*]pyrene results in N^2-BPDE-dG through its metabolite benzo[*a*]pyrene-7,8-diol-9,10-epoxide (BPDE).[25] In addition,

aldehydes can attack the N^2 position of guanine to yield N^2-alkyl-dG.[26–28] The levels of N^2-MedG in mouse tissues were increased from 1.2-1.7 per 10^6 nucleosides to 1.9-4.2 per 10^6 nucleosides following a 4-week exposure to 1.5 mg/kg of methanol, which can be metabolized to formaldehyde.[28] Previous research in our laboratory demonstrated that N^2-alkyl-dG could be efficiently and accurately bypassed in mammalian cells proficient in translesion synthesis; however, loss of Pol κ, Pol ι or REV1 could result in mutagenic bypass of these lesions.[29,30] Moreover, Pol η promotes the transcriptional bypass of these minor-groove DNA lesions.[24] Bulky N^2-BPDE-dG is a known substrate for NER;[31] nonetheless, no systematic research has been conducted about how NER responds to N^2-alkyl-dG lesions differing in sizes. Moreover, while *Escherichia coli* AlkB protein was shown to be capable of reverting various N-alkylated DNA lesions,[32] it remains unclear whether minor-groove N^2-alkyl-dG lesions could be subjected to a similar repair mechanism in human cells.

By taking advantage of metabolic incorporation, herein we examined systematically the repair of N^2-methyl- and N^2-*n*-butyl-2′-deoxyguanosine (N^2-MedG and N^2-*n*BudG) in mammalian genome and its modulation by TLS polymerases, NER machinery and oxidative dealkylation enzymes (**Figure 3.1.**). In addition, a comparative study on N^2-MedG and N^2-nBudG facilitates the assessment about the effects of alkyl group size on the metabolic incorporation and repair of N^2-alkyl-dG lesions.

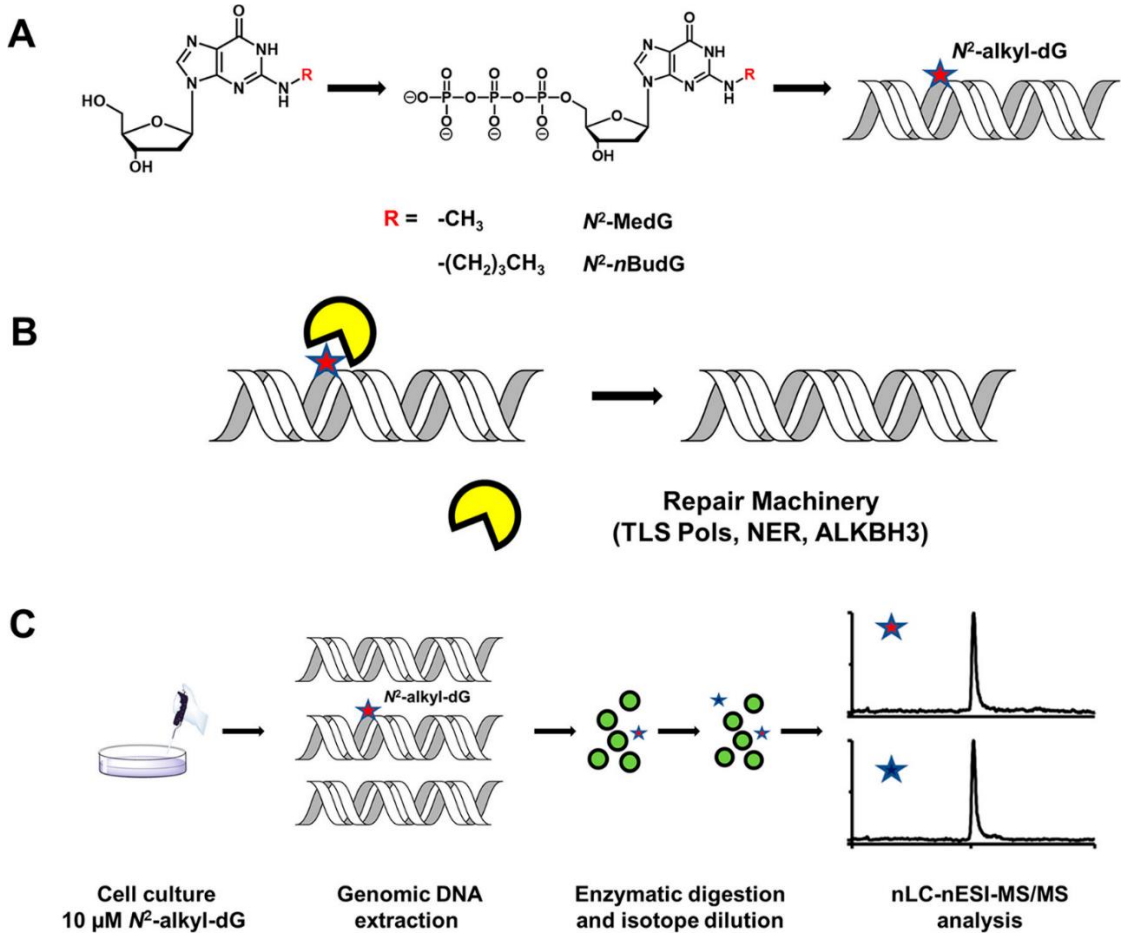

Figure 3.1. LC-MS/MS for assessing the incorporation and repair of N^2-alkyl-dG in genomic DNA. (A) Genomic incorporation of N^2-MedG and N^2-*n*BudG. (B) Repair of N^2-MedG and N^2-*n*BudG. (C) Schematic diagram showing the experimental workflow. Cells proficient or deficient in DNA repair were exposed with 10 μM of N^2-MedG or N^2-*n*BudG, and then incubated in fresh medium without the modified nucleosides for 3 or 8 h. The cells were harvested and genomic DNA extracted. Oligodeoxynucleotides containing a site-specifically inserted and stable isotope-labeled N^2-MedG or N^2-*n*BudG were spiked into the genomic DNA, which were subsequently digested to mononucleosides. The nucleoside mixtures were subjected to LC-MS/MS analysis.

3.2. Experimental sections

3.2.1. Materials

If not mentioned otherwise, all chemicals were purchased from Sigma-Aldrich (St. Louis, MO), and all enzymes were obtained from New England Biolabs (Ipswich, WA). HEK293T cells with *POLH*, *POLI*, *POLK*, *REV1* and *REV3L* genes being individually ablated by CRISPR were described previously,[30,36] while ALKBH1, ALKBH2, and ALKBH3 single knockout cells were generated following published procedures.[30,36] Repair-competent Chinese hamster ovary cells (CHO-AA8) and the isogenic ERCC1 knockout cells (CHO-7–27) were kindly provided by Prof. Michael Seidman (National Institute of Aging, Bethesda, MD).[37] Repair-proficient human skin fibroblasts (GM00637) and its XPA-deficient counterpart (GM04429) were generous gifts from Prof. Gerd P. Pfeifer (Van Andel Institute, Grand Rapids, MI).

3.2.2. Syntheses of N^2-MedG, N^2-*n*BudG and their corresponding stable isotope-labeled counterparts

Uniformly ^{15}N-labeled N^2-MedG ([$^{15}N_5$]-N^2-MedG) was synthesized previously.[24,33] N^2-MedG, N^2-*n*BudG, d_9-N^2-*n*BudG were prepared following published procedures.[34,35]

Syntheses N^2-*n*BudG and d_9-N^2-*n*BudG

N^2-*n*BudG was synthesized from 2-fluoro-6-*O*-(trimethylsilylethyl)-2′-deoxyinosine (**Scheme 3.1.**). Briefly, 2-fluoro-6-*O*-(trimethylsilylethyl)-2′-deoxyinosine (4.0 mg, 0.01 mmol) was dissolved in 80 µL dimethyl sulfoxide (DMSO), to which solution were added *n*-butylamine (5.0 µL, 0.05 mmol) and anhydrous *N*,*N*-diisopropylethylamine (DIEA, 3.8 µL, 0.02 mmol). The reaction mixture was stirred at 55°C for 3 days. The resulting mixture was dried *in vacuo*, reconstituted in 0.1 M acetic acid (100 µL) to deprotect the trimethylsilylethyl group. The solution was neutralized with an equal volume of 0.1 M sodium bicarbonate. The crude product was dried *in vacuo* and redissolved in 1 mL doubly distilled water.

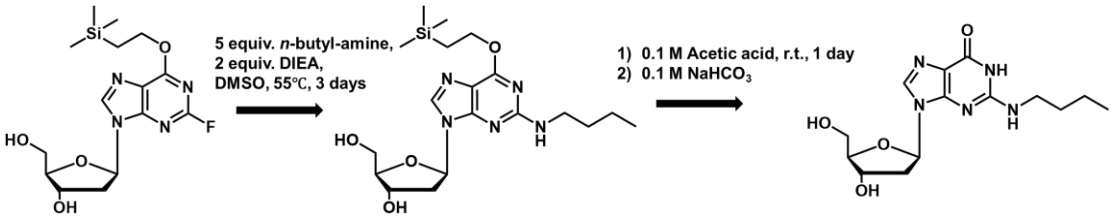

Scheme 3.1. Synthesis of N2-nBudG from 2-fluoro-6-O-(trimethylsilylethyl)-2'-deoxyinosine.

A similar approach was employed for the preparation of d_9-N^2-*n*BudG (**Scheme 3.2.**). In brief, 2-fluoro-6-*O*-(trimethylsilylethyl)-2′-deoxyinosine (5.7 mg, 0.015 mmol) was dissolved in 80 µL DMSO, to which solution were added d_9-*n*-butylamine (Toronto Research Chemicals, 37.9 µL, 0.045 mmol) dissolved in 100 µL DMSO and anhydrous DIEA (5.4 µL, 0.030 mmol). The reaction mixture was allowed to stir at 55 °C for 5 days. The resulting mixture was subsequently dried *in vacuo*. To the mixture was

subsequently added 0.1 M acetic acid (100 µL) and the mixture was stirred at room temperature for 24 h. The solution was again neutralized with sodium bicarbonate, and dried *in vacuo*.

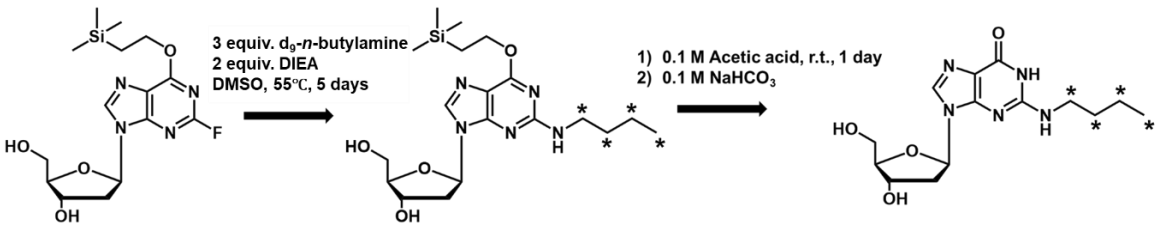

Scheme 3.2. Synthesis of d9-N2-nBudG. Asterisks represent those hydrogens that were replaced with deuterons.

Synthesis N^2-MedG

N^2-MedG was synthesized from 2-fluoro-6-*O*-(trimethylsilylethyl)-2′-deoxyinosine (**Scheme 3.3.**). Briefly, 2-fluoro-6-*O*-(trimethylsilylethyl)-2′-deoxyinosine (3.9 mg, 0.01 mmol) was dissolved in 80 µL anhydrous dimethyl sulfoxide (DMSO, Sigma Aldrich), to which solution were added methylamine (33% wt in absolute ethanol, Sigma Aldrich) (6.3 µL, 0.05 mmol) and anhydrous *N*,*N*-diisopropylethylamine (DIEA, 3.8 µL, 0.02 mmol). After stirring the reaction mixture at 55°C for 3 days, the reaction mixture was dried *in vacuo*, reconstituted in 5% acetic acid (100 µL) to deprotect the trimethylsilylethyl group. The solution was neutralized with an equal volume of 0.1 M sodium bicarbonate. The crude product was dried *in vacuo* and redissolved in 1 mL doubly distilled water.

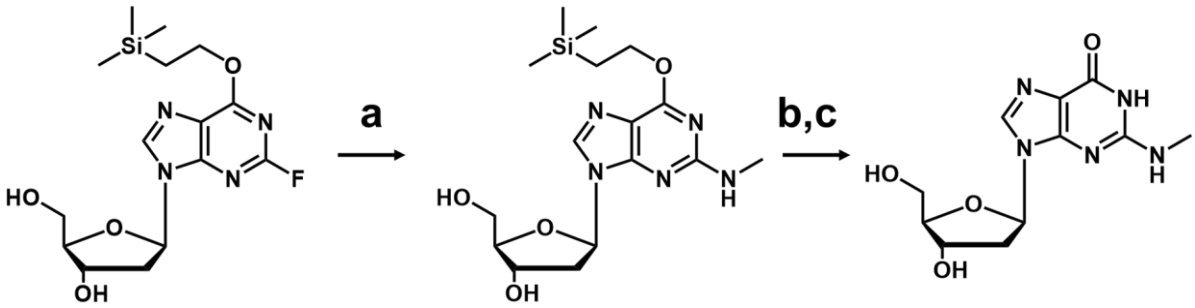

Scheme 3.3. Synthetic route for N2-MedG. a) Methylamine (5 equiv.)/ DIEA (2 equiv.)/ anhydrous DMSO, 55 °C, 3 days. b) 5% acetic acid, overnight. c) 0.1 M sodium bicarbonate.

3.2.3. HPLC purification of N^2-*n*BudG, d_9-N^2-*n*BudG and N^2-MedG

An ODS-silica column (10 × 250 mm, 10 μm in particle size, 100 Å in pore size, Soochow High Tech Chromatography Co.) was employed to purify N^2-*n*BudG, d_9-N^2-*n*BudG and N^2-MedG. Doubly distilled water and methanol were selected as mobile phases A and B, respectively. The gradient compromised of 10% B at 0-2 min and 10-80% B at 2-75 min, with the flow rate being 2.5 mL/min. The purified N^2-*n*BudG (**Figure 3.2.**), d_9-N^2-*n*BudG (**Figure 3.3.**) and N^2-MedG (**Figure 3.4.**) were confirmed by ESI-MS and MS/MS analyses, respectively.

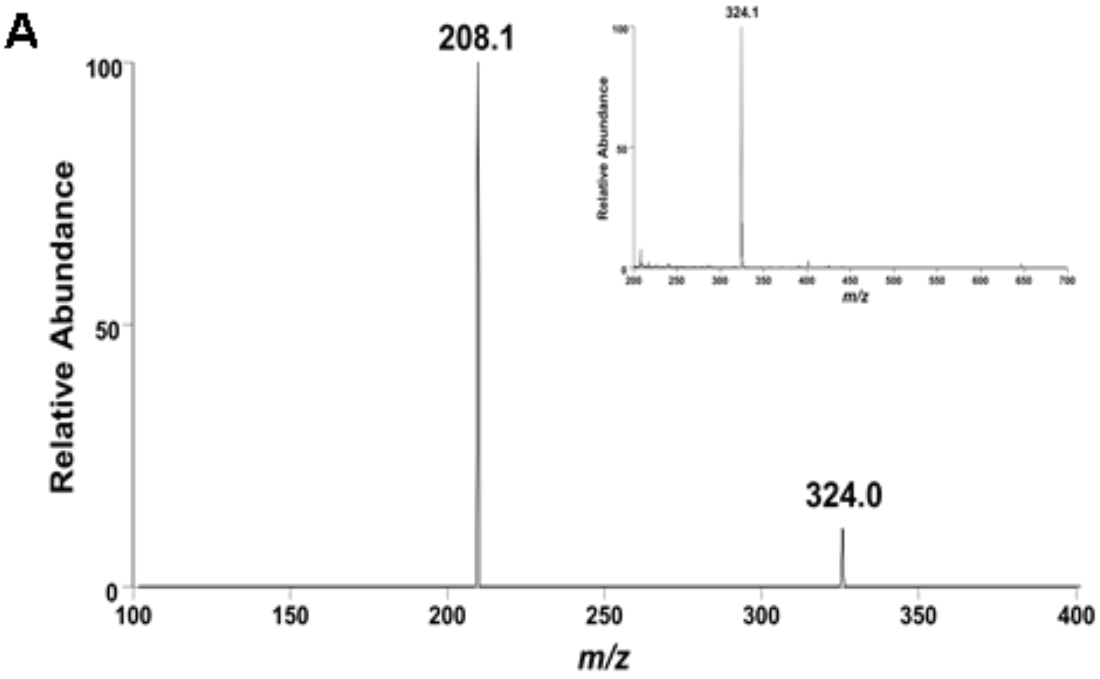

Figure 3.2. Positive-ion ESI-MS (insets) and MS^2 of N^2-*n*BudG. A neutral loss of deoxyribose (116 Da) was found in MS^2.

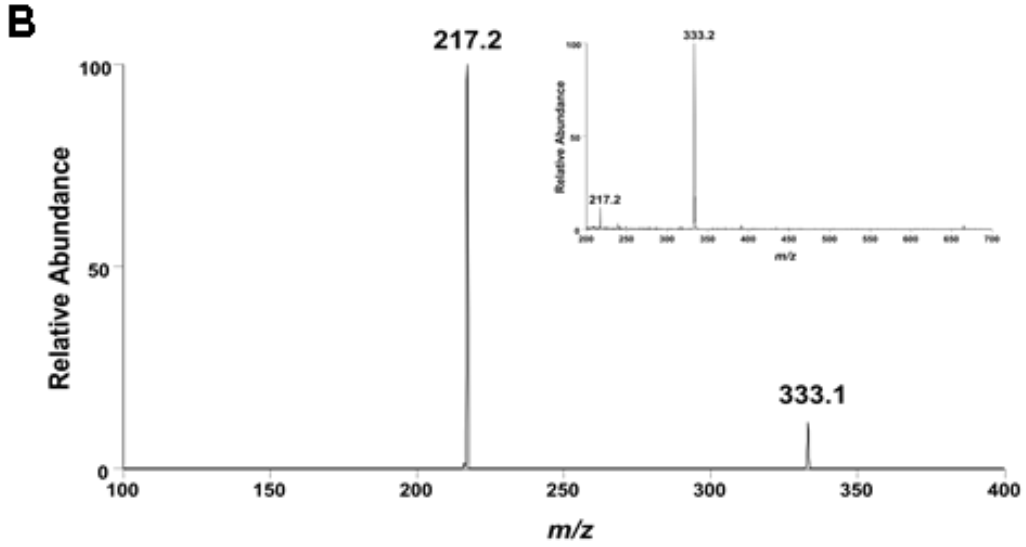

Figure 3.3. Positive-ion ESI-MS (insets) and MS^2 of d$_9$-N^2-*n*BudG. A neutral loss of deoxyribose (116 Da) was found in MS^2.

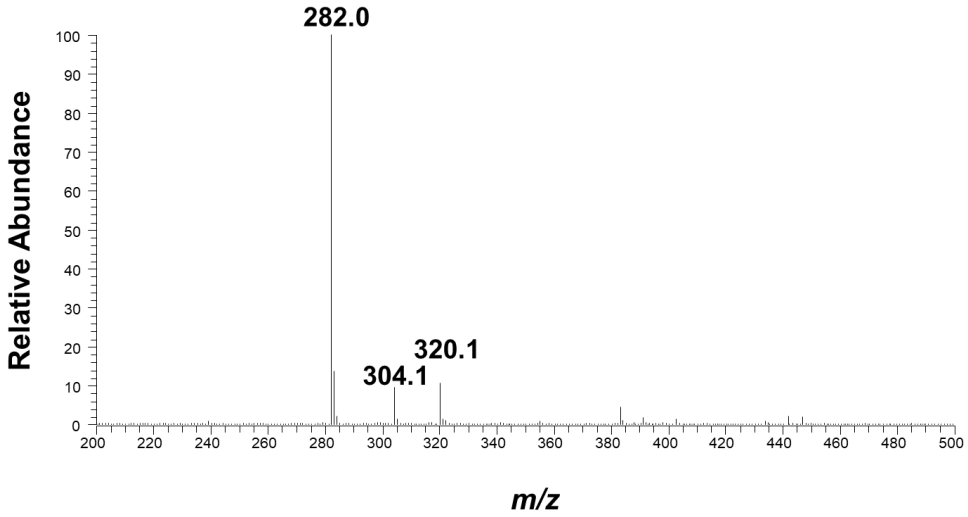

Figure 3.4. Positive ESI-MS analysis of the purified N^2-MedG.

3.2.4. Incorporation of N^2-*n*BudG and N^2-MedG into genomic DNA

HEK293T cells, TLS polymerase-deficient cells, NER-deficient cells and ALKBH1-3 knockout cells were seeded in 6-well plates at 37°C in a 5% CO_2 atmosphere. N^2-MedG and N^2-*n*BudG were added to the culture medium at a final concentration of 10 μM. After incubation for 3 h (for N^2-*n*BudG) or 16 h (for N^2-MedG), the cells were harvested immediately, or cultured for another 3 or 8 h in fresh media without the modified nucleoside, and harvested afterwards. Genomic DNA was extracted from cells using Qiagen DNeasy Blood & Tissue Kit, and approximately 6 μg DNA was recovered from a single well of cells.

3.2.5. Enzymatic digestion

Extracted genomic DNA was subjected to enzymatic digestion following previously published procedures.[14,24,38] In brief, 1.0 μg cellular DNA was digested with 10 units of nuclease P1 and 0.00125 unit of phosphodiesterase II in a buffer with 30 mM sodium acetate (pH 5.6), 1 mM $ZnCl_2$, and 2.5 nmol of *erythro*-*9*-(2-hydroxy-3-nonyl)adenine (EHNA, adenosine deaminase inhibitor). The above mixture was incubated at 37°C for 24 h. After then, 1.0 unit of alkaline phosphatase, 0.0025 unit of phosphodiesterase I and one tenth volume of 0.5 M Tris-HCl (pH 8.9) were added. The resulting mixture was incubated at 37°C for another 4 h, and subsequently neutralized with 1.0 M formic acid. The enzymes in the digestion mixture were then removed by

chloroform extraction. The aqueous phase was dried *in vacuo* and reconstituted in water for LC-MS/MS analysis.

3.2.6. Online nLC-MS/MS analysis of N^2-*n*BudG and N^2-MedG in cellular DNA

HPLC separation was conducted on a Dionex Ultimate 3000 HPLC module (Thermo Fisher) with an in-house packed trapping column (150 μm × 40 mm) and an analytical column (75 μm × 200 mm), both packed with Magic C18 AQ (200 Å, 5 μm, Michrom BioResource, Auburn, CA) reversed-phase materials. Mobile phases A and B comprised of 0.1% formic acid in doubly distilled water and acetonitrile, respectively. The sample was loaded onto the trapping column with mobile phase A at a flow rate of 2.5 μL/min in 8 min, and the analyte (N^2-*n*BudG) and its stable isotope-labeled standard were then eluted from the column by using a 20-min linear gradient of 0−95% mobile phase B at a flow rate of 300 nL/min.

The LC effluent was directed to a TSQ-Altis mass spectrometer operated in the multiple-reaction monitoring (MRM) mode. The MRM transitions corresponding to the neutral loss of a 2-deoxyribose (116 Da) from the protonated ions ($[M+H]^+$) of N^2-*n*BudG (i.e. *m/z* 324→208) and d_9-N^2-*n*BudG (i.e. *m/z* 333→217) were monitored (**Figure 3.5. B**). The voltage for electrospray was set at 2.0 kV and the temperature for the ion transport tube was maintained at 275°C. The widths for precursor and fragment ion selection were both 0.7 *m/z* unit, and the collision energy was set at 20 V.

N^2-MedG was quantified in a similar way except that a slower gradient was employed. In brief, the separation was conducted on a Dionex Ultimate 3000 module (Thermo Fisher Scientific Inc.) with a home-made trapping column (150 μm × 40 mm) and an analytical column (75 μm × 200 mm) packed with Magic C18 AQ (200 Å, 5 μm, Michrom BioResource, Auburn, CA) reversed-phase materials. Mobile phases A and B contained 0.1% formic acid in water and 0.1% formic acid in acetonitrile, respectively. The sample was loaded onto the trapping column with mobile phase A at a flow rate of 2.5 μL/min in 8 min, and the analyte (N^2-MedG) and its corresponding stable isotope-labeled standard were subsequently eluted from the column by using a 30-min linear gradient of 0−95% mobile phase B at a flow rate of 300 nL/min.

The LC effluent was directed to a TSQ-Altis triple-quadrupole mass spectrometer operated in the multiple-reaction monitoring (MRM) mode. The MRM transitions included the neutral loss of a 2-deoxyribose (116 Da) from the $[M+H]^+$ ions of N^2-MedG (i.e. *m/z* 282→166), as well as its stable isotope-labeled counterparts (*m/z* 287→171 for $[^{15}N_5]$-N^2-MedG) (**Figure 3.5. A**). The voltage for electrospray was 2.0 kV, and the temperature for the ion transfer tube was 275°C. The widths for precursor and fragment ion isolation were both 0.7 *m/z* unit, and the collision energy was 20 V.

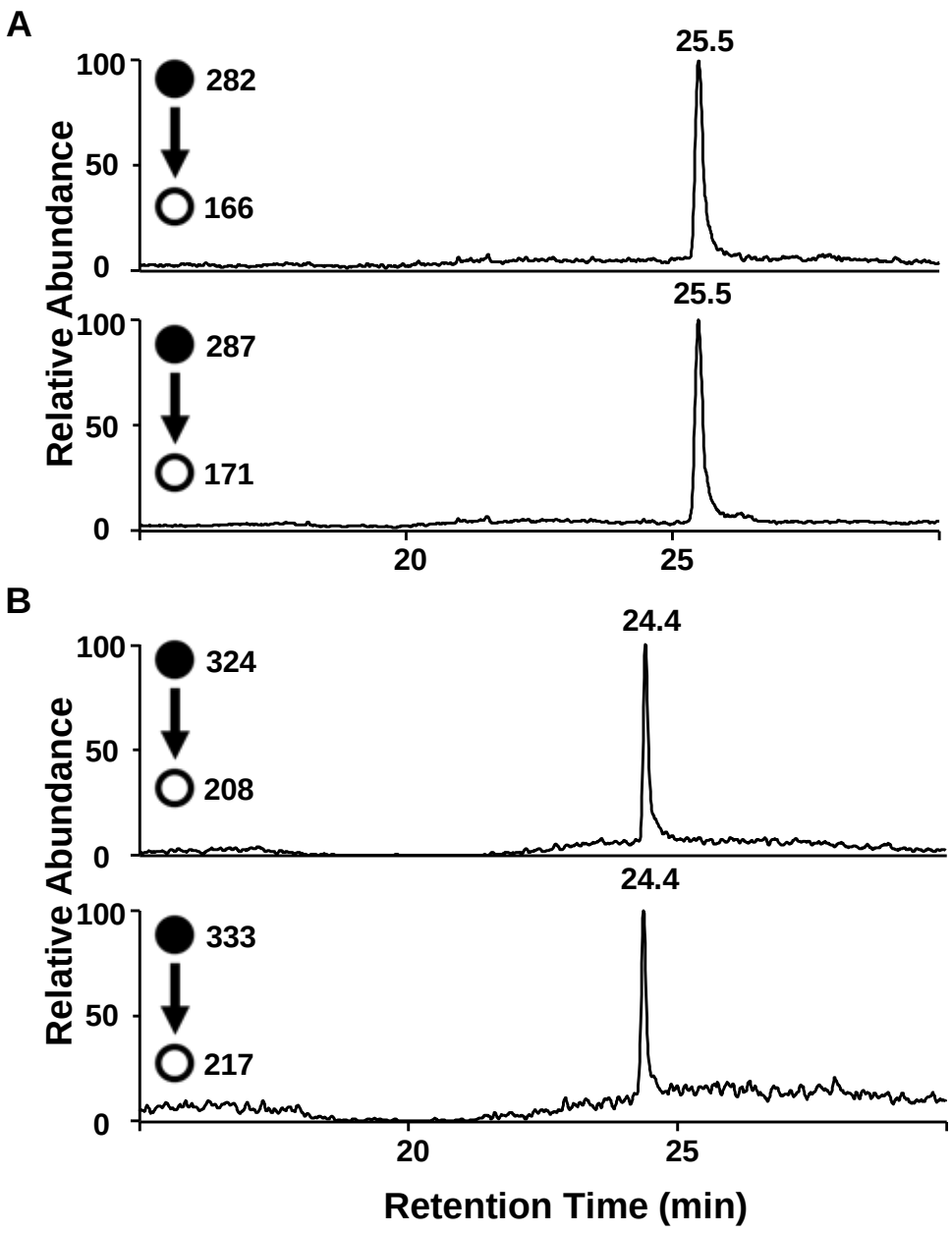

Figure 3.5. Representative selected-reaction monitoring chromatograms of the *m/z* 282 → 166 (A, top panel), 287 → 171 (A, bottom panel), 324 → 208 (B, top panel) and 333 → 217 (B, bottom panel) transitions for the $[M + H]^+$ ions of the unlabeled and stable isotope-labeled N^2-MedG (A), and N^2-*n*BudG (B), respectively, in the digested nucleosides of DNA extracted from CHO-AA8 cells treated with 10 μM N^2-MedG for 16 h or N^2-*n*BudG for 3 h, respectively.

3.2.7. Calibration curve for N^2-MedG

The calibration curve for N^2-MedG was constructed by spiking 1.0 µg calf thymus DNA with different amounts of an N^2-MedG-containing 12-mer ODN (5′-ATGGCGXGCTAT-3′, X= N^2-MedG) and a fixed amount (250 fmol) of [$^{15}N_5$]-N^2-MedG, followed by enzymatic digestion and LC-MS/MS analysis as mentioned above for the cellular DNA samples (**Figure 3.6.**).

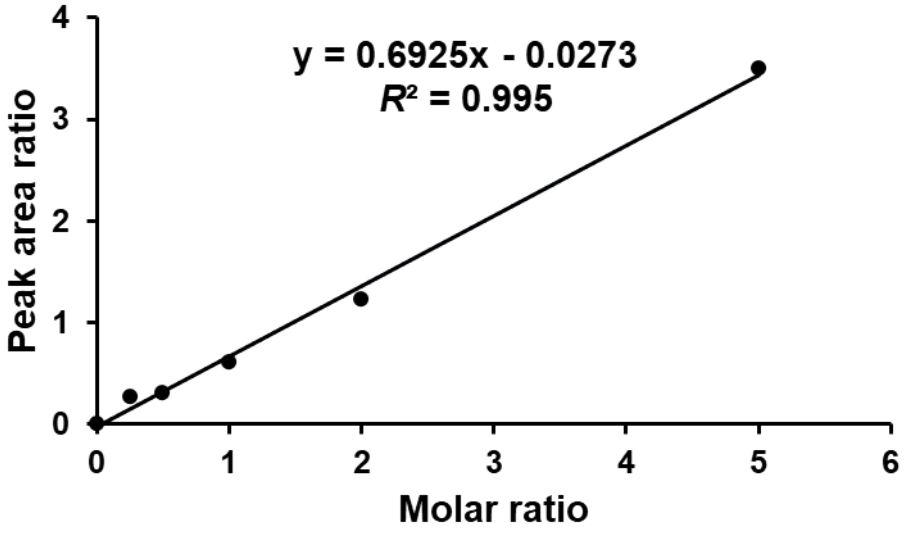

Figure 3.6. The calibration curve for the LC-MS/MS quantification of N^2-MedG. The samples used for the construction of the calibration curve compromised 1 μg calf thymus DNA, different amounts (0, 62.5, 125, 250, 500, 1250 fmol) of N^2-MedG containing 12-mer ODN, 5'-ATGGCGXGCTAT-3', where 'X' represents N^2-MedG) and a fixed amount of [$^{15}N_5$]-N^2-MedG (250 fmol), followed by enzymatic digestion and LC-MS/MS analysis as described in the main text. The calibration curve was constructed by plotting the peak area ratios found in the selected-ion chromatograms for the N^2-MedG /[$^{15}N_5$]-N^2-MedG vs. the molar ratio of N^2-MedG /[$^{15}N_5$]-N^2-MedG.

3.2.8. Calibration curve for N^2-*n*BudG

A calibration curve for N^2-*n*BudG was constructed by spiking 1.0 μg calf thymus DNA with different amounts (20, 40, 80, 200, 400, 800 and 2000 fmol) of an N^2-*n*BudG-containing 12-mer ODN and a fixed amount (400 fmol) of d_9-N^2-*n*Bu-dG; the samples were subjected to enzymatic digestion and LC-MS/MS analysis under the same conditions as described above for the cellular DNA samples (**Figure 3.7.**).

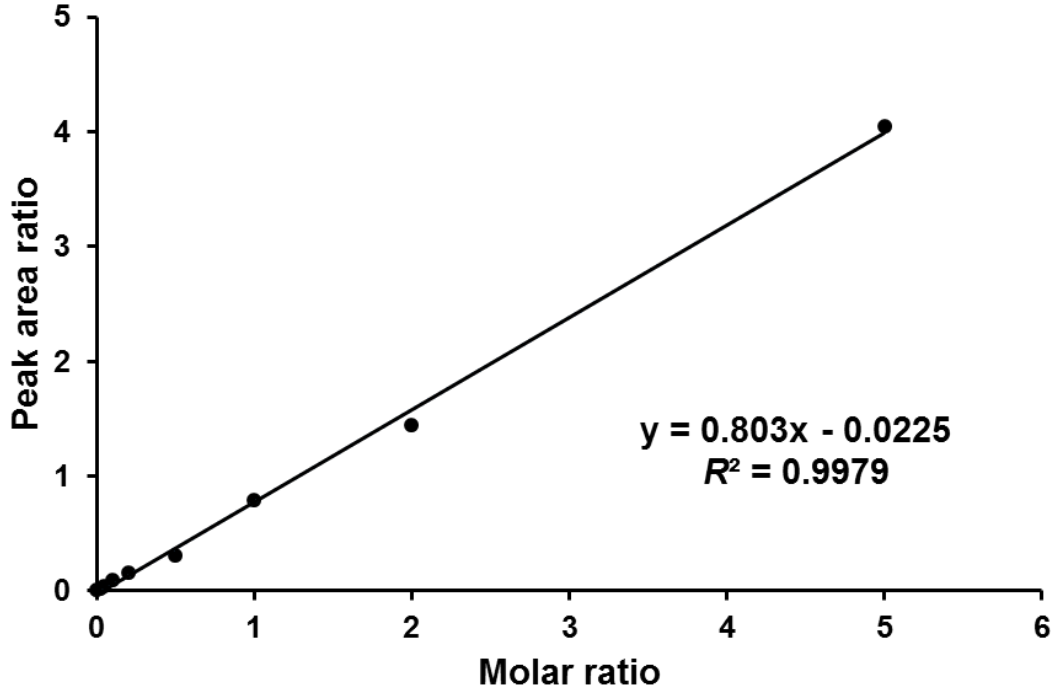

Figure 3.7. The calibration curve for the quantification of N^2-*n*Bu-dG. The samples used for the construction of the calibration curve compromised 1 μg calf thymus DNA, different amounts (20, 40, 80, 200, 400, 800 and 2000 fmol) of an N^2-*n*BudG containing oligodeoxyribonucleotide (ODN, 5′-ATGGCGXGCTAT-3′, where 'X' represents N^2-*n*BudG) and a fixed amount of d_9-N^2-*n*BudG (400 fmol). The calibration curve was constructed by plotting the peak area ratios found in the selected-ion chromatograms for the unlabeled/labeled N^2-*n*BudG vs. the molar ratios of the unlabeled/labeled N^2-*n*BudG.

3.3. Results

3.3.1. Pol κ and Pol η incorporate N^2-*n*BudG into genomic DNA

We found that incubating HEK293T cells with 10 μM N^2-*n*BudG for 3 hr results in the incorporation of a substantial level of N^2-*n*BudG into genomic DNA (**Figure 3.8.**). While individual ablation of Pol ι, Pol ζ or REV1 did not appreciably affect the incorporation of N^2-*n*BudG, losses of Pol κ and, to a lesser degree, Pol η gave rise to pronounced decreases in the incorporation of N^2-*n*BudG into genomic DNA. This is in keeping with the results from *in-vitro* biochemical assay, showing that Pol κ is highly efficient in inserting N^2-*n*BudG opposite a cytosine base in template DNA; Pol η also exhibits such a function, albeit at a much lower efficiency.

3.3.2. Pol κ is involved in the repair of N^2-*n*BudG, but not other TLS polymerases

Our LC-MS/MS results (**Figure 3.8.**) also revealed that, after removal of medium containing the modified nucleoside, cellular DNA displays a time-dependent decrease in the level of N^2-*n*BudG in parental HEK293T cells, or the isogenic cells depleted of Pol η, Pol ι, REV1, or Pol ζ, though the difference in the levels of N^2-*n*BudG in Pol η-deficient cells at 3 and 8 hr was not statistically significant. The loss of Pol κ, however, abrogated such a progressive decrease in the level of N^2-*n*BudG. These results, therefore, underscore that, among these TLS polymerases, Pol κ contributes to the removal of N^2-

*n*BudG from genomic DNA. In addition, our results suggest that Pol η may also assume a minor role in promoting the repair of N^2-*n*BudG in cells, but not as significant as Pol κ.

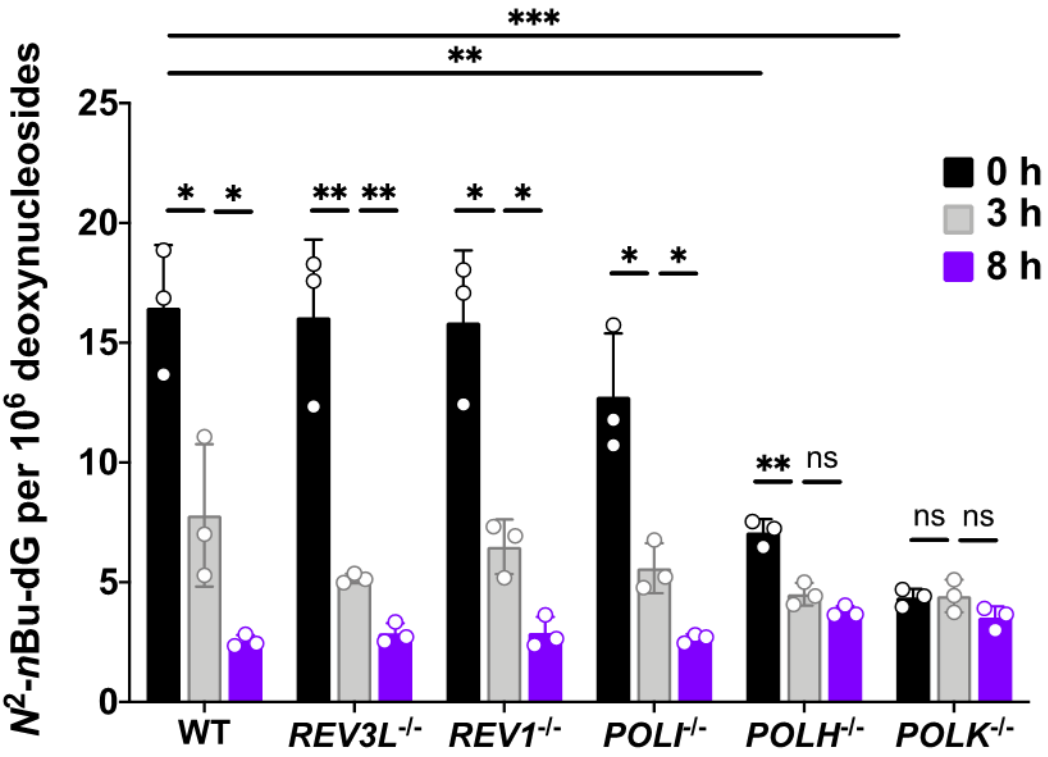

Figure 3.8. The frequencies of N^2-*n*BudG in cellular DNA isolated from parental and TLS polymerase-depleted HEK 293T cells. All cells were exposed to 10 μM of N^2-*n*BudG for 3 h. The cells were then harvested immediately, or after incubation in fresh media for another 3 or 8 h. The data represent the mean ± S.D. of results obtained from three independent experiments. *, 0.01 < *p* < 0.05; **, 0.001 < *p* < 0.01; ns, *p* > 0.05. The multiplicity adjusted *p* values were calculated by using multiple *t*-tests with Holm-Sidak correction for comparisons between 0 h and 3 h, and between 3 h and 8 h, by using one-way ANOVA and Dunnett's multiple comparisons test for the comparisons between parental HEK293T cells and the isogenic polymerase knockout cells at 0 h.

3.3.3. Pol κ and Pol η incorporate N^2-MedG into genomic DNA and contribute to its repair

To examine systematically the repair of N^2-MedG in mammalian cells, we extended our method for N^2-*n*BudG to include the quantification of N^2-MedG. In this respect, the N^2-alkyl-dG derivatives could be uptaken into cells and metabolically activated to yield the corresponding nucleoside triphosphates, which could be subsequently incorporated into genomic DNA by translesion synthesis DNA polymerases.[23,24] By using this method, we found that N^2-MedG was not detectable in genomic DNA isolated from HEK293T cells. After a 16-h incubation of HEK293T cells in a medium containing 10 μM N^2-MedG, we detected N^2-MedG at a level of approximately 90 modifications per 10^6 nucleosides (**Figure 3.9.**). It is of note that we did not observe any apparent alterations in the growth or survival of HEK293T cells upon exposure to N^2-MedG. Markedly lower levels of N^2-MedG were detected in genomic DNA from isogenic cells depleted of Pol κ or Pol η, underscoring their roles in the incorporation of N^2-MedG into genomic DNA. Other TLS Pols tested (i.e., Pol ι, REV1 and Pol ξ) did not exhibit any appreciable roles in the incorporation of N^2-MedG into genomic DNA, as their depletion did not result in any diminutions in the level of N^2-MedG incorporated into genomic DNA (**Figure 3.9.**).

Our time-dependent repair experiments suggest a possible role of TLS polymerases in the repair of N^2-MedG. Similar to our recently published result on N^2-*n*BudG,[24] Pol κ assumes an important role in the removal of N^2-MedG (**Figure 3.9.**). In

particular, while we observed a progressive decline in the level of N^2-MedG in genomic DNA of parental HEK293T cells at 0-8 h following exposure to the modified nucleoside, no appreciable drop in the level of N^2-MedG was detected for Pol κ-deficient cells (**Figure 3.9.**). However, different from our findings made for N^2-*n*BudG,[24] Pol η may also be involved in the repair of the less bulky N^2-MedG (**Figure 3.9.**). Deficiencies in other human TLS Pols investigated in this study, i.e., Pol ι, REV1 and Pol ξ, did not alter appreciably the time-dependent decreases in the levels of N^2-MedG, suggesting the lack of involvement of these polymerases in the repair of N^2-MedG in genomic DNA (**Figure 3.9.**).

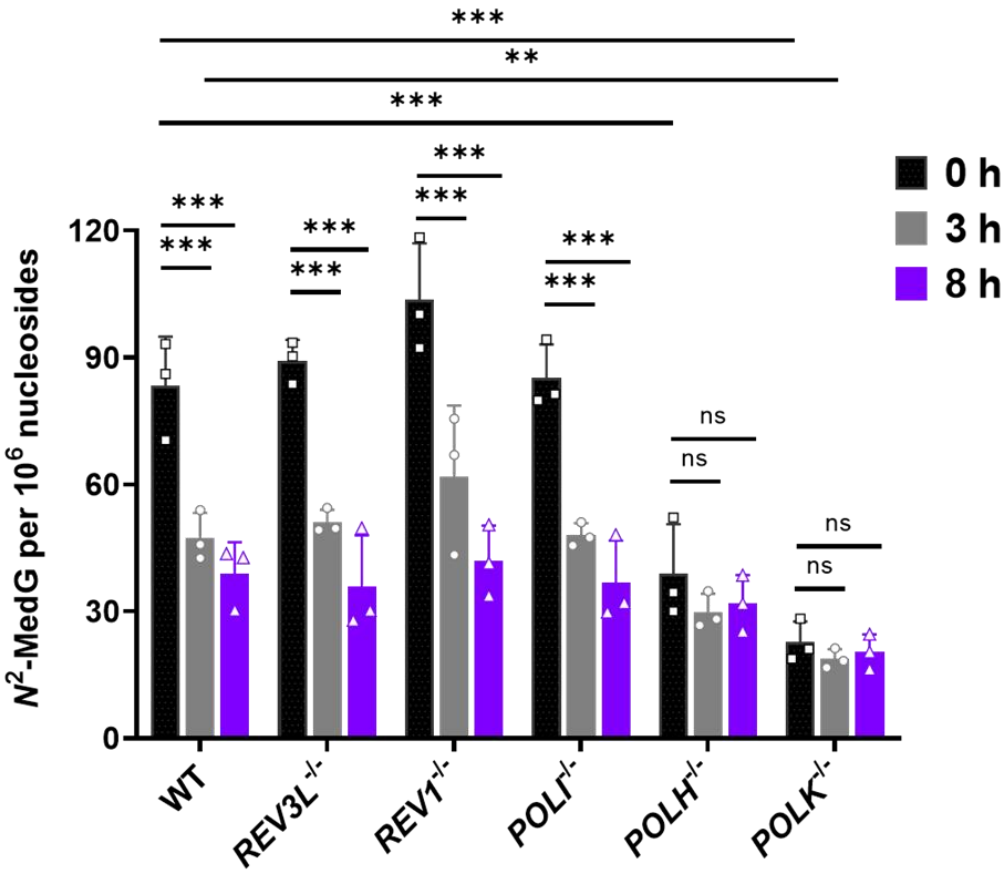

Figure 3.9. The frequencies of N^2-MedG in cellular DNA isolated from parental and TLS polymerase-depleted HEK293T cells. All cells were exposed to 10 μM of N^2-MedG for 16 h. The cells were then harvested immediately, or after incubation in fresh media for another 3 or 8 h. The data represent the mean ± S.D. of results obtained from three independent experiments. ns, $p > 0.05$; *, $0.01 < p < 0.05$; **, $0.001 < p < 0.01$; ***, $p < 0.001$. The p values were calculated by one-way ANOVA with Tuckey's multiple comparisons test.

3.3.4. The involvement of NER in the removal of N^2-alkyl-dG from human cells

We next conducted our time-dependent repair experiments in mammalian cells proficient in DNA repair or deficient in NER factors (**Figure 3.10.**). We found that depletion of two NER proteins, i.e., xeroderma pigmentosum complementation group A (XPA) protein and endonuclease ERCC1, both led to diminished removal of the two minor-groove N^2-alkyl-dG lesions, revealing the contributions of NER in the repair of these two lesions in mammalian cells.

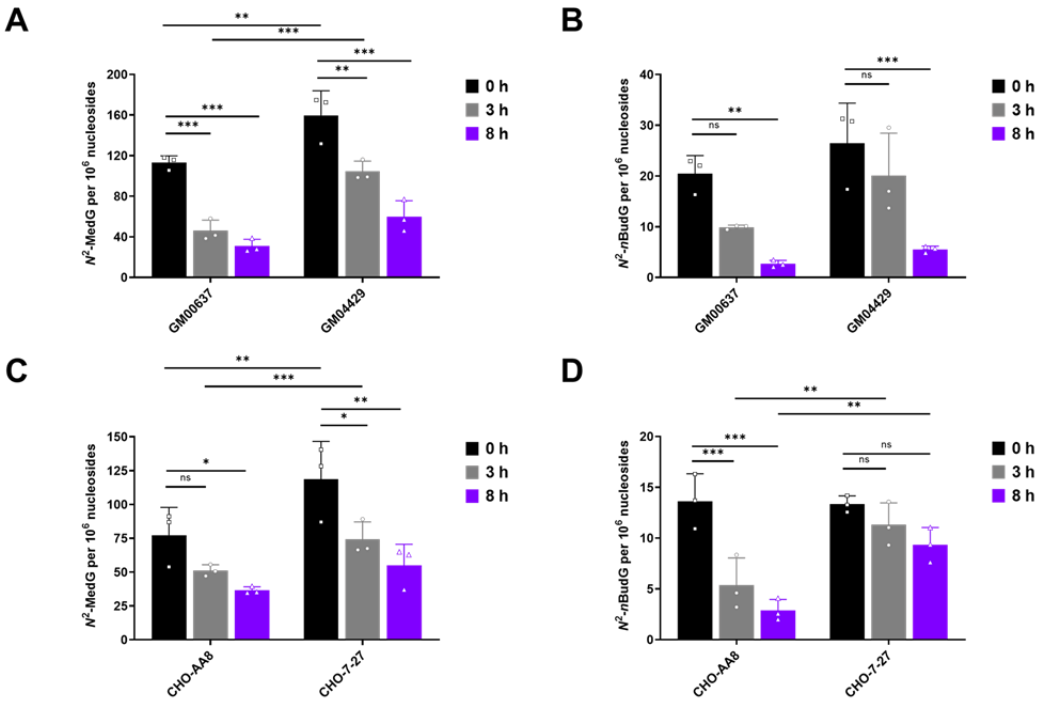

Figure 3.10. LC-MS/MS results of N^2-MedG (A, C) and N^2-*n*BudG (B, D) in cellular DNA isolated from NER-competent and -deficient cells. After a 16-h exposure to 10 μM of N^2-MedG or 3-h exposure to 10 μM of N^2-*n*BudG, the cells were then harvested immediately, or cultured in fresh medium without the modified nucleosides for another 3 or 8 h. The data represent the mean ± S.D. of results obtained from three biological replicates. ns, $p > 0.05$; *, $0.01 < p < 0.05$; **, $0.001 < p < 0.01$; ***, $p < 0.001$. The p values were calculated by one-way ANOVA with Tuckey's multiple comparisons test.

3.3.5. Human ALKBH3 may be involved in the removal of N^2-alkyl-dG lesions from the nucleotide pool

Our quantification results revealed a potential role of human AlkB analog ALKBH3, but not ALKBH1 or ALKBH2, in the reversal of the N^2-alkyl-dG lesions in the nucleotide pool (**Figure 3.11.**). We observed elevated level of N^2-MedG and N^2-*n*BudG in the genomic DNA of ALKBH3-depleted cells compared to isogenic HEK293T cells after exposure to the modified nucleosides, i.e., 160 vs. 90 N^2-MedG and 32 vs. 21 N^2-*n*BudG per 10^6 nucleosides, from ALKBH3 knockout cells and WT cells, respectively. Similar to what we observed for parental HEK293T cells, the levels of N^2-MedG and N^2-*n*BudG exhibit progressive decline over time in ALKBH3-deficient cells, suggesting that the two lesions in genomic DNA can still be repaired in ALKBH3-deficient background. Hence, increased levels of the N^2-MedG and N^2-*n*BudG observed in ALKBH3-deficient cells may arise from their diminished removal from the nucleotide pool.

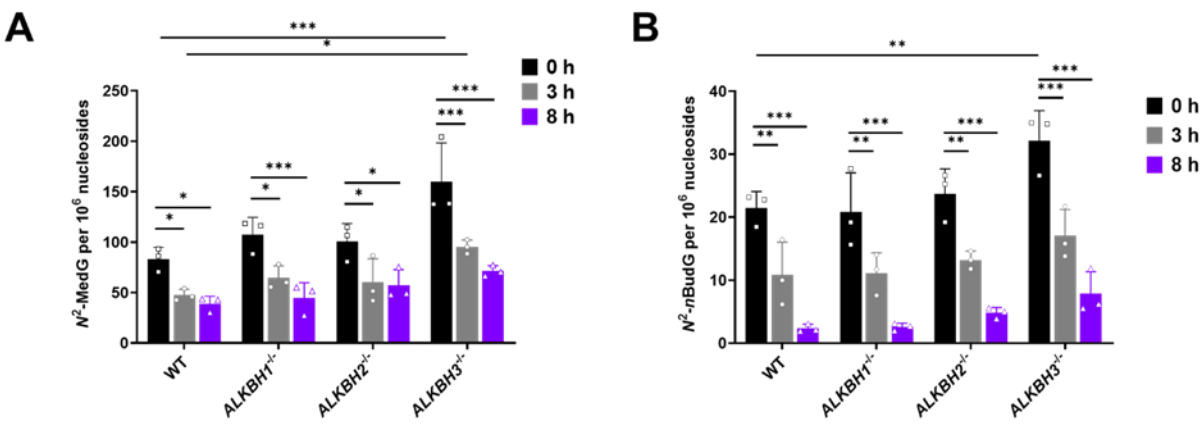

Figure 3.11. Elevated level of N^2-MedG (A) and N^2-*n*BudG (B) were observed in cellular DNA isolated from ALKBH3-depleted cells. After a 16-h exposure to 10 μM of N^2-MedG or 3-h exposure to 10 μM of N^2-*n*BudG, respectively, isogenic HEK293T cells and ALKBH1-3 individually knockout cells were then harvested for DNA extraction immediately, or after incubation in fresh media without N^2-MedG or N^2-*n*BudG for another 3 or 8 h. The data represent the mean ± S.D. of results obtained from three biological replicates. *, 0.01< p < 0.05; **, 0.001< p < 0.01; ***, p < 0.001. The p values were calculated by one-way ANOVA with Tuckey's multiple comparisons test.

3.4. Discussion

Substantial efforts have been made to assess the occurrence and repair of structurally defined DNA lesions.[6,9,39] Exposing laboratory animals or cultured cells with DNA damaging agents is widely adopted and represents one of the most reliable and efficient ways to discover novel DNA lesions and/or quantify DNA lesions.[6,11] After removing exogenous chemicals in diet or cell culture medium, researchers can further assess the repair of DNA lesions of interest by monitoring time-dependent decreases in the levels of DNA lesions. The method may provide important knowledge about the

occurrence and repair of DNA lesions induced by carcinogenic chemicals, thereby informing risk assessment.[9,11] The method, however, poses limitations sometimes. In particular, chemical exposure often gives rise to a wide-spectrum of lesions. For instance, exposure to 4-(methylnitrosamino)-1-(3-pyridyl)-1-butanone (NNK), a carcinogen found in tobacco and its combustion products, can induce a number of alkylation adducts formed on the nucleobases and backbone phosphates in DNA.[12,13,40] Metabolic labeling of genomic DNA with a structurally defined nucleoside can overcome this limitation by enabling selective incorporation of the modified nucleoside without the complicating effects of other DNA lesions.[22–24]

In this study, we employed a metabolic labeling method to introduce minor-groove N^2-MedG and N^2-*n*BudG into genomic DNA. After their incorporation into genomic DNA, we interrogated how their removals are modulated by DNA repair machinery and TLS polymerases. We found that Pol κ and Pol η play important roles in the incorporation of N^2-MedG into the human genome. Interestingly, both Pols also contribute to the repair of N^2-MedG. Pol η is known to confer intrinsic resistance to chemotherapy,[41] while Pol κ-deficient mouse embryonic fibroblasts display decreased NER of UV-induced DNA lesions.[42] Taken these previous findings with our results together, Pol κ and η may function in DNA repair, which further expands their roles beyond translesion synthesis. It remains unclear why Pol η does not prominently modulate the repair of the more bulky N^2-*n*BudG.[24]

NER is a versatile DNA repair pathway that removes a plethora of lesions from DNA.[43] Bulky BPDE adducts formed at the N^2 position of dG is a good substrate for NER.[31] Recent discovery from Patel and coworkers[27] demonstrates that NER is required to protect mammalian cells against formaldehyde toxicity and N^2-dG adduct induced by the aldehyde. In line with these previous findings, our results unveil that NER contributes to the repair of both N^2-MedG and N^2-*n*BudG.

The AlkB family of Fe(II)- and α-ketoglutarate-dependent dioxygenases perform direct reversal by oxidative dealkylation that removes various alkyl adducts.[44] It was first found in *E. coli* and was considered as "adaptive response" protein that protects against alkylation.[45–47] AlkB has many substrates, from simple alkyl chain adducts to small exocyclic etheno adducts.[32,44,48,49] Human genome encodes nine AlkB homologs (i.e., ALKBH1–8, FTO), and, among them, ALKBH2 and ALKBH3 are DNA repair enzymes.[44,50–52] Our results showed that N^2-MedG and N^2-*n*BudG are elevated in genomic DNA of ALKBH3-depleted cells compared to parental repair-proficient cells after exposure to these two modified nucleosides in culture medium. Nevertheless, the level of N^2-alkyl-dG in genomic DNA of ALKBH3-deficient cells decreased gradually with time, in a manner similar to that found for parental HEK293T cells. Hence, ALKBH3 may reverse N^2-alkyl-dG in the nucleotide pool prior to its incorporation into genomic DNA, and its depletion may lead to high levels of N^2-alkyl-dG in the nucleotide pool, which may ultimately result in the incorporation of a higher level of N^2-alkyl-dG into genomic DNA.

Taken together, we employed a metabolic labeling method to incorporate minor-groove N^2-MedG and N^2-*n*BudG into genomic DNA. We also conducted a systematic repair study on these two lesions. Our results revealed the roles of TLS polymerases, NER and ALKBH3 in the repair of these lesions in mammalian cells. It will be interesting to examine, in the future, whether the method can also be employed for assessing the metabolic incorporation and repair of bulky aromatic hydrocarbon-induced N^2-dG adducts, e.g., N^2-BPDE-dG.

References

(1) Friedberg, E. C.; Walker, G. C.; Siede, W.; Wood, R. D. *DNA Repair and Mutagenesis*; American Society for Microbiology Press, 2005.

(2) Lindahl, T.; Wood, R. D. Quality Control by DNA Repair. *Science* **1999**, *286* (5446), 1897–1905. https://doi.org/10.1126/science.286.5446.1897.

(3) Fu, D.; Calvo, J. A.; Samson, L. D. Balancing Repair and Tolerance of DNA Damage Caused by Alkylating Agents. *Nat. Rev. Cancer* **2012**, *12* (2), 104–120. https://doi.org/10.1038/nrc3185.

(4) Shrivastav, N.; Li, D.; Essigmann, J. M. Chemical Biology of Mutagenesis and DNA Repair: Cellular Responses to DNA Alkylation. *Carcinogenesis* **2010**, *31* (1), 59–70. https://doi.org/10.1093/carcin/bgp262.

(5) Bauer, N. C.; Corbett, A. H.; Doetsch, P. W. The Current State of Eukaryotic DNA Base Damage and Repair. *Nucleic Acids Res.* **2015**, *43* (21), 10083–10101. https://doi.org/10.1093/nar/gkv1136.

(6) Yu, Y.; Wang, P.; Cui, Y.; Wang, Y. Chemical Analysis of DNA Damage. *Anal. Chem.* **2018**, *90* (1), 556–576. https://doi.org/10.1021/acs.analchem.7b04247.

(7) Hofer, A.; Liu, Z. J.; Balasubramanian, S. Detection, Structure and Function of Modified DNA Bases. *J. Am. Chem. Soc.* **2019**, *141* (16), 6420–6429. https://doi.org/10.1021/jacs.9b01915.

(8) Tretyakova, N.; Villalta, P. W.; Kotapati, S. Mass Spectrometry of Structurally Modified DNA. *Chem. Rev.* **2013**, *113* (4), 2395–2436. https://doi.org/10.1021/cr300391r.

(9) Liu, S.; Wang, Y. Mass Spectrometry for the Assessment of the Occurrence and Biological Consequences of DNA Adducts. *Chem. Soc. Rev.* **2015**, *44* (21), 7829–7854. https://doi.org/10.1039/C5CS00316D.

(10) Tretyakova, N.; Goggin, M.; Sangaraju, D.; Janis, G. Quantitation of DNA Adducts by Stable Isotope Dilution Mass Spectrometry. *Chem. Res. Toxicol.* **2012**, *25* (10), 2007–2035. https://doi.org/10.1021/tx3002548.

(11) Hwa Yun, B.; Guo, J.; Bellamri, M.; Turesky, R. J. DNA Adducts: Formation, Biological Effects, and New Biospecimens for Mass Spectrometric Measurements in Humans. *Mass Spectrom. Rev.* **2020**, *39* (1–2), 55–82. https://doi.org/10.1002/mas.21570.

(12) Hecht, S. S. DNA Adduct Formation from Tobacco-Specific N-Nitrosamines. *Mutat. Res. Mol. Mech. Mutagen.* **1999**, *424* (1), 127–142. https://doi.org/10.1016/S0027-5107(99)00014-7.

(13) Leng, J.; Wang, Y. Liquid Chromatography-Tandem Mass Spectrometry for the Quantification of Tobacco-Specific Nitrosamine-Induced DNA Adducts in Mammalian Cells. *Anal. Chem.* **2017**, *89* (17), 9124–9130. https://doi.org/10.1021/acs.analchem.7b01857.

(14) Guo, S.; Leng, J.; Tan, Y.; Price, N. E.; Wang, Y. Quantification of DNA Lesions Induced by 4-(Methylnitrosamino)-1-(3-Pyridyl)-1-Butanol in Mammalian Cells. *Chem. Res. Toxicol.* **2019**, *32* (4), 708–717. https://doi.org/10.1021/acs.chemrestox.8b00374.

(15) LePage, G. A. Basic Biochemical Effects and Mechanism of Action of 6-Thioguanine. *Cancer Res.* **1963**, *23* (8_Part_1), 1202–1206.

(16) Elion, G. B. The Purine Path to Chemotherapy. *Science* **1989**, *244* (4900), 41–47. https://doi.org/10.1126/science.2649979.

(17) Salic, A.; Mitchison, T. J. A Chemical Method for Fast and Sensitive Detection of DNA Synthesis in Vivo. *Proc. Natl. Acad. Sci.* **2008**, *105* (7), 2415–2420. https://doi.org/10.1073/pnas.0712168105.

(18) Kantarjian, H.; Issa, J.-P. J.; Rosenfeld, C. S.; Bennett, J. M.; Albitar, M.; DiPersio, J.; Klimek, V.; Slack, J.; de Castro, C.; Ravandi, F.; Helmer, R.; Shen, L.; Nimer, S. D.; Leavitt, R.; Raza, A.; Saba, H. Decitabine Improves Patient Outcomes in Myelodysplastic Syndromes: Results of a Phase III Randomized Study. *Cancer* **2006**, *106* (8), 1794–1803. https://doi.org/10.1002/cncr.21792.

(19) Wang, H.; Wang, Y. LC-MS/MS Coupled with Stable Isotope Dilution Method for the Quantification of 6-Thioguanine and S6-Methylthioguanine in Genomic DNA of Human Cancer Cells Treated with 6-Thioguanine. *Anal. Chem.* **2010**, *82* (13), 5797–5803. https://doi.org/10.1021/ac1008628.

(20) Fantoni, N. Z.; El-Sagheer, A. H.; Brown, T. A Hitchhiker's Guide to Click-Chemistry with Nucleic Acids. *Chem. Rev.* **2021**, *121* (12), 7122–7154. https://doi.org/10.1021/acs.chemrev.0c00928.

(21) Zauri, M.; Berridge, G.; Thézénas, M.-L.; Pugh, K. M.; Goldin, R.; Kessler, B. M.; Kriaucionis, S. CDA Directs Metabolism of Epigenetic Nucleosides Revealing a Therapeutic Window in Cancer. *Nature* **2015**, *524* (7563), 114–118. https://doi.org/10.1038/nature14948.

(22) Liu, X.; Lai, W.; Li, Y.; Chen, S.; Liu, B.; Zhang, N.; Mo, J.; Lyu, C.; Zheng, J.; Du, Y.-R.; Jiang, G.; Xu, G.-L.; Wang, H. N6-Methyladenine Is Incorporated into Mammalian Genome by DNA Polymerase. *Cell Res.* **2021**, *31* (1), 94–97. https://doi.org/10.1038/s41422-020-0317-6.

(23) Prakasha Gowda, A. S.; Lee, M.; Spratt, T. E. N2-Substituted 2′-Deoxyguanosine Triphosphate Derivatives, Selective Substrates for Human DNA Polymerase κ. *Angew. Chem. Int. Ed Engl.* **2017**, *56* (10), 2628–2631. https://doi.org/10.1002/anie.201611607.

(24) Tan, Y.; Guo, S.; Wu, J.; Du, H.; Li, L.; You, C.; Wang, Y. DNA Polymerase η Promotes the Transcriptional Bypass of N2-Alkyl-2'-Deoxyguanosine Adducts in Human Cells. *J. Am. Chem. Soc.* **2021**, *143* (39), 16197–16205. https://doi.org/10.1021/jacs.1c07374.

(25) Pfeifer, G. P.; Denissenko, M. F.; Olivier, M.; Tretyakova, N.; Hecht, S. S.; Hainaut, P. Tobacco Smoke Carcinogens, DNA Damage and P53 Mutations in Smoking-Associated Cancers. *Oncogene* **2002**, *21* (48), 7435–7451. https://doi.org/10.1038/sj.onc.1205803.

(26) Cheng, G.; Shi, Y.; Sturla, S. J.; Jalas, J. R.; McIntee, E. J.; Villalta, P. W.; Wang, M.; Hecht, S. S. Reactions of Formaldehyde Plus Acetaldehyde with Deoxyguanosine and DNA: Formation of Cyclic Deoxyguanosine Adducts and Formaldehyde Cross-Links. *Chem. Res. Toxicol.* **2003**, *16* (2), 145–152. https://doi.org/10.1021/tx025614r.

(27) Mulderrig, L.; Garaycoechea, J. I.; Tuong, Z. K.; Millington, C. L.; Dingler, F. A.; Ferdinand, J. R.; Gaul, L.; Tadross, J. A.; Arends, M. J.; O'Rahilly, S.; Crossan, G. P.; Clatworthy, M. R.; Patel, K. J. Aldehyde-Driven Transcriptional Stress Triggers an Anorexic DNA Damage Response. *Nature* **2021**, *600* (7887), 158–163. https://doi.org/10.1038/s41586-021-04133-7.

(28) Pontel, L. B.; Rosado, I. V.; Burgos-Barragan, G.; Garaycoechea, J. I.; Yu, R.; Arends, M. J.; Chandrasekaran, G.; Broecker, V.; Wei, W.; Liu, L.; Swenberg, J. A.; Crossan, G. P.; Patel, K. J. Endogenous Formaldehyde Is a Hematopoietic Stem Cell Genotoxin and Metabolic Carcinogen. *Mol. Cell* **2015**, *60* (1), 177–188. https://doi.org/10.1016/j.molcel.2015.08.020.

(29) Yuan, B.; You, C.; Andersen, N.; Jiang, Y.; Moriya, M.; O'Connor, T. R.; Wang, Y. The Roles of DNA Polymerases κ and ι in the Error-Free Bypass of N2-Carboxyalkyl-2′-Deoxyguanosine Lesions in Mammalian Cells*. *J. Biol. Chem.* **2011**, *286* (20), 17503–17511. https://doi.org/10.1074/jbc.M111.232835.

(30) Wu, J.; Du, H.; Li, L.; Price, N. E.; Liu, X.; Wang, Y. The Impact of Minor-Groove N2-Alkyl-2′-Deoxyguanosine Lesions on DNA Replication in Human Cells. *ACS Chem. Biol.* **2019**, *14* (8), 1708–1716. https://doi.org/10.1021/acschembio.9b00129.

(31) Shafirovich, V.; Kolbanovskiy, M.; Kropachev, K.; Liu, Z.; Cai, Y.; Terzidis, M. A.; Masi, A.; Chatgilialoglu, C.; Amin, S.; Dadali, A.; Broyde, S.; Geacintov, N. E. Nucleotide Excision Repair and Impact of Site-Specific 5',8-Cyclopurine and Bulky DNA Lesions on the Physical Properties of Nucleosomes. *Biochemistry* **2019**, *58* (6), 561–574. https://doi.org/10.1021/acs.biochem.8b01066.

(32) Li, D.; Fedeles, B. I.; Shrivastav, N.; Delaney, J. C.; Yang, X.; Wong, C.; Drennan, C. L.; Essigmann, J. M. Removal of N-Alkyl Modifications from N2-Alkylguanine and N4-Alkylcytosine in DNA by the Adaptive Response Protein AlkB. *Chem. Res. Toxicol.* **2013**, *26* (8), 1182–1187. https://doi.org/10.1021/tx400096m.

(33) Cui, Y.; Wang, P.; Yu, Y.; Yuan, J.; Wang, Y. Normalized Retention Time for Targeted Analysis of the DNA Adductome. *Anal. Chem.* **2018**, *90* (24), 14111–14115. https://doi.org/10.1021/acs.analchem.8b04660.

(34) Harris, T. M.; Harris, C. M. Synthesis of N2-Substituted Deoxyguanosine Nucleosides from 2-Fluoro-6-O-(Trimethylsilylethyl)-2′ -Deoxyinosine. *Curr. Protoc. Nucleic Acid Chem.* **2000**, *00* (1), 1.3.1-1.3.19. https://doi.org/10.1002/0471142700.nc0103s00.

(35) Cao, H.; Jiang, Y.; Wang, Y. Stereospecific Synthesis and Characterization of Oligodeoxyribonucleotides Containing an N2-(1-Carboxyethyl)-2‘-Deoxyguanosine. *J. Am. Chem. Soc.* **2007**, *129* (40), 12123–12130. https://doi.org/10.1021/ja072130e.

(36) Wu, J.; Li, L.; Wang, P.; You, C.; Williams, N. L.; Wang, Y. Translesion Synthesis of O4-Alkylthymidine Lesions in Human Cells. *Nucleic Acids Res.* **2016**, *44* (19), 9256–9265. https://doi.org/10.1093/nar/gkw662.

(37) Rolig, R. L.; Layher, S. K.; Santi, B.; Adair, G. M.; Gu, F.; Rainbow, A. J.; Nairn, R. S. Survival, Mutagenesis, and Host Cell Reactivation in a Chinese Hamster Ovary Cell ERCC1 Knock-out Mutant. *Mutagenesis* **1997**, *12* (4), 277–283. https://doi.org/10.1093/mutage/12.4.277.

(38) Wang, J.; Yuan, B.; Guerrero, C.; Bahde, R.; Gupta, S.; Wang, Y. Quantification of Oxidative DNA Lesions in Tissues of Long-Evans Cinnamon Rats by Capillary High-Performance Liquid Chromatography-Tandem Mass Spectrometry Coupled with Stable Isotope-Dilution Method. *Anal. Chem.* **2011**, *83* (6), 2201–2209. https://doi.org/10.1021/ac103099s.

(39) Yuan, B.-F. Assessment of DNA Epigenetic Modifications. *Chem. Res. Toxicol.* **2020**, *33* (3), 695–708. https://doi.org/10.1021/acs.chemrestox.9b00372.

(40) Ma, B.; Villalta, P. W.; Zarth, A. T.; Kotandeniya, D.; Upadhyaya, P.; Stepanov, I.; Hecht, S. S. Comprehensive High-Resolution Mass Spectrometric Analysis of DNA Phosphate Adducts Formed by the Tobacco-Specific Lung Carcinogen 4-(Methylnitrosamino)-1-(3-Pyridyl)-1-Butanone. *Chem. Res. Toxicol.* **2015**, *28* (11), 2151–2159. https://doi.org/10.1021/acs.chemrestox.5b00318.

(41) Albertella, M. R.; Green, C. M.; Lehmann, A. R.; O'Connor, M. J. A Role for Polymerase η in the Cellular Tolerance to Cisplatin-Induced Damage. *Cancer Res.* **2005**, *65* (21), 9799–9806. https://doi.org/10.1158/0008-5472.CAN-05-1095.

(42) Ogi, T.; Lehmann, A. R. The Y-Family DNA Polymerase Kappa (Pol Kappa) Functions in Mammalian Nucleotide-Excision Repair. *Nat. Cell Biol.* **2006**, *8* (6), 640–642. https://doi.org/10.1038/ncb1417.

(43) Marteijn, J. A.; Lans, H.; Vermeulen, W.; Hoeijmakers, J. H. J. Understanding Nucleotide Excision Repair and Its Roles in Cancer and Ageing. *Nat. Rev. Mol. Cell Biol.* **2014**, *15* (7), 465–481. https://doi.org/10.1038/nrm3822.

(44) Fedeles, B. I.; Singh, V.; Delaney, J. C.; Li, D.; Essigmann, J. M. The AlkB Family of Fe(II)/α-Ketoglutarate-Dependent Dioxygenases: Repairing Nucleic Acid Alkylation Damage and Beyond. *J. Biol. Chem.* **2015**, *290* (34), 20734–20742. https://doi.org/10.1074/jbc.R115.656462.

(45) Samson, L.; Cairns, J. A New Pathway for DNA Repair in Escherichia Coli. *Nature* **1977**, *267* (5608), 281–283. https://doi.org/10.1038/267281a0.

(46) Falnes, P. Ø.; Johansen, R. F.; Seeberg, E. AlkB-Mediated Oxidative Demethylation Reverses DNA Damage in Escherichia Coli. *Nature* **2002**, *419* (6903), 178–182. https://doi.org/10.1038/nature01048.

(47) Trewick, S. C.; Henshaw, T. F.; Hausinger, R. P.; Lindahl, T.; Sedgwick, B. Oxidative Demethylation by Escherichia Coli AlkB Directly Reverts DNA Base Damage. *Nature* **2002**, *419* (6903), 174–178. https://doi.org/10.1038/nature00908.

(48) Mishina, Y.; Yang, C.-G.; He, C. Direct Repair of the Exocyclic DNA Adduct 1,N6-Ethenoadenine by the DNA Repair AlkB Proteins. *J. Am. Chem. Soc.* **2005**, *127* (42), 14594–14595. https://doi.org/10.1021/ja055957m.

(49) Li, D.; Delaney, J. C.; Page, C. M.; Yang, X.; Chen, A. S.; Wong, C.; Drennan, C. L.; Essigmann, J. M. Exocyclic Carbons Adjacent to the N6 of Adenine Are Targets for Oxidation by the Escherichia Coli Adaptive Response Protein AlkB. *J. Am. Chem. Soc.* **2012**, *134* (21), 8896–8901. https://doi.org/10.1021/ja3010094.

(50) Duncan, T.; Trewick, S. C.; Koivisto, P.; Bates, P. A.; Lindahl, T.; Sedgwick, B. Reversal of DNA Alkylation Damage by Two Human Dioxygenases. *Proc. Natl. Acad. Sci.* **2002**, *99* (26), 16660–16665. https://doi.org/10.1073/pnas.262589799.

(51) Dango, S.; Mosammaparast, N.; Sowa, M. E.; Xiong, L.-J.; Wu, F.; Park, K.; Rubin, M.; Gygi, S.; Harper, J. W.; Shi, Y. DNA Unwinding by ASCC3 Helicase Is Coupled to ALKBH3-Dependent DNA Alkylation Repair and Cancer Cell Proliferation. *Mol. Cell* **2011**, *44* (3), 373–384. https://doi.org/10.1016/j.molcel.2011.08.039.

(52) Fu, D.; Samson, L. D. Direct Repair of 3,N(4)-Ethenocytosine by the Human ALKBH2 Dioxygenase Is Blocked by the AAG/MPG Glycosylase. *DNA Repair* **2012**, *11* (1), 46–52. https://doi.org/10.1016/j.dnarep.2011.10.004.

Chapter 4 Genomic incorporation and repair of 2,6-diaminopurine in mammalian cells

4.1. Introduction

2,6-diaminopurine (Z) was first identified in bacteriophages, where it replaces adenine (A) in the phage genome.[1,2] The Z-containing genome is resistant to a spectrum of bacterial endonucleases, empowering bacteriophages a selective advantage.[3,4] While there are two hydrogen bonds in the canonical A:T base pair, Z pairs with T through three hydrogen bonds, which alters physicochemical properties of the DNA double helix.[5,6] Despite its prevalence in phage genomes, Z has never been found in the genomes of other organisms.[7,8] In this vein, researchers failed to identify the genes essential in the biosynthesis of Z in higher organisms.[8] Despite its lack of biosynthesis in higher organisms, genomic incorporation of Z from exogenous sources or enzyme-catalyzed reductive amination at O^6 position of guanine may allow higher organisms to bear Z in their genomes.[9,10] Thus, it is of great importance to investigate the occurrence and fate of Z in the human genome.

No reports showed the presence of Z in the genome of higher organisms; however, Z and its derivatives have been explored as drug candidates.[11] Base Z was documented as an antimetabolite of the nucleotide salvage pathway and strongly inhibits the growth of tumor cells.[12–14] 2,6-Diaminopurine-2′-deoxyriboside (dZ) was found as a substrate for deoxycytidine kinase.[15] In addition, the 5′-triphosphate derivative of dZ (dZTP) can be utilized by Klenow fragments to elongate nascent DNA *in vitro*.[16]

Although dZTP was found in the nucleotide pool after exposing cells with Z or dZ,[11] the genomic incorporation and the clearance of Z in mammalian cells have not yet been reported.

The advances of LC-MS instrumentation and sample preparation methods in the past decades facilitate the analysis of DNA modification and push the limit of detection (LOD) down to a few femtomoles or even attomoles.[17–19] With advanced instrumentation, it is the time to revisit the natural occurrence of dZ in the genomes of higher organisms. It is also worth investigating if dZ can be metabolically incorporated into the human genome. Many non-canonical nucleobase/nucleoside were found to be incorporated into the genome when cells are exposed to them.[20,21] For example, 6-thioguanine and 5-aza-2′-deoxycytidine are readily incorporated into the genome and it is one of the first class of chemotherapeutic drugs.[20,22] 5-ethynyl-2′-deoxyuridine (EdU) can also be incorporated into genomic DNA efficiently and its 'clickable' property allows for a number of applications in biorthogonal assays.[23,24] Beyond replicative DNA polymerases, recent reports have shown the involvement of translesion synthesis (TLS) DNA polymerases in catalyzing the insertion of modified deoxynucleoside triphosphates (dNTPs) into nascent DNA.[25–28] For instance, Pol λ and Pol κ were found to be involved in the incorporation of N^6-methyl-2′-deoxyadenosine and N^2-substituted-dG, respectively, into the genomic DNA of mammalian cells.[25–28] Thus, it is important to examine if any TLS polymerases are involved in the genomic incorporation of dZ in mammalian cells.

Metabolic labeling constitutes a new tool for systematic evaluation of DNA damage repair.[25] Different from conventional method by exposing laboratory chemicals

or cultured cells to DNA damaging agents,[18,29] metabolic labeling involves culturing of mammalian cells in a medium containing the modified nucleobases/nucleosides.[25] Metabolic labeling method enables selective incorporation by introducing a specific type of DNA modification into genome, which avoids the complicating effects from other DNA lesions in the repair study.[25] By exposing cells that are proficient or deficient in DNA repair to dZ under otherwise the same conditions, the difference in the occurrences of dZ in the genome may reveal the plausible repair pathways for dZ.

Herein, we employed a metabolic labeling method that successfully incorporates dZ into the genome of mammalian cells. We also investigated the roles of TLS polymerases in dZ incorporation, and identified a plausible repair pathway for Z in human cells (**Figure 4.1.**).

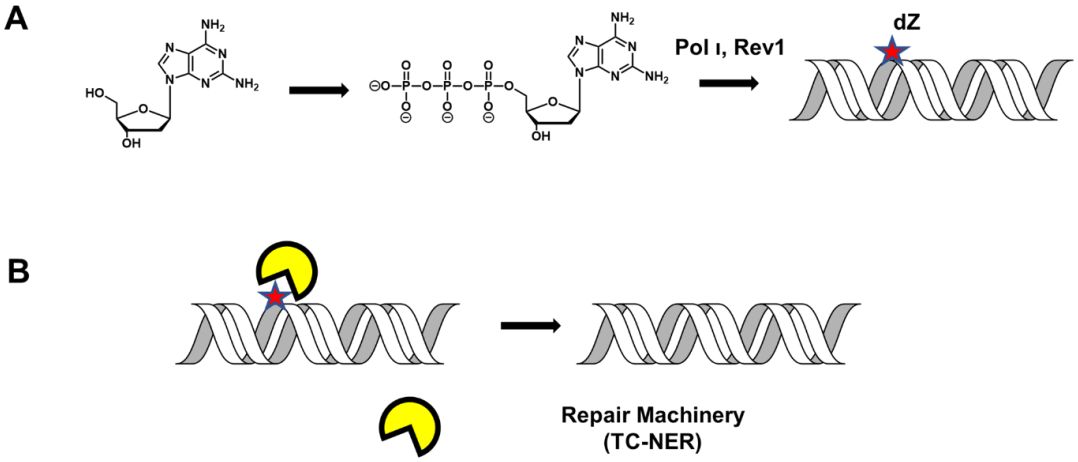

Figure 4.1. LC-MS/MS for assessing the genomic incorporation and repair of dZ in mammalian cells. (A) TLS Pol ι and Rev1 may be involved in the genomic incorporation of dZ. (B) Repair of dZ is modulated by TC-NER.

4.2. Experimental sections

4.2.1. Materials

All chemicals were obtained from Sigma-Aldrich (St. Louis, MO) and enzymes were obtained from New England Biolabs (Ipswich, WA) if not otherwise mentioned. *Erythro*-9-(2-hydroxy-3-nonyl)adenine (EHNA) hydrochloride was purchased from Tocris Bioscience (Ellisville, MO). 2,6-diaminopurine-2′-deoxyriboside (dZ) was purchased from Fisher Scientific (Waltham, MA). HEK293T cells with *XPC*, *CSB*, *POLH*, *POLI*, *POLK*, *REV1*, and *REV3L* genes being individually ablated by CRISPR were generated previously.[30,31]

4.2.2. Genomic incorporation of dZ

Parental HEK293T cells and the isogenic cells deficient in individual TLS polymerases and nucleotide excision repair (NER) factors were seeded in 6-well plates at 37°C in a 5% CO_2 atmosphere. dZ was added to the culture medium at a final concentration of 100 μM. After incubation for 12 h, the cells were harvested immediately or continued to be cultured in fresh media without the nucleoside for another 12 or 24 h, and harvested afterwards. Genomic DNA was extracted from the cells using Qiagen DNeasy Blood & Tissue Kit, and approximately 5 μg of DNA was recovered from a single well of cells.

4.2.3. Enzymatic Digestion

Extracted genomic DNA was enzymatically digested following previously published procedures. In brief, 500 ng of cellular DNA was digested with 5 units of nuclease P1 and 0.00063 unit of phosphodiesterase II in a buffer with 30 mM sodium acetate, 1 mM $ZnCl_2$, and 2.5 nmol of EHNA (adenosine deaminase inhibitor). The pH was subsequently adjusted to 5.6, and the above mixture was incubated at 37°C for 48 h. After then, 0.5 unit of alkaline phosphatase, 0.0013 unit of phosphodiesterase I and one tenth volume of 0.5 M Tris-HCl (pH 8.9) were added. The resulting mixture was incubated at 37°C for another 4 h and neutralized with 1.0 M formic acid. Chloroform extraction was conducted to remove the digestion enzymes. The aqueous phase was dried in a SpeedVac (Fisher Scientific) and reconstituted in water for LC-MS/MS analysis.

4.2.4. Online nLC-MS/MS analysis of dZ in genomic DNA

Online nLC-MS/MS analysis of dZ was conducted following previously described procedures.[25,28] In brief, the separation was conducted on a Dionex Ultimate 3000 module (Thermo Fisher Scientific, Inc.) with a homemade trapping column (150 μm × 40 mm) and an analytical column (75 μm × 200 mm). Both trapping column and analytical column were packed with Magic C18 AQ (200 Å in pore size, 5 μm in particle size, Michrom BioResource, Auburn, CA) reversed-phase materials. Mobile phases A and B contained 0.1% formic acid in water and 0.1% formic acid in acetonitrile, respectively. The samples wwere loaded onto the trapping column with 5% mobile phase

B at a flow rate of 3 μL/min in 7 min, and the analyte (dZ) was subsequently eluted from the column by using a 35-min linear gradient of 5-14% mobile phase B at a flow rate of 300 nL/min.

The LC effluent was directed to a TSQ-Altis triple-quadrupole mass spectrometer operated in the multiple-reaction monitoring (MRM) mode. The MRM transitions included the neutral loss of a 2-deoxyribose (116 Da) from the $[M + H]^+$ ions of dZ (i.e., *m*/*z* 267 → 151) and dA (i.e., *m*/*z* 252 → 136) (**Figure 4.2.**). We also monitored dG (i.e., *m*/*z* 268 → 152), which eluted 1.4-min later than dZ. The voltage for electrospray was 2.0 kV, and the temperature for the ion transfer tube was 275 °C. The widths for precursor and fragment ion isolation were both 0.7 *m*/*z* unit, and the collision energy was 20 V.

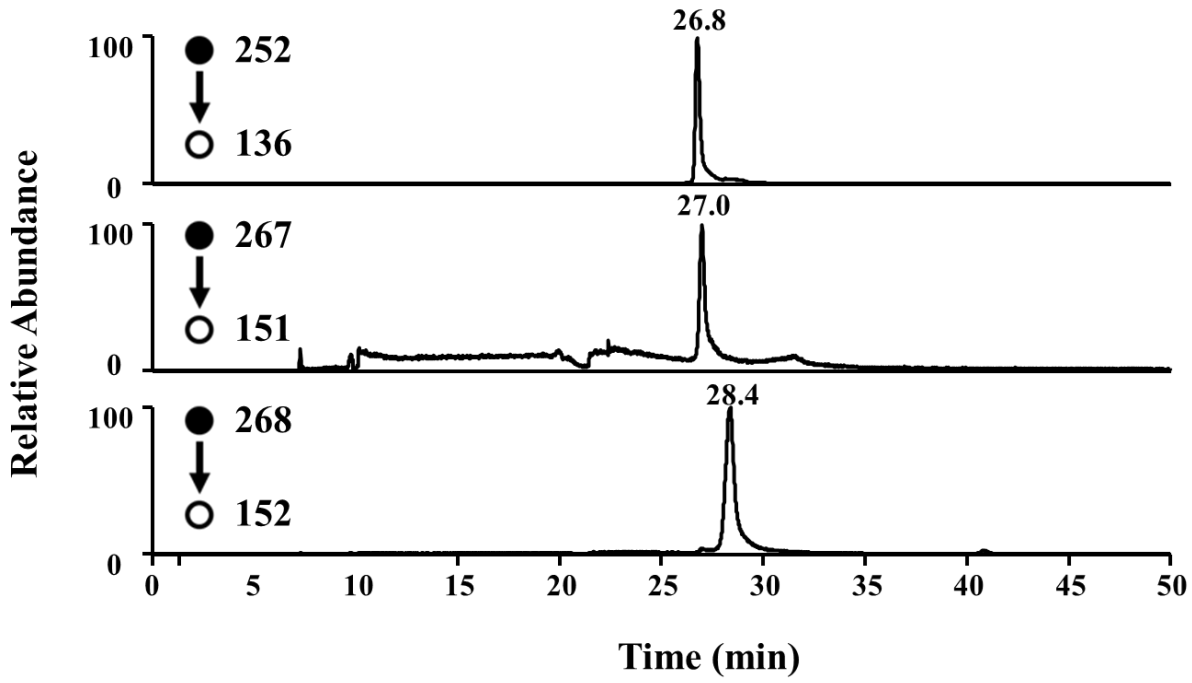

Figure 4.2. Representative selected-ion chromatograms of the *m/z* 252 → 136 (top panel), 267 → 151 (middle panel), 268 → 152 (bottom panel) transitions for the $[M + H]^+$ ions of dA, dZ and dG, respectively, in the digested nucleosides of DNA extracted from CSB-depleted HEK293T cells treated with 100 μM dZ for 12 h.

4.3. Results

4.3.1. dZ is not present in the human genome

To ask if dZ is naturally present in the human genome, we extracted genomic DNA from HEK293T cells, digested it with a mixture of enzymes, and subjected the ensuring nucleosides to nLC-MS/MS analysis. Our results revealed no appreciable peak in the SIC for the *m*/*z* 267 → 151 transition in the expected retention time window of dZ, indicating that dZ does not exist in the genome of HEK293T cells.

4.3.2. Pol ι and Rev1 incorporate dZ into genomic DNA

We found that incubating HEK293T cells with 100 μM dZ for 12 hr results in the incorporation of a substantial level of dZ into genomic DNA (**Figure 4.3., 4.4.**). The resulting dZ in the genome is measured to be 18.1 ± 6.6 modifications per 10^4 dA, or 4.4 ± 1.6 modifications per 10^4 deoxynucleosides. While individual ablation of Pol κ did not appreciably affect dZ incorporation, losses of Pol ι and REV1 led to substantial diminutions in the incorporation of dZ into genomic DNA (**Figure 4.3.**).

4.3.3. Pol ξ and η may modulate the repair of dZ in human cells

Individual ablations of Pol ξ and η lead to increases in the occurrence of dZ compared to parental HEK293T cells, indicating a plausible repair mechanism modulated

by Pol ξ and η. (**Figure 4.3.**) In contrast, gradual decreases in the levels of dZ were found in temporal experiments. It is still unclear how Pol ξ and η modulate the repair of dZ, though some reports showed that Pol ξ and η may be involved in cell cycle arrest.[43]

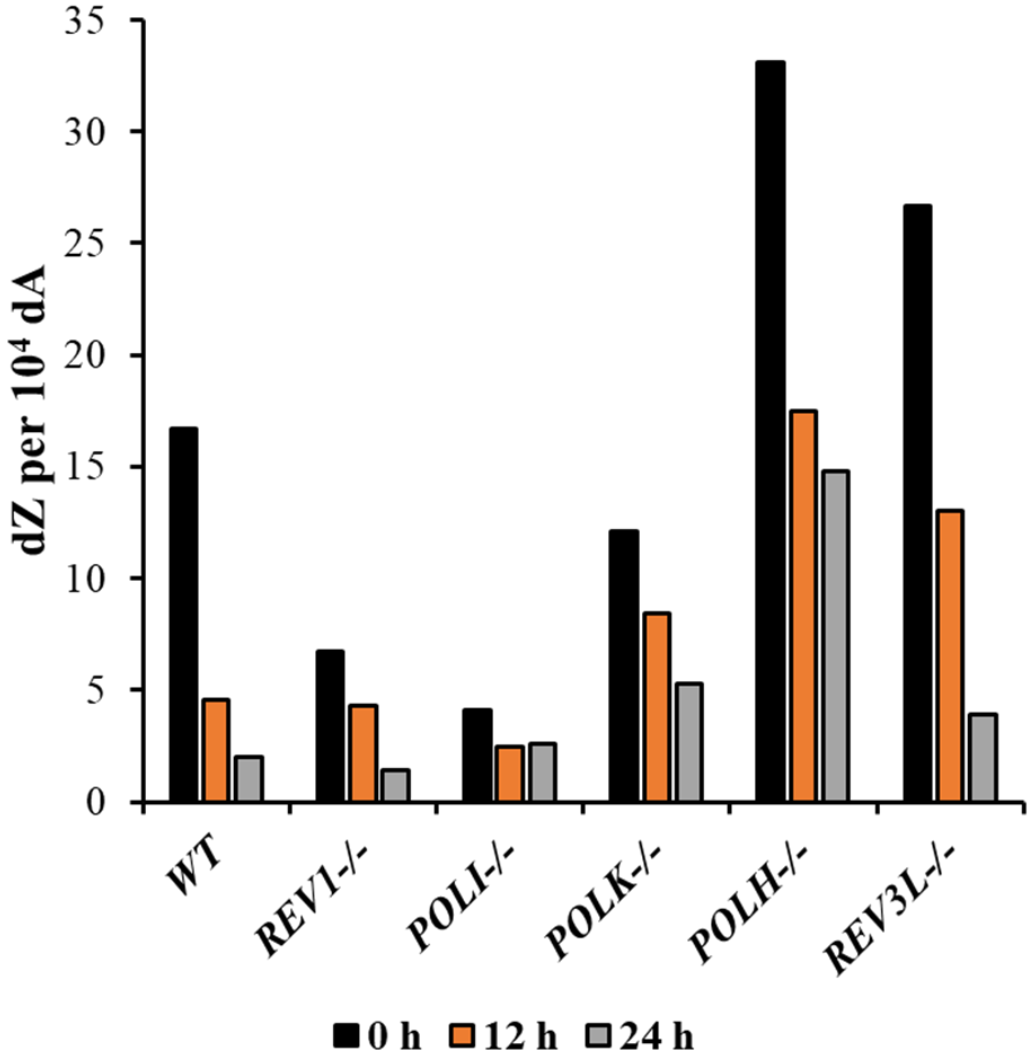

Figure 4.3. The frequencies of dZ in cellular DNA isolated from parental and TLS polymerase-depleted HEK 293T cells. All cells were exposed to 100 µM of dZ for 12 h. The cells were then harvested immediately, or after incubation in fresh media for another 12 or 24 h. The data represent the mean of two measurements on one biological replicate, except for parental HEK293T cells, which represent the mean obtained from three biological replicates.

4.3.4. The involvement of TC-NER in the removal of dZ from human cells

We next conducted time-dependent repair experiments in mammalian cells proficient in DNA repair or deficient in NER factors (**Figure 4.4.**). There are two sub-pathways of NER, i.e., transcription-coupled NER (TC-NER) and global genome NER (GG-NER),[32,33] which are initiated by transcriptional stalling and DNA helix distortion, respectively. These two subpathways uniquely require Cockayne syndrome B (CSB) and xeroderma pigmentosum complementation group C (XPC) proteins, respectively.[34] Our results showed that genetic ablation of CSB, but not XPC, led to diminished removal of dZ, revealing the contributions of TC-NER, but not GG-NER, in the removal of dZ from mammalian cells.

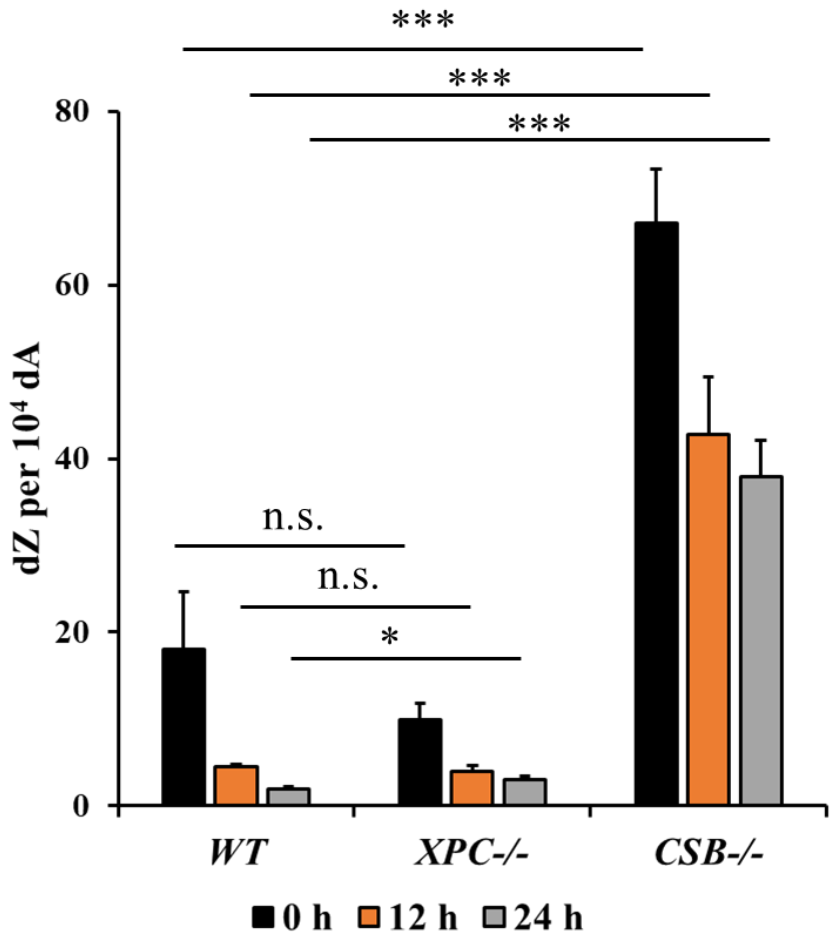

Figure 4.4. The frequencies of dZ in cellular DNA isolated from parental and XPC- or CSB-depleted HEK 293T cells. All cells were exposed to 100 μM of dZ for 12 h. The cells were then harvested immediately, or after incubation in fresh media for another 12 or 24 h. The data represent the mean ± S.D. of results obtained from three biological replicates. ns, $p > 0.05$; *, $0.01 < p < 0.05$; **, $0.001 < p < 0.01$; ***, $p < 0.001$. The p values were calculated by one-way ANOVA with Tuckey's multiple comparisons test.

4.4. Discussion

If cells recognize a foreign nucleobase in the genome, a DNA damage repair machinery is activated. Base excision repair (BER) is responsible for removing most lesions resulting from oxidation, deamination and alkylation.[35] NER, however, is involved in the repair of bulky lesions such as cyclobutane pyrimidine dimer (CPD) and pyrimidine(6–4)pyrimidone (6-4 photoproducts) formed from UV radiation, benzo[*a*]pyrene diolepoxide adducts, and some pyridyloxybutyl (POB) adducts.[34,36] GG-NER pathway senses the distortion in DNA helix. Another subpathway of NER was later found to handle unrepaired DNA lesions that result in transcriptional blockage, which is known as TC-NER.[33] An increasing body of literature has demonstrated that TC-NER is distinct from GG-NER.[37] For example, Patel demonstrated that TC-NER, but not GG-NER, is required for protecting mammalian cells against formaldehyde toxicity and its resulting N^2-MedG.[38] In our recent report, we found that NER is responsible for the repair of N^2-MedG, as well as bulkier N^2-*n*BudG, where TC-NER is involved in the removal of both lesions.[25] In addition, bulkier N^2-*n*BudG is also suspected to be a substrate for GG-NER, probably due to the distortion it brings to the DNA double helix.[25] Taken together, we may conclude that a small modification that does not significantly distorts DNA helix (e.g., a methyl group in N^2-MedG), as long as it blocks transcription machinery, is prone to be removed via a TC-NER mechanism.

The discovery of an alternative purine base, i.e., Z, in bacteriophage has attracted substantial interest from researchers in multiple disciplines.[1,11,12,16] Since Z was first discovered in the 1970s,[1,39] researchers have mainly focused on its antimetabolite

properties.[11] In the past year, three reports published back-to-back in Science elucidated the biogenesis pathways of Z: Zhou and Sleiman found the biochemical mechanisms that produces Z,[2,40] while Pezo uncovered a specialized DNA polymerase that incorporates Z into DNA while excluding A.[41] These findings improved tremendously our understanding of Z; however, it is still unclear if Z is naturally present or incorporated into the genomes of higher organisms. Our quantification results showed that Z is not naturally present in mammalian cells, though it can be incorporated into the genome of HEK293T cells. We can deduce that dZ from exogenous sources has the potential to be a drug that targets DNA. Thus, it is of importance to document the repair and other biological consequences when dZ is introduced into the genome. A shuttle vector-based method was utilized to study the transcriptional bypass, mutagenesis, and repair of Z on a transfected plasmid in mammalian cells recently in our lab.[7] Z was found to substantially impede transcriptional elongation, but not elicit any mutant transcripts, and is readily removed by TC-NER in mammalian cells.[7] However, it is still unclear how Z is incorporated into the genome and how repair machinery responds to Z in genomic DNA. To fill the knowledge gap, we incorporated dZ into mammalian genome for the first time utilizing a metabolic labeling approach. In line with previous findings, TC-NER, but not GG-NER, is essential in the removal of genomic incorporated dZ.[7] The rapid and efficient removal of Z may provide an explanation why higher organisms excluding Z in the genome, though Z presents superior stability in paring with T than A.

This report also supports novel roles of TLS polymerases in incorporating this non-canonical nucleoside into genomic DNA of mammalian cells. Genomic

incorporation of unnatural bases was extensively utilized in chemotherapy, antiviral medication, and biorthogonal applications.[20,23] The DNA polymerases involved in the process have long been thought to be carried out by replicative DNA polymerases; however, TLS polymerases has been shown to be able to modulate incorporation of some modified bases. Pol λ was involved in the genomic incorporation of N^6-MedA,[26] Pol κ was found responsible for the incorporation of N^2-modified-dG, while Pol η.[27,28,42] In this report, Pol ι and Rev1 stand out in mediating the incorporation of dZ into human genome, and these two TLS polymerases are the first time found involve in genomic incorporation of noncanonical nucleosides. In line with previous findings of Pol λ, Pol κ It is worth investigating the roles of other TLS polymerases in catalyzing the incorporation of non-canonical bases into the genome. Multiple cancer cells are known to have a higher level of TLS polymerases in handling unrepaired DNA lesions, avoiding apoptosis and eventually developing resistance to chemotherapeutic drugs.[43] A modified, not naturally occurring nucleobase that strongly inhibits the transcription machinery can be a potential chemotherapeutic agent.[44,45] Since replicative polymerases cannot accommodate the modified bases and TLS polymerases are present at relatively low levels in normal cells, cancer cells are more likely to uptake more modified base and incorporate it into the genome compared to normal cells. The modified bases may stall transcription and replication machineries, and as a result, control the growth and division of cancer cells.

Taken together, here we reported the incorporation of Z into genomic DNA of human cells for the first time. It is worth noting that Pol ι and Rev1 contribute to the incorporation, while we cannot rule out the involvement of other DNA polymerases (e.g.,

replicating polymerases). Z is not bulky in size, and it may not distort DNA double helix and thus may not be recognized by the GG-NER machinery. However, TC-NER readily removes Z from genomic DNA. Future directions can be investigation on the genomic incorporation and repair of a structurally related, adenine derivative, 2-aminopurine (2-AP).

References

(1) Kirnos, M. D.; Khudyakov, I. Y.; Alexandrushkina, N. I.; Vanyushin, B. F. 2-Aminoadenine Is an Adenine Substituting for a Base in S-2L Cyanophage DNA. *Nature* **1977**, *270* (5635), 369–370. https://doi.org/10.1038/270369a0.

(2) Zhou, Y.; Xu, X.; Wei, Y.; Cheng, Y.; Guo, Y.; Khudyakov, I.; Liu, F.; He, P.; Song, Z.; Li, Z.; Gao, Y.; Ang, E. L.; Zhao, H.; Zhang, Y.; Zhao, S. A Widespread Pathway for Substitution of Adenine by Diaminopurine in Phage Genomes. *Science* **2021**, *372* (6541), 512–516. https://doi.org/10.1126/science.abe4882.

(3) Szekeres, M.; Matveyev, A. V. Cleavage and Sequence Recognition of 2,6-Diaminopurine-Containing DNA by Site-Specific Endonucleases. *FEBS Lett.* **1987**, *222* (1), 89–94. https://doi.org/10.1016/0014-5793(87)80197-7.

(4) Chollet, A.; Kawashima, E. DNA Containing the Base Analogue 2-Aminoadenine: Preparation, Use as Hybridization Probes and Cleavage by Restriction Endonucleases. *Nucleic Acids Res.* **1988**, *16* (1), 305–317. https://doi.org/10.1093/nar/16.1.305.

(5) Haaima, G.; Hansen, H. F.; Christensen, L.; Dahl, O.; Nielsen, P. E. Increased DNA Binding and Sequence Discrimination of PNA Oligomers Containing 2,6-Diaminopurine. *Nucleic Acids Res.* **1997**, *25* (22), 4639–4643. https://doi.org/10.1093/nar/25.22.4639.

(6) Cheong, C.; Tinoco, I.; Chollet, A. Thermodynamic Studies of Base Pairing Involving 2,6-Diaminopurine. *Nucleic Acids Res.* **1988**, *16* (11), 5115–5122. https://doi.org/10.1093/nar/16.11.5115.

(7) Tan, Y.; You, C.; Park, J.; Kim, H. S.; Guo, S.; Schärer, O. D.; Wang, Y. Transcriptional Perturbations of 2,6-Diaminopurine and 2-Aminopurine. *ACS Chem. Biol.* **2022**. https://doi.org/10.1021/acschembio.2c00369.

(8) Czernecki, D.; Bonhomme, F.; Kaminski, P.-A.; Delarue, M. Characterization of a Triad of Genes in Cyanophage S-2L Sufficient to Replace Adenine by 2-Aminoadenine

in Bacterial DNA. *Nat. Commun.* **2021**, *12* (1), 4710. https://doi.org/10.1038/s41467-021-25064-x.

(9) Afanasyev, O. I.; Kuchuk, E.; Usanov, D. L.; Chusov, D. Reductive Amination in the Synthesis of Pharmaceuticals. *Chem. Rev.* **2019**, *119* (23), 11857–11911. https://doi.org/10.1021/acs.chemrev.9b00383.

(10) Reid, D. A.; Reed, P. J.; Schlachetzki, J. C. M.; Nitulescu, I. I.; Chou, G.; Tsui, E. C.; Jones, J. R.; Chandran, S.; Lu, A. T.; McClain, C. A.; Ooi, J. H.; Wang, T.-W.; Lana, A. J.; Linker, S. B.; Ricciardulli, A. S.; Lau, S.; Schafer, S. T.; Horvath, S.; Dixon, J. R.; Hah, N.; Glass, C. K.; Gage, F. H. Incorporation of a Nucleoside Analog Maps Genome Repair Sites in Postmitotic Human Neurons. *Science* **2021**, *372* (6537), 91–94. https://doi.org/10.1126/science.abb9032.

(11) Weckbecker, G.; Cory, J. G. Metabolic Activation of 2,6-Diaminopurine and 2,6-Diaminopurine-2′-Deoxyriboside to Antitumor Agents. *Adv. Enzyme Regul.* **1989**, *28*, 125–144. https://doi.org/10.1016/0065-2571(89)90068-X.

(12) Huang, M.-C.; Hatfield, K.; Roetker, A. W.; Montgomery, J. A.; Blakley, R. L. Analogs of 2′-Deoxyadenosine: Facile Enzymatic Preparation and Growth Inhibitory Effects on Human Cell Lines. *Biochem. Pharmacol.* **1981**, *30* (19), 2663–2671. https://doi.org/10.1016/0006-2952(81)90535-9.

(13) Paterson, A. R.; Yang, S. E.; Lau, E. Y.; Cass, C. E. Low Specificity of the Nucleoside Transport Mechanism of RPMI 6410 Cells. *Mol. Pharmacol.* **1979**, *16* (3), 900–908.

(14) Cory, J. G.; Sato, A.; Carter, G. L.; Bacon, P. E.; Montgomery, J. A.; Brown, N. C. The Utility of Combinations of Drugs Directed at Specific Sites of the Same Target Enzyme--Ribonucleotide Reductase as the Model. *Adv. Enzyme Regul.* **1985**, *23*, 181–192. https://doi.org/10.1016/0065-2571(85)90047-0.

(15) Ives, D. H.; Wang, S. M. Deoxycytidine Kinase from Calf Thymus. *Methods Enzymol.* **1978**, *51*, 337–345. https://doi.org/10.1016/s0076-6879(78)51045-8.

(16) Farnham, P. J.; Platt, T. Effects of DNA Base Analogs on Transcription Termination at the Tryptophan Operon Attenuator of EScherichia Coli. *Proc. Natl. Acad. Sci. U. S. A.* **1982**, *79* (4), 998–1002. https://doi.org/10.1073/pnas.79.4.998.

(17) Liu, S.; Wang, Y. Mass Spectrometry for the Assessment of the Occurrence and Biological Consequences of DNA Adducts. *Chem. Soc. Rev.* **2015**, *44* (21), 7829–7854. https://doi.org/10.1039/C5CS00316D.

(18) Hwa Yun, B.; Guo, J.; Bellamri, M.; Turesky, R. J. DNA Adducts: Formation, Biological Effects, and New Biospecimens for Mass Spectrometric Measurements in Humans. *Mass Spectrom. Rev.* **2020**, *39* (1–2), 55–82. https://doi.org/10.1002/mas.21570.

(19) Yuan, B.-F. Assessment of DNA Epigenetic Modifications. *Chem. Res. Toxicol.* **2020**, *33* (3), 695–708. https://doi.org/10.1021/acs.chemrestox.9b00372.

(20) Elion, G. B. The Purine Path to Chemotherapy. *Science* **1989**, *244* (4900), 41–47. https://doi.org/10.1126/science.2649979.

(21) LePage, G. A. Basic Biochemical Effects and Mechanism of Action of 6-Thioguanine. *Cancer Res.* **1963**, *23* (8_Part_1), 1202–1206.

(22) Wang, H.; Wang, Y. LC-MS/MS Coupled with Stable Isotope Dilution Method for the Quantification of 6-Thioguanine and S6-Methylthioguanine in Genomic DNA of Human Cancer Cells Treated with 6-Thioguanine. *Anal. Chem.* **2010**, *82* (13), 5797–5803. https://doi.org/10.1021/ac1008628.

(23) Salic, A.; Mitchison, T. J. A Chemical Method for Fast and Sensitive Detection of DNA Synthesis in Vivo. *Proc. Natl. Acad. Sci.* **2008**, *105* (7), 2415–2420. https://doi.org/10.1073/pnas.0712168105.

(24) Fantoni, N. Z.; El-Sagheer, A. H.; Brown, T. A Hitchhiker's Guide to Click-Chemistry with Nucleic Acids. *Chem. Rev.* **2021**, *121* (12), 7122–7154. https://doi.org/10.1021/acs.chemrev.0c00928.

(25) Guo, S.; Li, L.; Yu, K.; Tan, Y.; Wang, Y. LC-MS/MS for Assessing the Incorporation and Repair of N2-Alkyl-2′-Deoxyguanosine in Genomic DNA. *Chem. Res. Toxicol.* **2022**. https://doi.org/10.1021/acs.chemrestox.2c00101.

(26) Liu, X.; Lai, W.; Li, Y.; Chen, S.; Liu, B.; Zhang, N.; Mo, J.; Lyu, C.; Zheng, J.; Du, Y.-R.; Jiang, G.; Xu, G.-L.; Wang, H. N6-Methyladenine Is Incorporated into Mammalian Genome by DNA Polymerase. *Cell Res.* **2021**, *31* (1), 94–97. https://doi.org/10.1038/s41422-020-0317-6.

(27) Prakasha Gowda, A. S.; Lee, M.; Spratt, T. E. N2-Substituted 2′-Deoxyguanosine Triphosphate Derivatives, Selective Substrates for Human DNA Polymerase κ. *Angew. Chem. Int. Ed Engl.* **2017**, *56* (10), 2628–2631. https://doi.org/10.1002/anie.201611607.

(28) Tan, Y.; Guo, S.; Wu, J.; Du, H.; Li, L.; You, C.; Wang, Y. DNA Polymerase η Promotes the Transcriptional Bypass of N2-Alkyl-2'-Deoxyguanosine Adducts in Human Cells. *J. Am. Chem. Soc.* **2021**, *143* (39), 16197–16205. https://doi.org/10.1021/jacs.1c07374.

(29) Balbo, S.; Turesky, R. J.; Villalta, P. W. DNA Adductomics. *Chem. Res. Toxicol.* **2014**, *27* (3), 356–366. https://doi.org/10.1021/tx4004352.

(30) Wu, J.; Li, L.; Wang, P.; You, C.; Williams, N. L.; Wang, Y. Translesion Synthesis of O4-Alkylthymidine Lesions in Human Cells. *Nucleic Acids Res.* **2016**, *44* (19), 9256–9265. https://doi.org/10.1093/nar/gkw662.

(31) Wu, J.; Du, H.; Li, L.; Price, N. E.; Liu, X.; Wang, Y. The Impact of Minor-Groove N2-Alkyl-2′-Deoxyguanosine Lesions on DNA Replication in Human Cells. *ACS Chem. Biol.* **2019**, *14* (8), 1708–1716. https://doi.org/10.1021/acschembio.9b00129.

(32) Gillet, L. C. J.; Schärer, O. D. Molecular Mechanisms of Mammalian Global Genome Nucleotide Excision Repair. *Chem. Rev.* **2006**, *106* (2), 253–276. https://doi.org/10.1021/cr040483f.

(33) Marteijn, J. A.; Lans, H.; Vermeulen, W.; Hoeijmakers, J. H. J. Understanding Nucleotide Excision Repair and Its Roles in Cancer and Ageing. *Nat. Rev. Mol. Cell Biol.* **2014**, *15* (7), 465–481. https://doi.org/10.1038/nrm3822.

(34) Chatterjee, N.; Walker, G. C. Mechanisms of DNA Damage, Repair, and Mutagenesis. *Environ. Mol. Mutagen.* **2017**, *58* (5), 235–263. https://doi.org/10.1002/em.22087.

(35) Bauer, N. C.; Corbett, A. H.; Doetsch, P. W. The Current State of Eukaryotic DNA Base Damage and Repair. *Nucleic Acids Res.* **2015**, *43* (21), 10083–10101. https://doi.org/10.1093/nar/gkv1136.

(36) de Boer, J.; Hoeijmakers, J. H. J. Nucleotide Excision Repair and Human Syndromes. *Carcinogenesis* **2000**, *21* (3), 453–460. https://doi.org/10.1093/carcin/21.3.453.

(37) Hanawalt, P. C.; Spivak, G. Transcription-Coupled DNA Repair: Two Decades of Progress and Surprises. *Nat. Rev. Mol. Cell Biol.* **2008**, *9* (12), 958–970. https://doi.org/10.1038/nrm2549.

(38) Mulderrig, L.; Garaycoechea, J. I.; Tuong, Z. K.; Millington, C. L.; Dingler, F. A.; Ferdinand, J. R.; Gaul, L.; Tadross, J. A.; Arends, M. J.; O'Rahilly, S.; Crossan, G. P.; Clatworthy, M. R.; Patel, K. J. Aldehyde-Driven Transcriptional Stress Triggers an Anorexic DNA Damage Response. *Nature* **2021**, *600* (7887), 158–163. https://doi.org/10.1038/s41586-021-04133-7.

(39) Grome, M. W.; Isaacs, F. J. ZTCG: Viruses Expand the Genetic Alphabet. *Science* **2021**, *372* (6541), 460–461. https://doi.org/10.1126/science.abh3571.

(40) Sleiman, D.; Garcia, P. S.; Lagune, M.; Loc'h, J.; Haouz, A.; Taib, N.; Röthlisberger, P.; Gribaldo, S.; Marlière, P.; Kaminski, P. A. A Third Purine Biosynthetic Pathway Encoded by Aminoadenine-Based Viral DNA Genomes. *Science* **2021**, *372* (6541), 516–520. https://doi.org/10.1126/science.abe6494.

(41) Pezo, V.; Jaziri, F.; Bourguignon, P.-Y.; Louis, D.; Jacobs-Sera, D.; Rozenski, J.; Pochet, S.; Herdewijn, P.; Hatfull, G. F.; Kaminski, P.-A.; Marliere, P. Noncanonical DNA Polymerization by Aminoadenine-Based Siphoviruses. *Science* **2021**, *372* (6541), 520–524. https://doi.org/10.1126/science.abe6542.

(42) Guo, S.; Li, L.; Yu, K.; Tan, Y.; Wang, Y. LC-MS/MS for Assessing the Incorporation and Repair of N 2-Alkyl-2′-Deoxyguanosine in Genomic DNA. *Chem. Res. Toxicol.* **2022**.

(43) Albertella, M. R.; Green, C. M.; Lehmann, A. R.; O'Connor, M. J. A Role for Polymerase η in the Cellular Tolerance to Cisplatin-Induced Damage. *Cancer Res.* **2005**, *65* (21), 9799–9806. https://doi.org/10.1158/0008-5472.CAN-05-1095.

(44) Kantarjian, H.; Issa, J.-P. J.; Rosenfeld, C. S.; Bennett, J. M.; Albitar, M.; DiPersio, J.; Klimek, V.; Slack, J.; de Castro, C.; Ravandi, F.; Helmer, R.; Shen, L.; Nimer, S. D.; Leavitt, R.; Raza, A.; Saba, H. Decitabine Improves Patient Outcomes in Myelodysplastic Syndromes: Results of a Phase III Randomized Study. *Cancer* **2006**, *106* (8), 1794–1803. https://doi.org/10.1002/cncr.21792.

(45) Zauri, M.; Berridge, G.; Thézénas, M.-L.; Pugh, K. M.; Goldin, R.; Kessler, B. M.; Kriaucionis, S. CDA Directs Metabolism of Epigenetic Nucleosides Revealing a Therapeutic Window in Cancer. *Nature* **2015**, *524* (7563), 114–118. https://doi.org/10.1038/nature14948.

Chapter 5 Conclusions and future directions

It is of great importance to dissect how the integrity of human genome is compromised and the mechanisms through which the resulting DNA modifications are repaired. Efforts have been made in the development of reliable analytical methods for quantitative and qualitative measurement of DNA adducts. LC-MS/MS is the most adopted platform for this need. In the thesis, LC-MS/MS-based methods were developed, enabling us to understand the formation (or genomic incorporation) and repair of PHB adducts resulting from tobacco specific nitrosamines, dZ and N^2-alkyl-dG.

In Chapter 2, an LC-MS/MS method for the simultaneous quantification of the pyridylhydroxybutyl lesions O^2-PHBdT, O^4-PHBdT and O^6-PHBdG, where O^4-PHBdT was reported, for the first time, found to be induced in mammalian cells upon exposure to pyridylhydroxybutylating agents. The method demonstrated high sensitivity in quantification of targeted DNA lesions and its capacity to snapshot the levels of lesions in a repair study at different time intervals. The method may serve as a tool to investigate the involvement of DNA pyridylhydroxybutylation as a biomarker related to tobacco-induced cancer. Researchers can also conduct investigations on other pyridylhydroxybutyl sites on the bases and phosphate backbones. Using a similar isotope dilution method, the formation and repair of novel pyridylhydroxybutyl lesions can also be evaluated.

In Chapter 3, a metabolic labeling method was employed to incorporate minor-groove N^2-MedG and N^2-*n*BudG into genomic DNA. Systematic repair study was

conducted on these two lesions. Results revealed the roles of TLS polymerases, NER and ALKBH3 in the repair of these lesions in mammalian cells. It will be interesting to examine, in the future, whether the method can also be employed for assessing the metabolic incorporation and repair of bulky aromatic hydrocarbon-induced N^2-dG adducts, e.g., N^2-BPDE-dG. Another direction of future research is to investigate the metabolic incorporation of other modified/non-canonical nucleosides into the human genome by TLS polymerases. In addition, it is worth noting that the metabolic labeling of genomic DNA with a structurally defined nucleoside enables selective incorporation of the modified nucleoside without the complicating effects of other DNA lesions. The proposed method may overcome the difficulties in selective introducing DNA lesions by traditional chemical labeling, which may show great potential in DNA damage repair research and risk assessment.

In Chapter 4, genomic incorporation of Z in human cells was found for the first time. Pol ι and Rev1 may contribute to the incorporation, though the involvement of other DNA polymerases (e.g., replicating polymerases) is still not clear. Z is not bulky in size, and it may not distort DNA double helix and thus may not be recognized by the GG-NER machinery. However, TC-NER readily removes Z from genomic DNA. Since the percentage of adenine in human genome may be affected by the exposure of dZ, the relative quantification based on the ratio of dZ and dA may be biased. A rigorous isotope dilution method is required, in this case, a stable isotope-labeled dZ needs to be prepared. Future directions may include investigation on the genomic incorporation and repair of a structurally related, adenine derivative, 2-aminopurine (2-AP). In addition, the discovery

of genomic incorporation of noncanonical nucleosides carried out by TLS polymerases may be utilized in combinatory medication to enhance chemotherapeutic practices since cancer cells usually express higher level of TLS polymerases compared to normal cells to cope with continuous threat and stress in the genome. Modified nucleosides which stall transcription and incorporated by TLS polymerases, but not replicative DNA polymerases is of great potential to trigger cell deaths in cancer cells but not normal cells.